Doctoral dissertation

Investigation of surface properties of boron doped diamond for developing neuron -machine interface

Farnoosh Vahidpour

Promoter:

Prof. Dr. Miloš Nesládek | UHasselt

Co-promoters:

Prof. Dr. Ken Haenen (UHasselt & IMEC vzw)

Prof. Dr. Michele Giugliano (University of Antwerp)

Chair: Prof. Dr. Karin Coninx (Universiteit Hasselt)

Supervisor:

Prof. Dr. Miloš Nesládek (Universiteit Hasselt & IMEC vzw)

Co-promoters:

Prof. Dr. Ken Haenen (Universiteit Hasselt & IMEC vzw)

Prof. Dr. Michele Giugliano (University of Antwerp)

Members of the jury:

Stoffel Janssens (OIST- Japan)

Hans-Gerhard Boyen (Universiteit Hasselt)

Cristian Pablo Pennisi (Aalborg University- Denmark)

Irena Kratochvilova (Institute of Physics Czech Academy Sciences- Czech Republic)

Marcel Ameloot (Universiteit Hasselt)

Mieke Buntinx (Universiteit Hasselt)

Contents

Acknowledgement

During the last five years, I have been grateful to meet and work with people who made the path towards my PhD defence more straight forward, nice and exciting. They have changed my life and will not be forgotten.

First of all, I take the opportunity to thank my promoter, Professor Miloš Nesládek. I am grateful for being a member in your group. I am deeply appreciative for your trust and confidence you had in me and it was a great pleasure working under your supervision. I acknowledge your valuable guidance through all the steps in the last five years.

I thank very much my co-promoter professor Ken Haenen whose useful discussions were helping me a lot in solving problems and have a better view during my research.

I would like to express my sincerest gratitude to Professor Michele Giugliano for our collaborations and helping with my experiments in University of Antwerp. I also acknowledge Prof. Dr. Hans-Gerhard Boyen and Prof. Dr. Marcel Ameloot and his group for valuable discussions and their kind collaborations in my experiments.

Thanks to all the jury members, for spending their valuable time to read my thesis and give valuable comments to improve the manuscript. Prof. Dr. Cristian Pablo Pennisi, Prof. Dr. Irena Kratochvilova, Prof. Dr. Mieke Buntinx, Dr. Stoffel Janssens, thank you very much.

I truly appreciate the scientific collaboration with Dr. Zuzana Vlčková Živcová and friendly guidance and supportive discussions from Václav Petrák, Vlaďka Petráková and Vilma Ratautaite.

I am grateful to Prof. Dr. Dario Farina and his group in Universitätmedizin Göttingen for their scientific collaboration.

Furthermore, I acknowledge the assistance I received from all technicians in physics and chemistry labs in IMO as well as the help and guidance of the secretary of IMO. Thank you very much.

Besides, I would like to thank all of my colleagues at IMO, especially in WBGM and NPF groups. First of all, Dr. Paulius Pobedinskas, who was not yet a doctor when I started my PhD, but he was my first teacher in IMO, who thought me the

work in the lab and clean room step by step, patiently. I am thankful to you Paulius, for being always such a great teacher.

I would like to thank Sien and Matthew for the late-at-night SEM measurements of my samples. Matthew, thanks for being such an understanding and easy going colleague. Your creativity and ideas helped me a lot in progressing my work, seriously! Sien, we have good memories together at Science Slam, remember? And good old times in coffee breaks…

I thank Pieter for helping me honestly at any time he could, and my hardworking master student, Ali, for suggesting ideas, discussing and progressing with the project.

Yaso, I am grateful to have such a nice colleague and friend. Thanks for being helpful and understanding.

I am appreciative to my former colleague, Elena, for showing me a new outlook of scientific research during my PhD.

I am grateful I spent four year of research in the office with very nice and understanding office mates: Emilie, Tim and Wouter. Dear Emilie, I am happy I was working close to you so we could chat and discuss details of our work and life every day, and I benefit a lot from your expertise. Thanks a million.

Johnny, IMO is not IMO without you! Keep your cool attitude at work with your different point of view! Thanks for helping me with technical problems in the lab and for introducing me a new world of art!

Wiebke, Thank you for being a forever-friend and colleague for me. More friend than colleague! I enjoy a lot talking to such an open and honest person. The lab felt totally different after you graduated!

Ilaria, I appreciate you for bringing such a positive attitude in the lab and the office. You are such a great person!

Very special thanks go to my dear Iranian friends at UHasselt for their support: Sedigheh, Rozhin, Mehran, Ali, Aziz, Farnaz, Elham and Majid.

And thanks to all of my lovely international and Belgian friends in UHasselt, from chemistry, biology and statistics department of UHasselt, for being supportive and always together, for parties and ice cream evenings at Keysel Creymke…

Deeply from the bottom of my heart, I am thankful to my dearest friends in Belgium: Keivan and Homayoun, Kaat and Lisa, for their helps at any time, and

happy and sad times together. Special thanks to Lisa for talking to me and following up the news regarding my work and studies.

I am very thankful to Jan and Archana for their support and thoughtful and useful discussions which helped me have a better view of work and life.

And, I wrote my thesis in Jülich, Germany, as I lived (and still do) on the second floor of the cosy house of a very nice couple. I thank them for their warm welcome and support:

Liebe Ingrid und lieber Manfred, Ich bedanke mich sehr für alles was ihr bis jetzt für uns gemacht habt. Ich bin dankbar für eure Liebe, Freundlichkeit und Unterstützung, die die ganze Wohnung gemütlich und bequem machte. Darüber freue ich mich immer!

My endless love and care goes to my dear family. My dearest parents, and my lovely brother and sister. I love you so much and thank you for your everyday attention:

پدر و مادر عزیز و دوست داشتنی ام، محبت ها، نگرانی ها، و به فکر بودن های شما در هیچ کجا پیدا نمیشه !از اینکه دوری رو تحمل میکنید و چیزی به زبون نمیارید ممنون و شرمنده م. امیدوارم بتونم تا حد ممکن جبران کنم. بلاخره دو میلیمتر به پایان رسید ! دمتون گرم بخاطر همه توجه ها و همفکری ها ! عشق منید شما!

برادر با معرفت و متوجه ام، بدون تو این آرامش وجود نداشت !برادر عزیزمی!

خواهر با فکر مشوقم، با حمایت ها و راهنماییهای تو تونستم انقدر پیشرفت کنم. ممنونم واسه همه چیز!

And my dearest Roohy, you are very critical with science and research, and that is why I want to thank you, for shedding light into my outlook to help me find my way in a better approach. Your honest support and guidance helped me grow, and I truly appreciate it. With love…

Nederlandse samenvatting

Op basis van de huidige kennis van diamantoppervlakken hebben we 2-dimensionale micro electrode arrays (MEA) oftewel multi-elektrodenreeksen ontwikkeld voor het interfacen van neuronen. Diamant biedt namelijk de unieke mogelijkheid om zowel elektrische geleidende (boor gedoteerd diamant) als isolerende (niet-gedoteerd diamant) oppervlakken te creëren. Platte diamant MEAs worden gefabriceerd vanuit dunne, synthetische diamant films, zowel nanokristallijn diamant (NCD) als boor-gedoteerd nanokristallijn diamant (BNCD), geproduceerd met behulp van PECVD (Plasma enhanced chemische dampdepositie). De fabricatiemethoden worden beschreven en de elektrochemische eigenschappen van de elektrodes worden onderzocht. De functionaliteit van de diamantelektrodes wordt onderzocht met behulp van corticale hersensneden van ratten.

Om toegepast te kunnen worden als kunstmatige interface voor neurale cellen voor het centrale en perifere zenuwstelsel is het belangrijk dat de MEAs zich kunnen aanpassen aan het zenuwweefsel, d.w.z. flexibel zijn. Daarom worden in deze thesis flexibele diamant/polymeer elektrodes ontwikkeld voor *in vivo* elektromyografie (EMG) experimenten op basis van alle kennis en ervaring ontleend aan het fabriceren van diamant elektrodes voor neurale detectie en diamant-neuron interfacing. Het actieve en geleidende deel van de elektrodes bestaat uit BNCD en de isolerende laag is biocompatibel polyimide. Om de fabricatie van de elektrodes te verwezenlijken was voldoende kennis en creativiteit nodig, hetgeen uiteindelijke bereikt werd. Fabricatiemethodes voor deze flexibele elektrodes, inclusief de gerelateerde materiaalwetenschap, worden besproken in deze thesis. De ontwikkelde elektrodes worden onderzocht aan de hand van elektrische impedantie spectroscopie (EIS) metingen uitgevoerd in biologische media. Bovendien kunnen de flexibele elektrodes niet alleen voor neuraal interfacing gebruikt worden maar ook voor neuromusculaire interfacen, die intensief bestudeerd worden in neuroprothetische apparaten.

De motivatie van deze thesis is dan ook het gebruik van diamantoppervlakken als een platform voor neurale interfacing, waarbij praktisch getoond wordt hoe de diamantelektrodes ontwikkeld en gekarakteriseerd worden, en om aan te tonen hoe het gebruik van de diamantfilm als actieve elektrode metingen van

het neurale signaal beïnvloeden. Naast de ontwikkeling van diamantelektrodes voerden we baanbrekende experimenten uit om de invloed van de oppervlaktelaag (coating) van het diamant op neuronenculturen te onderzoeken. Het doel was om de ontegenzeglijke invloed van de polyethyleenimine (PEI) monolaag op diamant te onthullen vanuit chemische en elektrochemisch standpunt. De belangrijke rol van de coatingsmethode werd bestudeerd met behulp van EIS metingen. Bovendien werden er corticale neuronen gecultiveerd op het gecoat oppervlak en werden de resultaten *in vitro* waargenomen.

De inhoud van de thesis

Deze thesis is opgedeeld in volgende hoofdstukken:

1. Inleiding
2. State of the art van Brain-Machine (let. Hersenen-Machine) interfaces: tot MEAs

   In dit hoofdstuk wordt eerder onderzoek naar MEAs en de ontwikkeling van Mens-Machine interfaces uitvoerig besproken. Kritieke punten voor het gebruik van diamant MEAs worden benadrukt, verschillende technieken worden besproken en de meest belovende resultaten voor ons doel worden geëxtraheerd.
3. Micro-elektrode arrays uit puur diamant met gefunctionaliseerde oppervlakken voor hersensnede neurale analyse [inclusief gedetailleerde fabricatie van MEA].

   In dit hoofdstuk worden MEAs ontwikkeld bestaande uit isolerende en geleidende diamantfilms. Het homogene oppervlak van diamant wordt gebruikt als elektrodeoppervlak voor *in vitro* neurale analyse van hersensneden.
4. Functionele Diamant/polyimide elektrodes: Flexibele elektromyografie MEAs [inclusief gedetailleerde fabricatie van EMG MEA].

   In dit hoofdstuk worden flexibele MEAs met geïntegreerd polyimide ontwikkeld. De elektrodes worden gekarakteriseerd en voorbereid voor biologische *in vivo* experimenten.
5. Functionele Bio-moleculaire Monolagen op Diamant: Een nieuw platform voor de constructie van artificiële neurale interfaces.

In dit hoofdstuk wordt de functionalisatie van diamantfilms met polyethyleenimine (PEI) monolagen experimenteel bestudeerd. Er wordt aangetoond dat deze oppervlaktefunctionalisatie leidt tot betere functionele eigenschappen van diamant. De oppervlakte-eigenschappen en samenstelling, elektrochemische eigenschappen en neurale cultivering op diamant worden nauwkeurig onderzocht in dit hoofdstuk.

De thesis wordt besloten met een algemene conclusie en vooruitzichten.

Een deel van experimenten werden uitgevoerd in het kader van het Europese MERIDIAN project.

Summary

The main goal of this thesis is to study how diamond films advance the construction of the hybrid biological-solid state interfaces and to construct Micro-Electrode Arrays (MEAs) for neural recordings. First, a literature study was carried out to review diamond applications in biology for *in vitro* and *in vivo* and for Microelectrode arrays (MEAs). In order to develop diamond MEAs, nano crystalline diamond (NCD) and boron-doped nano crystalline diamond (BNCD) were synthetized on fused silica substrates, featuring the insulating and conductive properties, respectively. These diamond films were employed for construction of neuron-device interfaces. The fabrication of the electrode arrays was achieved by performing different microfabrication techniques such as photo lithography, metal deposition and wet and dry etching. The resulting flat diamond MEAs on fused silica were characterized by different techniques. Finally, cortical brain slices from rats were used to evaluate the neural signal measurements on the diamond MEA.

The next goal was to construct flexible diamond MEAs as implantable electrodes. These flexible diamond electrodes were to function as Electromyography (EMG) for experiments *in vivo*. To provide mechanical flexibility, polyimide as a biocompatible polymer was employed, which featured also interesting chemical and physical properties. The NCD served as the insulating part and BNCD was integrated as the conductive electrode material. The polyimide preformed as the second insulating layer. However, the first series of NCD-BNCD-polyimide electrodes showed mechanical problems. Therefore, the fabrication plan was carefully investigated, adapted and finally a new plan was introduced, to improve and advance the electrodes. The final successful flexible diamond-polyimide MEAs consisted of BNCD-polyimide with gold interlayers. The electrodes were carefully characterized in every step by different techniques.

In the path towards developing the neuron-machine interface, a new method was explored and introduced, using Polyethyleneimine (PEI) monolayers. This precise coating method was developed and applied to treat the surface of diamond to enable the neuron growth from primary neural cultures. The PEI monolayer on diamond surface plays a key role as a neural adhesion promoter, to yield a high density of neurons on the surface. This cationic monolayer

polymer which was coated on diamond surface, also demonstrated notably interesting electrochemical properties which was characterized thoroughly. It was shown that the formed monolayer of PEI on diamond surface is extremely adherent and resistant. The PEI monolayer has the benefit of non-toxicity and provides better performance for construction of brain-machine interfaces than thicker PEI layers.

List of abbreviations

Abbreviations

ACSF	Artificial Cerebrospinal Fluid
AFM	Atomic Force Microscopy
BDD	Boron Doped Diamond
BNCD	Boron Doped Nano-Crystalline Diamond
BSCD	Boron-doped Single Crystalline Diamond
CAM	Cell Adhesion Molecule
CMOS	Complementary Metal Oxide Semiconductor
CNS	Central Nervous System
CNT	Carbon Nano Tube
CPE	Constant Phase Element
CTE	Coefficient of Thermal Expansion
CV	Cyclic Voltammetry
CVD	Chemical Vapour Deposition
DI	deionized
DIV	Days *in Vitro*
DLS	Dynamic Light Scattering
DMEM	Dulbecco Modified Eagle's Medium
EBL	Electron Beam Lithography
ECM	Extra Cellular Matrix
EDX	Energy Dispersive X-ray spectroscopy
EEG	Electroencephalography
EIS	Electro Impedance Spectroscopy
EMG	Electromyography
eV	Electron Volt
FBS	Fetal Bovine Serum

fEPSP	Field Excitatory Post Synaptic Potential
FET	Field Effect Transistor
fMRI	Functional Magnetic Resonance Imaging
HBSS	Hanks Balanced Salt Solution
IC	Integrated Circuit
MEA	Micro-Electrode Array
MEM	Minimal Essential Medium
MWPECVD	Micro Wave Plasma Enhanced Chemical Vapour Deposition
NCD	Nano-Crystalline Diamond
PBS	Phosphate Buffer Saline
PCB	Printed Circuit Board
PNS	Peripheral Nervous System
RF	Radio Frequency
RIE	Reactive Ion Etching
rpm	Revolutions per Minute
SEM	Scanning Electron Microscopy
Sccm	Standard Cubic Centimetre per Minute
SWNT	Single Wall Nano Tube
UNCD	Ultra-Nano Crystalline Diamond
UV	Ultra Violet
XPS	X-ray Photoelectron Spectroscopy

Chemical Elements and Compounds

Ag	Silver
AgCl	Silver Chloride
AlN	Aluminium Nitride
Ar	Argon
Au	Gold

CaCl$_2$	Calcium Chloride
CH$_4$	Methane
COOH	Carboxyl group
Cr	Chromium
EtOH	Ethanol
HF	Hydrofluoric Acid
HNO$_3$	Nitric Acid
H$_2$SO$_4$	Sulfuric Acid
IrO	Iridium Oxide
ITO	Indium TiN Oxide
KCl	Potassium Chloride
MgCl$_2$	Magnesium Chloride
NaCl	Sodium Chloride
NaHCO$_3$	Sodium bicarbonate
NaH$_2$PO$_4$	Monosodium phosphate
NaOH	Sodium Hydroxide
OH	Hydroxyl group
PDL	Poly-D-Lysine
PDMS	Polydimethylsiloxane
PEI	Polyethyleneimine
PEIE	Polyethyleneimine Ethoxylated
PI	Polyimide
PLL	Poly-L-Lysine
Pt	Platinum
SDS	Sodium Dodecyl Sulphate
Si	Silicon
SiN	Silicon Nitride
SiO$_2$	Silicon dioxide

Ti	Titanium
TiN	Titanium Nitride
TMAH	Thetramethyleamoniumhydroxide
TMB	Trimethyl borane
W	Tungsten

Symbols and Constants

ω	Frequency
ε	Permittivity
ρ	Resistivity
Φ	Potential
μ	Micro
Ω	Ohm
C	Capacitance
E_f	Fermi level Energy
E_{vb}	Valance Band Energy
F	Farad
K	Boltzmann Constant
N	Number of Acceptors
T	Temperature
Z	Diffusion Impedance

List of figures

1   Introduction

The current research in neuro-electronics attempts mimicking human brain architecture by computer electronics (for example Human Brain Flagship EU Project). The similarity with the function of Central Nervous System (CNS) is that signals are processed centrally by electronics; the chips and Integrated Circuit (IC) devices and are transmitted through connections, similarly to axons in neural systems. However, the principle of the signal transmission is entirely different. In ICs the signals are carried by electrons whilst in nerve cells the signal transmission is ionic-based. Neurons are thus electrically excitable cells allowing the process of transmitting information through electrical and chemical signals. Neurons can connect in synapses to each other and form neural networks. The electrical signal is then transmitted in this network. To be able to monitor, read out and stimulate neural signals, an active bio-electronic device as an interface between the electronic device and the neural cells is needed. In this paradigm, devices called Micro-Electrode Arrays (MEAs) have been discovered and used as a tool for reading *in vitro* but also *in vivo* neural signals. Since the biological response can be influenced by the presence of the foreign material in biological environment, the choice of material for construction of MEAs is of importance and has to be carefully inspected. The MEA devices also bring new potential for medical therapies, such as curing neurological diseases like Alzheimer, Parkinson, retinal diseases, etc. However, to minimize any adverse biological reaction for MEAs with biological tissue, MEAs are to be adequately designed and constructed from fully biocompatible material.

Diamond, as a carbon-based material, seems to be an exceptional choice for interfacing cells to biological systems, holding many promises due to its excellent properties, such as biocompatibility, chemical inertness, wide electrochemical potential window (3.5 V), possibility for surface functionalization and long term stability allowing electrophysiological experiment studies. Recently, also luminescence properties of nano diamonds allowed cell tracking in cultures of living cells [1]–[3].

The functionality of the solid state- biological interfaces is the critical component of neuron–man made diamond devices. Based on the knowledge of the

properties of diamond surfaces, we developed two-dimensional diamond MEAs for neuron interfacing for *in vitro* cultures. Plasma-enhanced chemical vapour deposition (PECVD) technique was used to fabricate diamond thin films, in the form of either Nano Crystalline Diamond (NCD) or Boron-doped Nano Crystalline Diamond (BNCD). These materials have been further used to produce diamond MEAs. Boron doping from gas phase during diamond growth offers a unique possibility to alter conductivity of otherwise insulating diamond films and to make them electrically conductive. To achieve suitable functional properties of diamond MEAs, electrochemical properties of the electrodes were examined. Specifically, impedance spectroscopy measurements were carried out in biological environment to study performance of MEAs and used as a feedback for construction of MEAs. Further on, for the application as artificial interfaces to neural cells for central and peripheral nervous system, it is important that MEAs can adapt to the neural tissue, i.e. to be flexible. Therefore, we developed flexible diamond-polymer electrodes for *in vivo* experiments. Methods for fabrication of these flexible electrodes are explained. The flexible electrodes can be used not only for neural interfaces but also for neuromuscular interfaces which are intensively studied topic in neuro-prosthetic device field.

Along with fabrication of the diamond electrodes, we investigated the compatibility of the diamond surface modified with Polyethylenimine (PEI) coatings for culturing primary neural cells. We have developed a method to form monolayers of PEI on diamond, which strongly chemically bonded to diamond surface, as revealed by X-ray photoelectron spectroscopy (XPS). The electrochemical properties of PEI layer on diamond were studied by electrochemical impedance spectroscopy (EIS) measurements and the behaviour of the polymer monolayer on diamond was evaluated.

The organization of the thesis

This thesis is organized in the following chapters:

    1- Introduction

    2. State of the art of Brain-Machine interfaces: path towards MEAs.

In this chapter, we have reviewed the research activities on MEAs and on construction of the man-machine interfaces. Critical issues are highlighted regarding the use of diamond MEAs.

3. Application of diamond functional surface micro-electrode arrays for brain-slice neural analysis (including detailed MEA fabrication).

In this chapter, it is described how the MEAs are constructed from insulating and conductive diamond films. The MEAs are used for *in vitro* brain slice neural analysis.

4. Functional Diamond-Polyimide Electrodes for Electromyography (EMG) application (including detailed Fabrication of EMG MEAs).

In this chapter, we described how the flexible diamond microelectrode arrays were integrated with Polyimide. The electrodes are characterized and prepared for biological *in vivo* experiments.

5. Functional Bio-molecular Monolayers on Diamond using PEI: A novel paradigm for construction of Man-Machine Interface.

In this chapter, we explain the surface functionalization of diamond film with PEI monolayers that is studied experimentally. This surface functionalization allows better functional properties of diamond MEAs. Growth of neurons was demonstrated on PEI coated diamond MEAs.

The thesis is then followed by a general conclusion and outlook.

Parts of the experiments were executed under the framework of European project MERIDIAN.

2 State of the art of Brain-Machine interfaces: path towards MEAs

Studying and understanding how the human brain works, has always been an important issue for curious human being. This most complex biological object discovered ever in the universe, weights in human only less than 2 kg, but contains billions of nerve cells of different types that are responsible for receiving, processing and sending information throughout the whole body. This information is encoded in the form of electrochemical signals that generate our feelings, thoughts, moves and senses. Nerve cells are building blocks of the nervous system. They do not proliferate like other cells. They divide shortly after the birth, then only expand and form network. Nerve cells constantly make new connections throughout the network. However, from many of them, we only have once in our life. When we get older, they might die and never replace again. That is when some neurological diseases might appear such as Alzheimer, Parkinson, Retinal degradation, etc. To avoid neural diseases and keep neurons working properly, we need to understand how neurons connect, communicate and organize in networks. These issues require neural signal monitoring and measuring them in a safe way. To enable detecting certain type of neural signals or signals from certain type of neurons, we need to measure neural signals in human brain or in an animal/mammalian brain with a measurement device.

There are several possibilities for measuring neural signals *in vivo* or *in vitro*; *in vivo* method is used for studying neural signals directly in animal models or in human, though this technique is invasive and it brings certain risks that is caused by insertion. Nevertheless, in some cases, we can gain sufficient amount of information by studying neural signal in networks in *in vitro* cultures. *In vitro* method studies the neural network outside of the body in the culture. One of the methods in this regime is patch clamp technique (Figure 2-1). Patch clamp allows the single cell studies as well as the measurements of the current coming from single or multiple ion channels in the cells. In this technique, a micropipette, as a patch pipette, penetrates into a cell membrane as it is used

for intracellular recording, together with a reference electrode. Here, different approaches can be used; for example, voltage clamp and current clamp. In the former, the voltage keeps constant and the changes of the current in the membrane ion channels are measured, and in the latter, current is kept constant and voltage changes are measured. However, this method is intracellular and invasive.
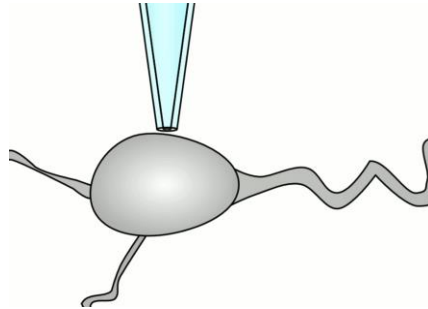
Figure 2-1. Schematic of the patch clamp micropipette approaching to the cell.

Another method is Microelectrode Arrays (MEAs) technique. MEAs are arrays of micro-sized electrodes, which are arranged along each other to measure neural signals. They are actually considered as neural interfaces that can connect the neurons to the devices. MEAs are divided in two subcategories: *in vivo* and *in vitro*. *In vivo* MEAs are implantable electrodes which can be tested in animal models and used in animals and humans, invasively. They have the advantage for studying the neurons in their biological environment. For studying the nerve cells outside of their biological environment, *in vitro* MEAs have been invented. As an extracellular and non-invasive technique, comparing with the patch-clamp, these MEAs can monitor, record or stimulate the neurons by means of the multiple electrode sites.

Microelectrode arrays have a history of less than 50 years. The first planar MEA was made in 1972 with gold and platinum as described in a review article in 2006 [4]. Two arrays of 15 electrodes were used to measure dissociated and cultured Myocytes from embryonic chicks onto the MEAs. Only in 1982, spontaneous electrophysiological activity of dissociated spinal cord neuron cultures was observed [4]. Since then, extensive research has been conducted

for material and methods development of custom and commercial MEAs as well as software development to control the devices. Several companies such as Multi Channel System (Germany) (Figure 2-2), Panasonic (Japan), Plexon (USA) and Ayanda (Switzerland), began the fabrication of commercial substrate-based MEAs. By development of CMOS technology, the transducers were also manufactured using Integrated Circuits (ICs). Max Plank Institute (Germany) introduced new Field Effect Transistor (FET) transducers [5]. Although this new technology made it possible to have single cell measurements, extra noises introduced in the system needed to be considered as well. That was a reason the type of the material (metals) used for the fabrication of the MEA needed to be chosen carefully as they could induce bio-toxicity and extra thermal noise.
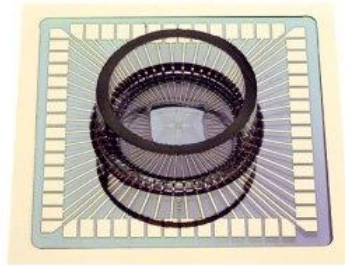
Figure 2-2. Standard titanium MEA from Multichannel Systems GmbH.

Besides this research, there have been several studies on in-cell recording of cells combined with patch clamping. Silicon nano wires coated with titanium and gold were used to control the membrane's potential, stimulation and recording of rat cortical cells [6]. Similarly, mushroom-shaped gold spine electrodes were fabricated to stimulate and record in cell extra-cellularly [7]. However, since the field of substrate-based MEAs remained important, from the same group in 2009, a combination of gold spine electrodes with titanium/gold/titanium nitride MEAs (from Multi-Channel Systems, Reutlingen, Germany) was used to measure from neuron cultures of the abdominal Ganglia of Aplysia californica [8].

As planar MEAs can provide important advantages such as long-term measurements, which is not possible with patch clamping, research on thin film have attracted a significant attention. With the progress in the material

technology, many research laboratories began to self-design and fabricate substrate-based MEAs for their specific research projects.

The efforts for understanding the neural networks and the complexity of the circuitry associated with it using thin film technology in research laboratories goes back by decades. In 1977, single unit activities of Snail helix pomatia were recorded using gold multi electrodes on Indium TiN Oxide (ITO) arrays which were insulated by a polymer [9]. In 1985, gold and ITO array of 50 microelectrodes were fabricated for signal recording of mouse spinal tissue cultures and the signal to noise ratio was shown satisfactory [10]. Few years later, a Japanese group fabricated MEA on glass plates [11]. 64 arrays were made of ITO, insulated by polyimide and the electrodes and connecting pads were covered by gold and nickel. Field Excitatory Post Synaptic Potentials (fEPSP) (the postsynaptic potential that makes the post synaptic neuron to fire an action potential) of Rat's hippocampal brain slice were recorded after stimulation and the stability of the signal was reported. While laboratory researches were going on, in a study in 2004, one of the commercially made MEAs from Multi-Channel Systems (Germany) has been used [12]. 30μm diameter titanium nitrides electrodes with 200μm spacing were insulated by Silicon Nitride. Surface of the MEA was treated with Polyethyleneimine (PEI) and Laminin. The type of the responses of NeoCortex cells after stimulations and the latencies was then studied.

In 2006, electrodes of gold and platinum on ITO arrays were designed and fabricated. They were insulated by Silicon Nitride and used for field potential measurements of Rat's hippocampal tissue [13]. A specific design for these electrodes was used to optimize stimulation pulse injection and the responses recording. Later on in 2011, PEI photo patterning was applied on ITO surface to define electrodes and study Rat's cortical neuron cultures [14]. The shape and alignment of these electrodes was designed to show that cortical neurons seeded on the photo-pattern treated ITO substrate had a homogeneous distribution and maintained their growth for several days *in vitro*.

2.1 Critical issues

As shown in the literature, MEAs have been produced of different materials and in different designs and configurations. As certain cultured neurons can only be studied by the MEA, this device requires specific properties to match the conditions of neural culture for signal measurements. One of these properties is the type of the materials in MEA. Several factors need to be taken care of, when choosing the materials to fabricate the electrodes. The biocompatibility comes to the first place. Biocompatibility of the materials in the MEA is their ability to be in contact with the biological environment, showing a proper host response without causing an adverse effect. There are not many conductive and insulating materials owning this property. The other important factors are the electrical conductivity or the impedance associated with the electrode material as well as insulating properties of the insulating material. The corrosion resistance of the electrode material has to be sufficient to avoid degradation in long-term electrophysiological measurements.

Another critical property of the MEA is the surface condition of the device. That demands the 'preparation' of the MEA surface for neural culture, which is a non-trivial topic. Nerve cells are very susceptible-to-the-environment cell types; and yet, cell culture is a complex environment in which cells grow in a controlled condition. For the cells to be adherent to an artificial surface, a highly biocompatible surface coated with Extra Cellular Matrix (ECM) components is needed to enhance the adhesion properties. It is already known that cells do not normally adhere directly to the surface, but rather bind to these specific attachment proteins that are adsorbed to the surface [15], [16]. The same corresponds for neural cells. However, since neurons are electrically excitable nerve cells, the ionic/electrochemical interface between neurons and the device seems to have overall a yet more critical role. Such interface, i.e. the nature of the connection between the cells and the MEA, has to be highly biocompatible as discussed. It has to allow transferring bi-directional neural signals with high fidelity and high signal to noise ratio. Additionally, external detection of these signals is required with high spatial resolution for extended periods of time [17].

When using MEAs as extra cellular and non-invasive techniques, the interface between the cells and the device comes to play a significant role. The cell or neuron's body and the MEA substrate form a cleft (a gap). The 'adhesion' between the neuron's membrane and the substrate is made electrostatically or chemically [17]. The neurons on the MEA are cultured in a growth medium, which is a liquid that is made and used to support the cell growth. It can contain different biological compositions such as amino acids, vitamins, glucose, salts, etc., according to different types of cells. In such environment, the cleft between the neuron and the MEA surface can be formed by an ionic- containing liquid solution. Efforts have been made to estimate the width of the cleft. It is shown that the cleft ranges up to 150nm [18]. It creates a resistance called 'Seal Resistance'. In order to measure neural activities with flat MEAs, it is an advantage to have a high seal resistance and consequently a high signal to noise ratio. Therefore, selecting the right material for planar MEA fabrication is critical and has a great impact on the interface between the cell and the device.

Having discussed about metallic electrodes, there are requirements that have to be satisfied. In fact, transducing electrical current (from the device) into the ionic current (from the neurons) and the opposite happens at the interface of the device and the tissue. The electrical charge is transferred by charge transfer phenomenon [19]. In the undesirable case of irreversible current injection, the release of the electrode material might result [19]. Such situation must be avoided, otherwise due to the local changes in the pH and changes in the material, it might lead to production of metal ions and cause damages to the tissue.

Ideally, for electrical stimulation, the electrode should have a large charge storage and large charge delivery capacity in order to deliver a sufficient amount of charge (within a 'relatively' small area).

For ideal neural signal measurements, a high resistance seal is necessary at the device and cell membrane interface. This high resistance provides stability for the measurements. It can as well insulate the signal from different types of noises such as thermal noise or noise from the device. Also the noise caused by the cleft, which is usually made between the elements that terminate the

surface of the device, and the proteins on the cell's membrane, can have a direct effect on the electrochemical recordings.

As discussed above, different materials have been employed for MEA fabrication and their biocompatibility and electrochemical properties are studied. The necessity of presenting new materials is to introduce 'the perfect' platform for neural cultures and neural signal measurements, and overcome the shortcomings that is unavoidable in case of the present materials.

2.2 Artificial diamond for neuro-electronics- state of the art

Developing a stable long lasting neuron-solid state interface is a key issue in man-machine interface science. The progress in material technology has allowed developing novel carbon-based materials [20], that might be suitable for such applications. Most of carbon-based materials show interesting bio-applicable properties. Therefore, an aim of this study was to develop diamond thin film as a new material for constructing man-machine interfaces and to benefit from its biocompatibility.

Carbon-based materials, including diamond, have emerged recently as a novel material exemplifying specific interests as an improved substrate for cell biology [21]–[26]. In addition, excellent mechanical and chemical stability [27], combined with biocompatibility and ability for surface functionalization [28], [29] exemplifies the possibilities of the neural interfacing surface.

Throughout this thesis, several forms of diamond are used or discussed. These forms include: single crystalline diamond, poly crystalline diamond, ultra-nano crystalline diamond, nano crystalline diamond (un-doped diamond), (Boron)-doped nano crystalline diamond and finally nano diamond particles. Although they are all certain forms of diamond, different techniques and tools are employed to produce these materials and yet, they represent different characteristics.

Prior to discussing the neuro-electronics applications of diamond, the details of these materials and their preparation methods are introduced.

Among several allotropes of carbon, crystalline diamond contains carbon atoms which are arranged in a variation of the face-centred cubic crystal structure called the diamond lattice (Figure 2-3).
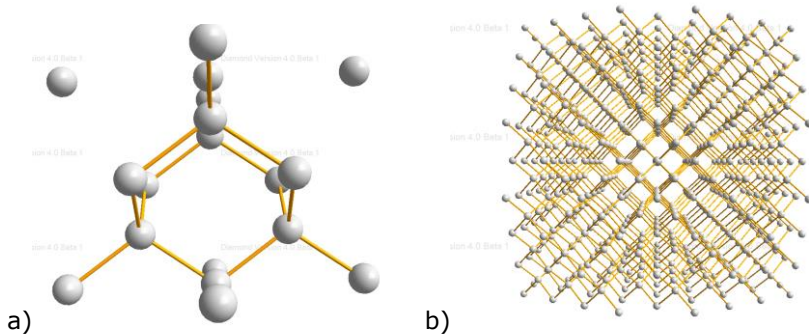
Figure 2-3. a) A diamond unit cell. b) A lattice of several unit cells

The diamond's excellent mechanical, physical, chemical and biological properties can be exploited by using a synthetic diamond produced by high pressure- high temperature (HPHT), and later on by Chemical Vapour Deposition (CVD) technique. This has made the opportunity to grow diamond in the form of a thin film on foreign substrates. CVD is used to deposit materials in different forms such as crystalline or amorphous on substrates. There are two sub-groups of CVD used for diamond growth: Hot filament assisted CVD and plasma assisted CVD. In the present project, plasma assisted CVD is employed to grow nano crystalline diamond on silicon or fused silica substrates. In this technique, the plasma activates the gas mixture of hydrogen and a simple carbon-based gas such as methane as precursor gas thermally, to enhance the chemical reactions between the atomic hydrogen and hydrocarbons from methane. Afterwards, the hydrocarbon radicals react to the surface of already containing diamond seeds, and initiate the diamond growth.

The growth on diamond or non-diamond substrate points the difference in the definition of single crystalline epitaxial diamond and poly-crystalline diamond.

- **Single crystalline diamond**

Single crystalline diamond can be made by HPHT and CVD techniques. To initiate the growth, there is always a necessity to employ diamond crystals as seed substrates. The CVD growth occurs in a chamber at ~600-1000°C. In the present work, the epitaxial layers on single crystal diamonds were grown in an ASTeX PDS-17 diamond reactor (Figure 2-4) using microwave plasma enhanced chemical vapour deposition (MPECVD) technique.
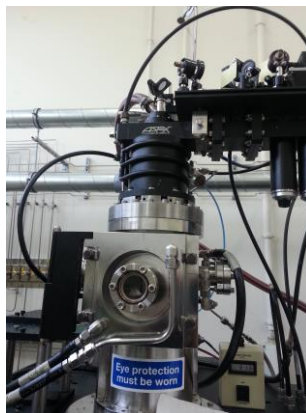
Figure 2-4. Diamond reactor ASTeX PDS-17.

- **Poly crystalline diamond**.

The CVD technique has made the opportunity to grow diamond also on non-diamond substrates, such as silicon. The diamond film grown on such foreign substrate is generally named Poly crystalline diamond (see Figure 2-5). In fact the poly crystalline feature of silicon substrate results in the poly crystallinity of diamond film, which means diamond crystals with different growth facets or grains [30]. The substrate must always be seeded by nano diamonds prior to the growth. The thickness of the layer vary from few tens of nanometres to microns.
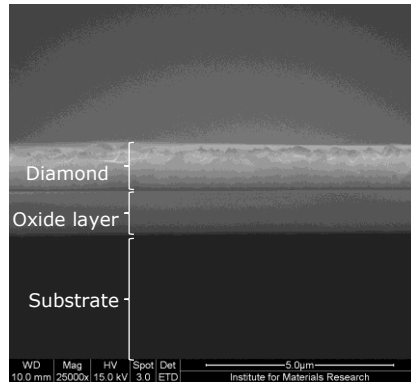
Figure 2-5. A cross-section SEM image of poly crystalline diamond grown on silicon substrate with thermal oxide layer.

- **Ultra-nano crystalline diamond (UNCD)**

Poly crystalline diamond is classified in different sub-groups, of which one is referred to as Ultra-nano crystalline diamond (UNCD). UNCD can be grown mainly with MPECVD technique. It is a form of diamond with 2-5 nm grain size and a smooth surface with 10-20nm RMS [31]. These interesting properties of UNCD and the ability to surface modification makes it possible to be used in electronic or biomedical devices such as Bio-microelectromechanical systems (BioMEMs).

- **Nano crystalline diamond (NCD)**

When the grain sizes of the diamond increases to few tens of nanometres, the resulting film is called Nano crystalline diamond (NCD) (Figure 2-6). NCD can be grown by Hot-Filament CVD (HF-CVD) or MPECVD process at temperatures of about 500–900°C, in a mixture of methane and hydrogen as feed gas, on large area substrates. The grain sizes differ according to the thickness of the grown film. Nano crystalline diamond offers the possibility of surface functionalization with surface treatment by hydrogen, oxygen, etc. This provides the opportunity to prepare different surface functionality such as wettability or hydrophilicity.
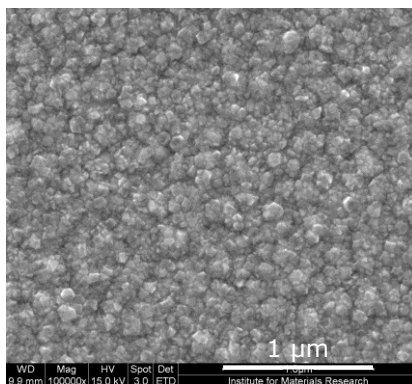
Figure 2-6. SEM image of a NCD film.

- **Boron-doped nano crystalline diamond**

(BNCD) can be grown in the same way as described for NCD films. Boron doping is introduced from gas phase during diamond growth as boron has been widely used as the dopant for producing conductive diamond. It offers a unique possibility to alter conductivity of otherwise insulating diamond films to make electrically conductive ones. BNCD can therefore be used for fabrication of various electronic and biomedical devices that are based on electrical conduction. All NCD and BNCD layers used in the experiments in this thesis are grown in ASTeX 6550 series diamond reactors.
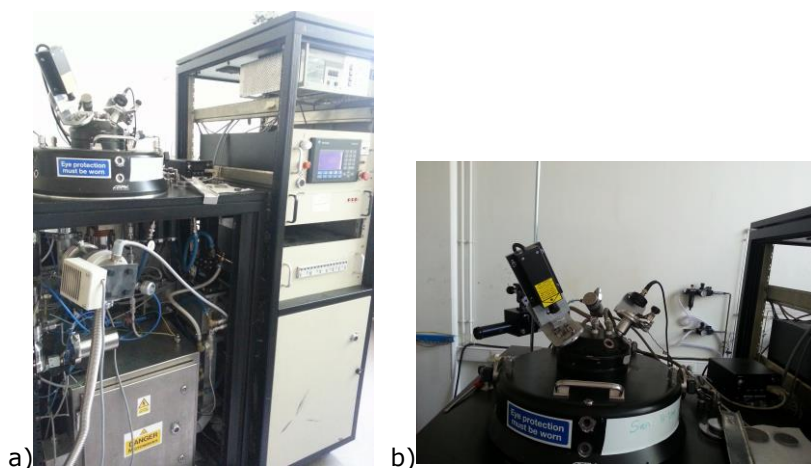
Figure 2-7. a) ASTeX 6550 series diamond reactor. b) The growth chamber.

- **Nano diamond particle**

Another diamond form discussed in this thesis is nano diamond particle. The nano diamond particles can be purified from the soot produced by detonating an oxygen deficient TNT/Hexogen composition. The resulting soot contains diamond crystals of 2-5nm in size. One of the most common applications of detonation nano diamonds is seed for CVD growth diamond. All the substrates that are used for CVD diamond growth can be treated by nano diamond particle or diamond powder as seeding material to introduce the nano crystalline property on the surface [32]. Nano diamond particles can be employed for biomolecule delivery in the cell lines as they have shown biocompatibility.

2.3 The Use of carbon materials in biological experiments and for construction of MEAs

Different forms of carbon-based materials have been employed for biological experiments. For example UNCD films and nano diamond particles have been used to cultivate neural cells. Functionalized UNCD has shown to be biocompatible and a desirable substrate for attachment of neurons and stem cells [33], [34]. Nano diamond particles have been employed for biomolecule delivery in the cell lines. Biocompatibility and the ability of diamond nano particles for biomolecule delivery has been also discussed [35]–[38]. Nano diamond coated surfaces were also found to be suitable surface for cell cultures [32], [39].

Electrode design for successful interfacing, either for stimulation or recording, requires good understanding of membrane phenomena, action potential generation, and the electrode behaviour. Looking to the literature, several research groups have aimed to prepare diamond based electrodes to measure neural activities. In 2006, a group in Ohio fabricated boron doped diamond probe to measure extracellular activity of Aplysia Californica as well as sensing serotonin [40]. This work continued by making implantable electrodes for *in vivo* application.

Different cell types have been used with diamond electrodes as well. For example diamond-based biosensors were fabricated, using conductive hydrogen terminated diamond single crystal, to measure spontaneous action potentials of mouse GT1-7 cells [41]. However, the active conductive area was relatively large; $\sim 1mm^2$. To reduce interference from neighbouring cells, smaller sized electrodes can be used to improve the spatial specificity. Also the extended temporal neuronal access is possible through extracellular arrays, without cellular damage that is caused by intracellular electrodes [7]. In 2012, diamond as transistor arrays has been fabricated, characterized and used for cardiomyocyte-like HL-1 cells' action potential measurements [42], [43]. One year after, in parallel with our work, two designs of electrode arrays were fabricated with BNCD and insulated by Si_3N_4. Spontaneous signals of an embryonic mouse hindbrain-spinal cord and *ex vivo* retina of a rat were extracellular measured [44]. Later on, the 64-channel BNCD electrode arrays were fabricated with several different passivation layers for comparison and were compared with gold electrodes [45]. These MEAs were used to monitor spontaneous cardiac action potentials of cardiomyocyte-like cell line HL-1. It was shown that on average BNCD electrodes could detect cardiac action potentials as well as gold electrodes.

Besides these studies, few other researches have shown the use of diamond micro electrodes *in vitro* for sensing norepinephrine (NE)-release from a laboratory test animal's mesenteric artery [46] or recording the overflow of 5-hydroxytryptamine (5-HT, serotonin) from enterochromaffin cells (EC) of the intenstinal mucosal layer [47], [48]. However, this material is insulating. BNCD as conductive diamond can be used as electrodes. The conductivity in diamond is promoted by the boron-doping. For the construction of B-doped neural devise, one has also to consider boron electrochemical properties. The electrochemical behaviour of BNCD has been discussed in several works [1], [27], [51]–[54]. BNCD exhibits a wide electrochemical potential window which makes it a perfect electrode material for MEA fabrication.

For use as an optically transparent electrode, lightly doped diamond shows a good optical transmission from 225 nm to the infrared. The transmission window is wider than that of ITO for example, another optically transparent electrode that is used [27].

In this thesis, diamond thin film surfaces are optimized to be used for fabrication of full diamond MEAs for *in vitro* analysis, in which only diamond coating is exposed to neurons. Instead of using a combination of BNCD Layer and insulating layer from another material, a new design for fabrication of diamond MEAs with NCD and BNCD is introduced and the fabrication methods are described in detail. The MEAs are further characterized. The diamond MEAs were used for acute neural signal measurements of rat's brain slices.

2.4 Diamond and diamond - polyimide MEAs

In the first experimental part of the thesis I have successfully prepared planar diamond MEAs for *in vitro* experiments and studying nerve cells, inside their biological environment. This has further motivated me to fabricate diamond implantable electrodes. It has also attracted my attention for using diamond films as implantable electrodes. Several experimental groups across the world have attempted to use diamond electrodes *in vivo,* or diamond as coating for implants [19], [40]. In neuro-electronics, a research group in Ohio published studies on neuro-dynamics properties of Aplysia Californica using Boron doped diamond coated probes and its fabrication processes [53], [54]. The electrode withstood the complex movements of an Aplysia californica for 9 days and there was no evidence of damage to the electrode. In a very recent study from an Australian group, *in vivo* biocompatibility of Nitrogen doped UNCD and Boron doped diamond was examined [55]. These diamond devices which were implanted for 4-15 weeks on the back muscle of Guinea pigs, showed minimum inflammatory response and fibrotic encapsulation comparing to medical grade silicone as control samples. All these results show that diamond implantable devices for various purposes perform promisingly. However, although implant material has to be biocompatible, any surgical insertion may cause inflammatory response as a physiological reaction to the inserted device. It is also therefore beneficial that the implantable devices are flexible. The implants may also result in damaging the tissue by degradation of the material or the device surface by biological environment.

Looking to the literature, flexibility of the implantable electrodes have been most commonly provided by different polymers such as Polyimide, Parylene, PDMS, SU8, etc. [56]. The use of Polyimide for metallic electrode implants has already been studied [57]. Later, the use of Polyimide for diamond electrode was reported in 2011. Implantable diamond electrodes were insulated with Polyimide and Parylene as retinal implants, which predicted no damages to the retinal tissue after 14 weeks *in vivo* in rat's retinal space [19]. Long-term stability of different types of Polyimide in PBS environment has been studied and showed no changes in chemical structure and physical properties after 20 months (at body temperature) with respect to the reference specimen [58].

In the present work, we fabricated diamond – polyimide flexible electrodes for Electromyography (EMG) application, by fully integrating diamond electrodes with polyimide. EMG electrodes can reveal a nerve or muscle dis-function, and be used to stimulate neural signal that are used for control of the muscle for neuro-prosthetics. The long term goal of such research is to monitor or record the electrical activity produced by skeletal muscles. The EMG MEAs were designed and manufactured in a way that it could be inserted directly in muscles to be tested in animal models.

In our design, polyimide was chosen as the flexible/insulating part of the implantable EMG electrodes, for its mechanical strength, insulating properties, and superior chemical resistance [56] and of course the availability of the process facilities in the lab. We have developed the full fabrication steps for our unique design in which BNCD was used as active areas of the electrodes and the conductive connections. The conductive parts were sandwiched between two polyimide layers. The final electrodes were characterized and prepared for the biological *in vivo* experiments.

2.5 Issues with the growth of neurons on diamond surface

It is claimed in the literature that the diamond surface can serve as an ideal platform for neural cell cultures, without any preparation and pre-treatment by

appropriate adhesion molecules [39] ,[59]. Some studies show that neurons were successfully cultured on oxygen terminated, hydrogen terminated, NH_2-terminated or UV treated bare diamond surfaces [33], [59]. However, the culturing period is often not mentioned or it is very short; i.e. shorter than seven days *in vitro* (7-DIV), which is not long enough to observe and confirm the maturity of neurons. As we were interested to prove the fascinating ability of diamond for neural cultures, we performed cortical neuron culturing on as-grown, O_2 terminated and H_2 terminated NCD surfaces. The cultures, however, unfortunately did not survive long. After several trials, we diagnosed that untreated diamond surfaces do not show to be ideal for neuron culture. Similar finding were found in another work from our group [60]. We have found out that neural cells are extremely dependent to the surface termination of diamond. Only some cases led to successful neuron growth, when neuron cultures were cultivated on diamond that was pre-treated by certain approaches before cell seeding. Different cell adhesive layers on diamond surface were applied to improve cell adhesion [61] as well as neural outgrowth [62], [63]. Coating with Extra Cellular Matrix (ECM) molecular promoters for functionalizing NCD has similarly been an important step for making diamond a permissive substrate for neurons. Example adhesion promoters such as Laminin and Poly-D-Lysine (PDL) have been applied to encourage culturing primary neural cells allowing neurons on the surface to adhere and outgrow [15], [16], [62]. These adhesive proteins are fundamental for cell differentiation, adhesion and survival, and different chain combinations in these molecules offers binding to the cells. Without the presence of any adhesive promoter, the adhesion, outgrowth and survival of neurons were shown to be insecure and unreliable. However, some of such coatings were to be relatively thick [64], which might lead to limited stability for prolonged operation and change the electrochemical properties of the electrode significantly.

In an attempt to reveal the importance of molecular promoters and their effect on electrode functioning, we studied PEI coating on the diamond films as neuron adhesion promoter and investigated the neural cultures grown on PEI surfaces. However, as PEI is potentially toxic, we have developed procedures how to work safely with PEI in terms of preparing neural cultures.

2.6 PEI and challenges

PEI is a polymer constructed by repeating unit composed of the amine group and two *CH$_2$CH$_2$* spacers (Figure 2-8). Linear and branched types of PEI are produced and present different properties. Due to PEI's polycationic character, it is widely used for many applications.
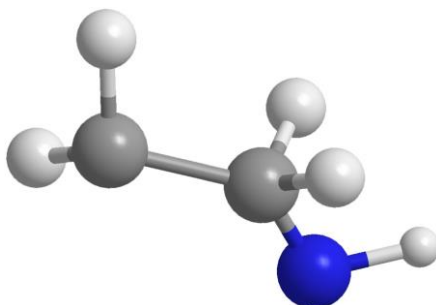
Figure 2-8. The unit cell of the linear PEI, containing two carbon atoms, one nitrogen and 5 hydrogen atoms.

Although PEI has been used vastly in the laboratories for surface preparation of neural cell seeding on other materials, little is known about the specific properties of this coating for the diamond films. When looking closely to the preparation procedure and the biological protocol that is meant for PEI coating on standard MEA surfaces, we found out that this protocol cannot be simply applied to diamond. In case of diamond surface, properties that influence the cell adhesion are not very well understood, specifically to which extend the PEI can remain on the diamond surface and how this might affect the toxicity and neural adhesion to surface or MEAs.

Following generally outlined protocol is used for PEI coating on MEAs in the biological laboratories:

Neural network preparation: MEA coating, cell seeding and maintenance

Before cell seeding, the MEAs are first cleaned by overnight treatment with Terg-A-Zyme proteolytic detergent solution (Sigma) at 1% w/v in bidistilled water followed by flushing for at least 4 times with fresh bidistilled water. After this,

the wet MEAs are autoclaved and next coated by overnight exposure to polyethylene-imine solution (PEI) with 1 ml at a concentration of 0.1 % w/v in sterile Milli-Q water. After this coating, the MEAs are rinsed 4 times with 1.5 ml sterile Milli-Q water and allowed to dry completely. The PEI-coating provides a positive surface charge that attracts the negatively charged cells. For cell-seeding on the MEAs, the cell concentration of the cell suspension is adjusted to 1.3 * 10e6 cells in 0.350 ml H-MEM medium. This volume is pipetted to the centre of the MEA, which is then left undisturbed in the cell-culture incubator for 60 min to allow sedimentation and adherence of the cells to the surface (electrodes and substrate). Once attached, 0.65 ml of medium at 37 ˚C is added slowly to the MEA dish to make it 1 ml. The MEA is then returned to the incubator and can be kept there stably up to several months (Baughman, 1986), while half the medium is replaced with fresh medium three times during the week. The incubator is set at 5 % CO_2, with saturated humidity at 37 ˚C and the MEAs are covered with a sterile MEA chamber cover with special Teflon polymer foil from Dupont that is permeable to gasses such as O_2 and CO_2 but not to water. This way protecting the cultures from contamination with the outside world and avoiding excessive evaporation of the culture medium is possible.

However, when applying the protocol to diamond surfaces, it turns out that the situation is much more complex. I realized that the mechanism and the know-how behind the surface washing of PEI and the resulting layer on the surface is not fully understood. Therefore, there was a motivation to discover the gaps in the technology, which could have been improved -from the material research point of view-, to advance the knowledge about PEI coating on diamond film.

PEI is indeed toxic; cytotoxicity of PEI with high volume or high molecular weight has already been established [35], [65]. As a result of this coating concept, some questions rise about using PEI for coating purposes:

- How biologists can use PEI as a coating for neuron growth if it is toxic?

- How to reduce this toxicity/cytotoxicity?

In an attempt to improve the biological protocol used for PEI coatings, I studied and prepared an optimized protocol in our material research lab, as discussed in the 5th chapter, hoping that the properties of PEI treatment on diamond surfaces can be revealed and it becomes more obvious and easy-to-apply for biologists but also physicists and material scientists.

By using a novel specific procedure, we were able to prepare functional PEI in the form of a 'monolayer' on diamond films that is strongly bound to the diamond surface and therefore not toxic. This protocol allows PEI monolayer coatings on diamond with high stability that can preserve the natural electrochemical properties of the original material. Therefore, the PEI monolayer coated diamonds were carefully characterized and electrochemical properties of this interface were investigated.

2.7   A brief introduction to electrochemistry for PEI analysis

Following is a brief description of the methods used for electrochemical experiments on PEI coated diamond surfaces; the principles of electrochemical impedance spectroscopy and cyclic voltammetry.

Electrochemical impedance spectroscopy (EIS) technique is an experimental method used to characterize the electrochemical systems. Using this technique, the dielectric and electric properties of elements can be investigated. This non-invasive technique measures the impedance response of the elements over a range of frequencies (ω) or time. Being surface sensitive, EIS is an important technique to characterize the modifications or treatments on the surface; specifically in this case, the diamond surface with PEI monolayer coating.

EIS is usually measured by applying an AC potential, E(t), to the electrochemical cell and measuring the current, I(t), through the cell. A model needs to be defined to analyse the contribution of the element of interest in each case.

The description impedance (Z) as follows:

$$Z(\omega) = \frac{E(t)}{I(t)} = \frac{E_0 \cos \omega t}{I_0 \cos(\omega t - \varphi)} ; \qquad\qquad (2\text{-}1)$$

$$Z = Z_{real} + iZ_{imaginary} \qquad\qquad (2\text{-}2)$$

where ω is the frequency, E(t) and I(t) are the voltage and the current at time t, and E_0 and I_0 are the voltage and current at time 0. To determine the impedance of a system, a voltage of small amplitude is applied and the response current is detected. From these two elements, the impedance Z of the system is calculated across a frequency range. The results of EIS measurements can be either presented in the form of Bode plot or Nyquist plot. The Bode plot describes the impedance versus frequency whereas a Nyquist plot shows the real part of the impedance against its imaginary part. By analysing the impedance, an equivalent circuit of the system can be found. This circuit consists of resistors, capacitors, inductors, or constant phase elements (CPE) of which each has a physical meaning.

The relationship between the capacitance and the voltage is established in the so-called Mott-Schottky plot. The Mott- Schottky plot allows us to experimentally determine the amount of band bending at the surface, as the theory is valid for the semiconductor- electrolyte junction. From the slope of the reversed square root of capacitance as the function of voltage, the donor density and the flat band potential at the surface of the examined material can be calculated. By using this technique, we could evaluate the electrochemical behaviour and the impact of the PEI coating on diamond.

Important electrochemical parameter is an electrochemical potential window. The electrochemical potential window of a material is the voltage range in which the substance is neither oxidized nor reduced. This range is important for evaluating the efficiency of the material as an electrode, because out of this potential range, the electrode materials gets electrolyzed, oxidized or reduced. By performing cyclic voltammetry (CV), one can determine the potential window of the material (see Figure 2-9). In principle, the potential of the material as the working electrode is ramped linearly by time. The current is plotted versus the applied voltage to give the CV trace. The cyclic voltammetry is used in our

experiments to evaluate the electrochemical potential window of diamond surfaces with and without PEI monolayer coatings.
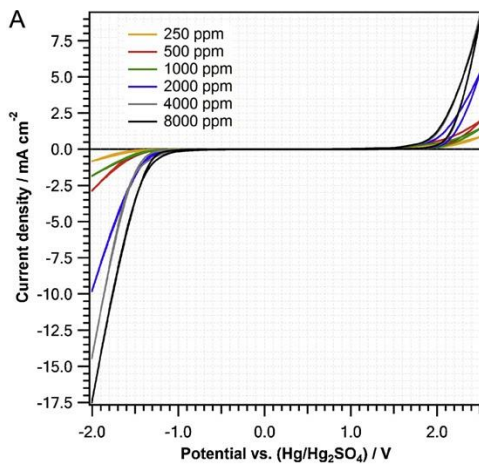
Figure 2-9. An example of cyclic voltammetry measurements on differently doped diamond surfaces[49].

3 Application of diamond functional surface micro-electrode arrays for brain-slice neural analysis

This Chapter is devoted to fabrication of diamond micro electrode arrays. It further deals with the techniques and methods used to engineer the MEA device, characterizing the electrodes and finally conducting biological experiments. Boron-doped Nano Crystalline Diamond is used as the conductive electrode material and Nano Crystalline Diamond is used as the insulating material. The surface termination of the diamond is investigated with regard to interaction with the cell medium which is used for cell cultures. The manufactured substrate-based diamond MEAs were used to measure the activity of Rat's cortical tissue slices. Along with the research, this work was submitted as an article to PSSA (Physica Status Solidi a):

Farnoosh Vahidpour, Lowry Curley, István Biró, Matthew McDonald, Dieter Croux, Paulius Pobedinskas, Ken Haenen, Michele Giugliano, Milos Nesládek; All-diamond functional surface micro-electrode arrays for brain-slice neural analysis

3.1 Abstract

Diamond-based microelectrode arrays were fabricated by using nano crystalline diamond as an insulating layer and conductive boron-doped for functional electrodes, in order to use them for analysis of brain slices. MEA surface is composed of only diamond exposed to the cells without presence of any metallic components on the surface of the MEAs. The impedance measurements showed negligible cross-talk between neighbouring diamond microelectrodes. Local field potentials related to neural signals were then successfully recorded from pharmacologically disinhibited rat cortical tissue slices, mechanically coupled on the surface of the MEA. The noise level of the diamond MEAs was found to be lower than that of commercial Pt-based MEAs, under identical measurement conditions.

3.2 Introduction

For over a decade, academic and industrial laboratories have worked on improving the technology for electrophysiological interfacing of neural tissue to substrate-integrated microelectrode arrays (MEAs). MEAs are devices which contain multiple areas or shanks through which neural signals are measured, recorded or transferred. They essentially serve as neural interfaces that connect the neurons to the electronic device. MEAs are nowadays employed both *in vivo* and *in vitro*, for example, for research of brain tissue or various neuro-pharmacological applications. The electrophysiological and imaging techniques allow the study of neuronal ion channels, synaptic plasticity, and functional differences in ion channel function within sub-regions of single cells [66]. For each of these specific purposes, the geometry, shape, and the material of the MEAs play critical roles. To date, MEAs are fabricated by employing a variety of conducting materials such as titanium nitride (TiN), iridium oxide (IrO), platinum (Pt), gold (Au), indium tin oxide (ITO), silicon (Si) and titanium (Ti) [7], [18], [69]–[73] as the electrode material. However, the electrode material stability is an important issue. In particular, upon electrical extracellular stimulation, the microelectrode and interface characteristic in the contact with the tissue can change, altering the MEA response [17], [18], [27], [72]. Most of the MEAs are formed by using different materials for electrodes and the insulating surfaces (such as Si_3N_4, SiO_2, polymers etc.), with distinctive characteristics for interaction with neural cells.

Artificial man-made CVD diamond is one of very interesting thin film materials for the MEA fabrication due to its biological inertness, chemical stability and availability of both highly insulating and highly conducting B-doped thin diamond films. It has been widely reported that NCD is biocompatible as deduced from both in *in vitro* [41], [45] and *in vivo* [19], [53] studies, exploring imaging, drug delivery, diagnostic or treatments contexts [48], [72]–[74]. Additionally diamond also exhibits reduced bio-fouling. Boron doped NCD (BNCD) is electrically conductive with a wide electrochemical potential window [49]. These properties make diamond an attractive platform for fabrication of active bio-electronic devices [27], [40], [42], [75]. Thus, one immediate application of

BNCD is MEAs for *in vitro* electrophysiological studies and pharmacological screening in neuroscience. The aim of this study is two – fold. We prepare MEAs in which the cells are exposed only to diamond surface, by using both metallically conductive as well as insulating diamond thin films for MEAs, providing thus homogenous surface for interaction with neural cultures. We study the interaction of both the conductive and isolating diamond surfaces with cellular environment and demonstrate the MEA functionality for using in the brain slices experiments.

3.3 Experimental methods

Substrate preparation. 49mm by 49mm fused silica substrates were employed for the fabrication of the MEAs. Fused silica has a relatively high melting point (~1700°C) and it is stable to high temperatures. Therefore, it can withstand the diamond growth processing at temperature of ~ 650°C. Another benefit of fused silica for constructing MEAs is its optical transparency, allowing optical imaging in transmission microscopy.

Before the diamond growth, fused silica substrates were cleaned according to the standard wafer cleaning procedure RCA-1 and RCA-2 [76]. To initiate diamond growth by microwave plasma enhanced CVD technique (MWPECVD), diamond nuclei have to be provided on the substrate surface. There are various approaches for such surface pre-treatment. One is submerging the substrate into a water based colloid of diamond nano particles, and the other is abrading the surface of the substrate using diamond powder [27]. In this study, we have applied the former approach [77]. A colloid of nano diamonds (NanoAmando®B from NanoCarbon Research Institute Ltd., Nagano, Japan) has been used. These detonation nano diamonds had the average diameter of ~5nm. The zeta potential of the particles was ~ 50 mV and the surface was predominantly graphitic with the traces of oxygen. The nano diamond colloid was ultra-sonicated prior to the seeding, to break up any large clusters of nano diamond particles to produce mono dispersion as confirmed by dynamic light scattering

(DLS). The cleaned fused silica substrates were immersed into this colloid for a minute. Then, the samples were spun with 4000 rpm for 40 seconds until dry, using a spin coater. The seeded substrates were flushed with Milli-Q water for the first 20 seconds to remove residual nano diamonds from the surface, leaving a nano diamond monolayer.

Detailed Fabrication steps of microelectrode arrays. To fabricate diamond MEAs, a fabrication plan was defined (Figure 3-1).
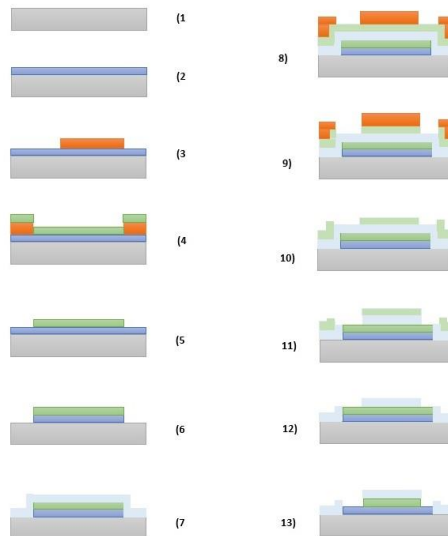
Figure 3-1. Schematic of complete plan steps for fabrication of diamond MEA**:** 1)Fused silica, 2) BNCD grown, 3)Photolithography, 4) Metal-1 deposition, 5)Lift off, 6)BNCD etching, 7)NCD grown, 8)Metal-2 deposition and Photolithography, 9)Metal-2 mask etching, 10)Photoresist acetone-cleaning, 11)NCD etching, 12)Metal-2 mask removal, 13)Metal-1 mask removal.

First, diamond layers were grown on the seeded substrates; 150nm thick films of BNCD (as the conductive layer) were grown in an ASTeX 6550 series using MW-PECVD technique. 375 sccm of H_2, 25 sccm (5%) Methane and 100 sccm (8000ppm) of Trimethyl borane (TMB) were used as gas mixture for the MW-PECVD growth. TMB was used in hydrogen mixture. 8000 ppm TMB formed the Boron concentration of about $3*10E 21$ cm^{-3}. The substrate temperature of 600°C was used for the diamond growth, selected to obtain relatively smooth

surface whilst keeping sufficiently high boron incorporation. The substrate temperature was controlled using a Williamson Pro 92-38 infrared pyrometer. These growth conditions were optimized to achieve a higher level of sp^3 [49], leading to a minimal sheet resistance (of about 500Ω/square) of the film grown under the conditions of 22 Torr pressure and 3500 Watt power for 90 minutes. Once the BNCD film growth was completed, the substrate went through the first photolithography step and metal deposition for patterning the BNCD. For that, the negative lift off photoresist NR9-3000PY (Futurrex Inc.) was spun on the BNCD film for 40 seconds with 3000 rpm. Then the photoresist was baked on the hotplate at 150°C for 1 minute. The surface was exposed to the UV light (Karl Suss MA55 mask aligner, i-line), using the photo mask shown in Figure 3-2. This photomask consisted of 56 circular contact areas at the centre of the mask with the diameter of 30μm and 200μm spacing. Each circle was connected to a 2mm by 2mm square at the edge of the design by means of a line. The widths of the lines changed from narrow to wide, reaching from the circles to the squares. However, these lines were designed to make sure that all electrodes have the same impedance and represent identical properties.
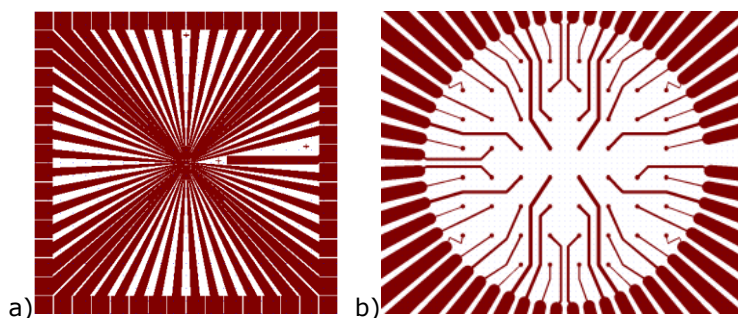
Figure 3-2. a) Design of the lithography mask for conductive areas. b) The zoomed center of the mask showing the circular channels.

After exposure, the process was followed by a post-exposure bake at 100°C on a hot plate for a minute and then the sample was developed in RD6 developer (Futurrex Inc.) for 17 seconds. The surface was then rinsed, dried and ready for metal deposition.

Following, a thin metal layer was deposited on the surface for negative lift-off lithographic processing. For this purpose, different metals were available such as chromium, aluminium, titanium or tungsten. However, because subsequently an un-doped diamond layer is grown on top of patterned metallic films, one has to be cautious in the metal selection to achieve optimal adhesion for diamond. In case chromium is selected, it is shown by experience that the adhesion of diamond to it is not sufficient. Aluminium on the other hand, has a low melting point in the high temperature and the pressure required for (following) diamond growth. Titanium makes good adhesion with diamond, but it is not suitable for the final etching step, including removing the metal on the BNCD electrode. When Ti is used, the HF is required for etching. HF solution can however, attack to the fused silica substrate as well. To avoid these risks, tungsten is chosen to mask the BNCD. It is shown by experience that tungsten exhibits a good adhesion to diamond, it can also resist the following diamond growth process, and the final etching step (by H_2O_2, 30%) is not harmful for the electrodes. Tungsten has a relatively low resistivity: $10^{-6}\Omega cm$ (compared to $\sim 10^{-2}\Omega cm$ for BNCD). Low resistive tungsten thin metallic layer can be used for enhancing the conductivity of the tracks transporting the electrical signal from the electrodes to the collecting pads, if deposited on BNCD and insulated by NCD layer. In fact, this metal layer is sandwiched between the BNCD and NCD layers. Our experiences indicate that tungsten (also a carbide former) adheres well to the diamond film and at the same time only ~ 50 nm of this film is sufficient to achieve good masking. Tungsten was deposited in an in house RF magnetron sputtering system using a tungsten target, 50 sccm of Argon and 100 Watt power under working pressure of few mTorr (Figure 3-4,a). The deposition conditions for W has been then optimized to achieve a stress-free and flatter film. After the W-film deposition, an acetone-assisted lift off of the metal was carried out to define the conductive microelectrodes (where cells are later exposed to BNCD surface for recording or stimulation), conductive tracks and the connection pads, see (Figure 3-2, Figure 3-3).
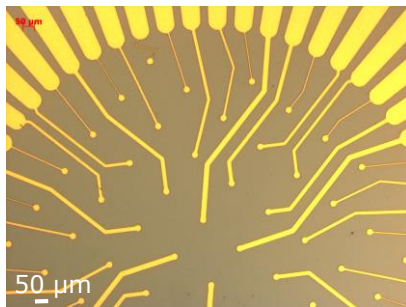
Figure 3-3. Tungsten mask on the BNCD surface.

The BNCD film with the mask was exposed to reactive ion etching (RIE) (Figure 3-4,b) using O_2 plasma under the conditions of 300 Watt, 30 sccm O_2 and a working pressure of few mTorr to etch the BNCD layer outside the intended electrode area. The oxygen etching was done in the same in house RF magnetron sputtering system. Checking under Scanning Electron Microscopy (SEM) and Energy-dispersive X-ray spectroscopy (EDX), the BNCD layer was etched in less than 10 minutes. One issue at this step is that by oxygen etching the BNCD with the metal mask, the top surface of the metal might probably form Oxide layer. This thin insulating layer can be destructive for some experiment, but for this experiment it is acceptable because the W film is thick enough to conduct the neural signals.
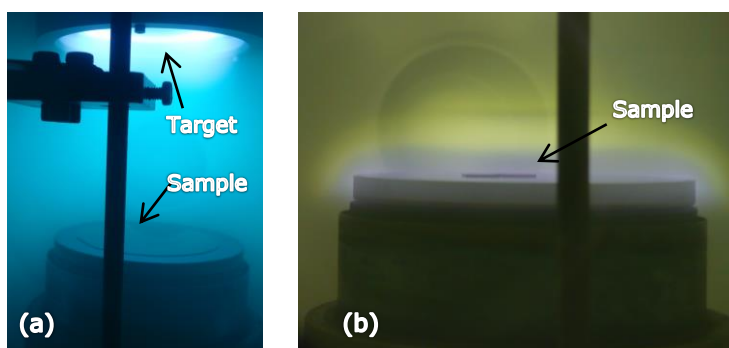
Figure 3-4. a) Argon plasma used for metal deposition. b) Oxygen plasma used for RIE etching of diamond

Next, a ~ 120nm NCD film was grown to form an insulating layer on the MEA structure as a protecting insulator for the BNCD microelectrode (Figure 3-5). For

the first series of the electrodes, the tungsten layer was kept on the BNCD surface and used later on as an etch-stop layer to protect the BNCD in diamond etching steps. The growth conditions for the NCD film were 495 sccm of H_2, 5 sccm (1%) of methane and 4000 Watt power at a gas pressure of 20 Torr. NCD layer was grown in a temperature between 650 to 700 °C. The growth conditions for NCD layer had to be optimized very carefully, because the NCD film had peeled off in several trials. The reason could be that the total diamond layer thickness on the Fused Silica exceeded 150-200nm. The thermal expansion coefficients of diamond and Fused Silica are not similar, that is why only thin diamond layers (<~200nm) can be grown on FS without a problem.
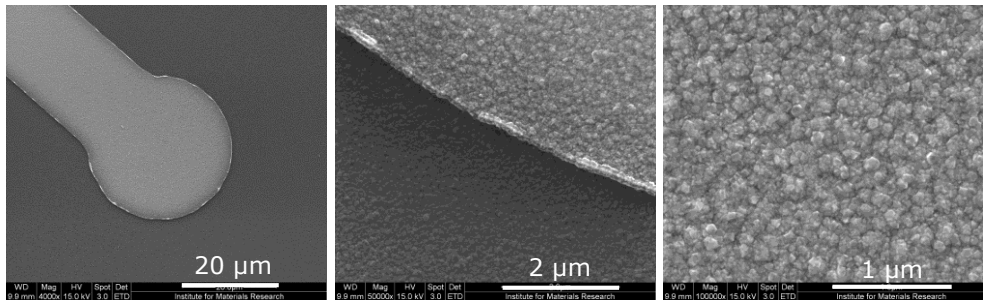
Figure 3-5. NCD film was grown on the patterned BNCD masked with W. The SEM images show the diamond structure on the electrodes.

After NCD growth, another step of photolithography and metal mask (chromium) deposition was applied using the second photolithographic mask (Figure 3-6) to mask the insulating areas, subsequently remove the NCD on microelectrodes and to open NCD by RIE down to BNCD. For that, since the patterning areas were only 20µm circles, there was a possibility to use Electron Beam Lithography (EBL) technique on the centre of the sample. However, the desirable positive lift off photoresist for this purpose was not available at that moment. Therefore, a step of metal deposition and photolithography was preceded. The chromium layer was deposited by applying Argon plasma and a chromium target. 100 Watt of power and 50 sccm Ar was used under the working pressure of few mTorr to coat the NCD surface. Then the photolithography was executed using negative photoresist NR7-1000Y (Futurrex

Inc.) with the same procedure as previously described for tungsten deposition. The "insulating" photomask shown in Figure 3-6 was used for the UV exposure with the mask aligner. This mask consisted of 56 circles at the centre of the mask with the diameter of 20µm and 200nm spacing. These circles were smaller than the circles on the conductive mask in order to avoid a gap between the edges of the BNCD conductive areas and insulating layer. All the square connecting pads were also covered.

a)   b)
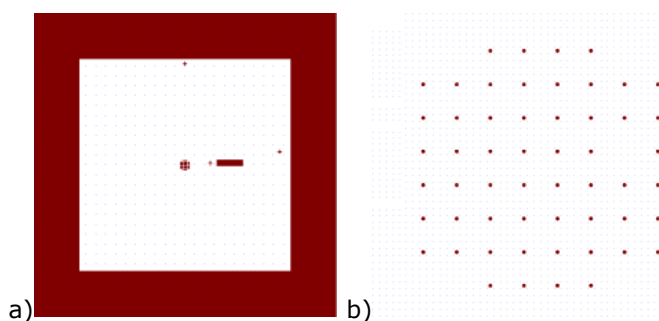
Figure 3-6. a) Design of the Lithography mask for NCD (insulating) areas. b) The zoomed centre of the mask showing channels with 20µm diameter and 200µm spacing.

After the photolithography, the areas shown in Figure 3-6 were open to the lower Cr layer and the rest was covered by photoresist. Therefore, the exposed Cr was chemically etched down to NCD layer, using the standard chromium etchant solution (Sigma Aldrich-Belgium). To make sure that the Cr is etched completely, the samples were measured with EDX to see the components on the surface. Then the photoresist was removed in Acetone. However, in the first few trials, the photoresist was not removed completely and some residues were left around the structure (Figure 3-7). It seems that once the surface with the photoresist was measured under the electron beam, the photoresist structure changed somehow that was not anymore removable by Acetone and other resist removers. Hot Acetone together with ultra-sonication, as well as warm resist remover RR41 (Futurrex Inc.) were tried, but couldn't completely dissolve the photoresist. Oxygen etching, though, helped to remove the contamination slightly.
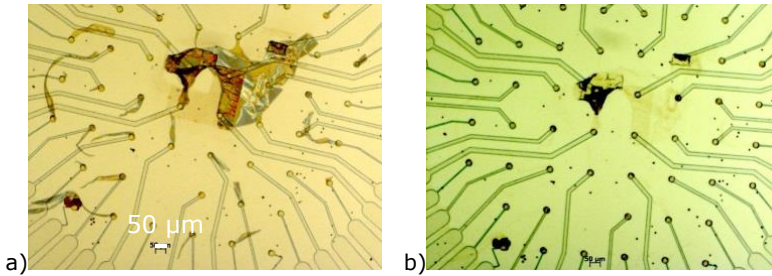
Figure 3-7. Photoresist residues stick to the surface after EDX measurements, a) before oxygen plasma cleaning, b) after oxygen plasma cleaning.

After this experience, NCD was etched in O_2 plasma RIE down to BNCD/W layer (Figure 3-8). For the sample with the photoresist contamination, NCD peeled off in some areas.
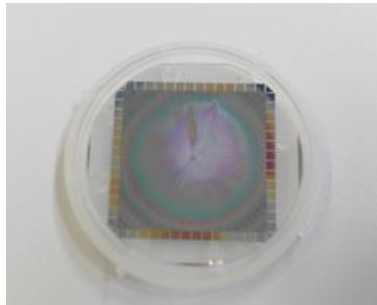
Figure 3-8. Diamond MEA after NCD deposition and patterning

After RIE processing, chromium mask was removed by wet etching, using standard Cr etchant (Sigma Aldrich, Belgium). Finally, tungsten layer was etched by H_2O_2 solution (30%, Sigma Aldrich, Belgium). For the samples with thicker diamond layers (>150nm), the NCD film cracked or peeled off in some areas at these steps. It could be that some pinholes were present in the NCD layer which made the etchant penetrate through and attack the tungsten. This made it very challenging to decide to continue with W etching, since the Cr etchant attacked also to the W layer. After few trials, some experience in timing and concentration of etching was gained and the final sample was fabricated: BNCD electrodes insulated with NCD. The circles of 20μm area at the centre of the electrodes which exposed BNCD areas, were insulated with NCD film along the wires. The diamond microelectrode array was produced according to the plan

shown in Figure 3-1. The surfaces available for interaction with neurons remained entirely made of diamond.

In order to fabricate full diamond MEAs, without metallic coating lines, the W layer was removed after the step of patterning the BNCD layer. The resistance of the BNCD was measured. Similar steps were taken for NCD growth and patterning. Only the step of NCD RIE etching needed to be done gradually and step by step. After each step of NCD etching, the resistance of the contacts (underlying BNCD layer) were controlled frequently by a Multimeter. Once the resistance of the contact areas was similar to what was measured after BNCD was patterned, it confirmed that the NCD layer was successfully removed. The final result was full diamond flat MEA, with BNCD exposed to the biological environment as conductive electrode, and full NCD insulation.

In our work the BNCD-W/NCD MEAs were intended for biological experiments using acute brain slices. The thin flat diamond MEA with microelectrode channels was used to monitor local responses of single neurons or populations of cells.

Surface termination and wettability of diamond. To study the wettability of both conductive and isolating diamond surfaces in cell experiments, two sets of fused silica substrates were prepared on which NCD and BNCD thin films were subsequently grown. One set of the NCD and BNCD coated substrates were hydrogen terminated; using hydrogen plasma exposure in the ASTeX reactor (800°C. 10 minutes, cooling in hydrogen). For the other set of substrates, the surfaces were oxygen terminated using UV induced ozone treatment in a PSD series digital UV-ozone system (Novascan Technologies, Inc.) for 30 minutes to create a homogeneously oxidized surface. The contact angles (water drop) for these substrates were measured, examining the surface wettability. The contact angles of these substrates were measured using OCA15EC Video Based Optical Contact angle Measurement Instrument.

To see any impact of the biological environment on the diamond surface wettability, the same set of samples were later treated with 1:1 Dulbecco's Modified Eagle's Medium (DMEM) and nutrient mixture F-12 from Sigma (Taufkirchen, Germany) containing 10% fetal bovine serum (FBS), and 1% penicillin/streptomycin. This medium is generally used to prepare substrates for

cell culturing, and because of its ion and charge content, the diamond surface properties can change due to physisorption of molecular or ionic species in the cell medium.

To investigate this effect, the incubation was carried out for a short (1-2 hours) and longer period (19 hours) in medium with FBS. After washing the surfaces in Milli-Q water, the contact angles were re-measured and compared.

Electrical characterization of diamond electrodes. Impedance spectroscopy was employed to characterize the diamond MEA and to evaluate the cross talk between the electrodes in dry condition (i.e. through the diamond layers), which is important to be minimized. For this measurement, HP 4194a Impedance/Gain-Phase analyser from Keysight technologies was employed. The impedance for the cross talk evaluation was measured between two microelectrodes using a 50 mV peak-to-peak excitation signal which was applied by the signal generator. The impedance was assessed in two conditions: wet (i.e., in phosphate-buffered saline PBS) and dry (Figure 3-9).

a)   b)
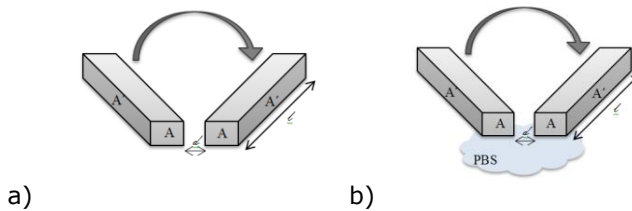
Figure 3-9. Schematic of the electrodes used in impedance measurements for cross talk evaluation in, a) dry condition and, b) wet condition (in PBS).

For the following experiments to characterize the impedance behaviour of the electrodes, Solartron 1260 Impedance/Gain-Phase analyzer from Solartron Group Ltd was employed.

Brain tissue slices preparation and MEA electrophysiology. Tissue preparation was performed by standard methods [78], closely following the guidelines of the Ethics Committee of the University of Antwerp. Briefly, 21 days old Wistar rats were anaesthetized with Isoflurane (IsoFlo, Abbott, USA), decapitated, and their brains excised. 300 μm thick tissue slices (parasagittal) of the somatosensory cortex were cut by a vibratome (VT1000 S, Leica

Microsystems, Diegem, Belgium) in ice-cold Artificial Cerebro-Spinal Fluid (ACSF) (Figure 3-10). The ACSF contained (in mM) 125 NaCl, 25 $NaHCO_3$, 2.5 KCl, 1.25 NaH_2PO_4, 2 $CaCl_2$, 1 $MgCl_2$, 25 glucose, balanced by 95% O_2, 5% CO_2 and adjusted to pH 7.3. The same solution was also employed after cut, to incubate slices at 36ºC for at least 45 min, during slice storage at room temperature, as well as during the electrophysiological recordings, performed at room temperature. All chemicals were obtained from Sigma-Aldrich (Diegem, Belgium).

Slices were trimmed, to a width of ~5-6mm, and gently placed over the active surface of the diamond MEAs, upon previous treatment with cellulose nitrate (Protran, Fisher Scientific, Belgium; 0.14mg/ml in 100% Methanol).

Wistar rat, p14–p50
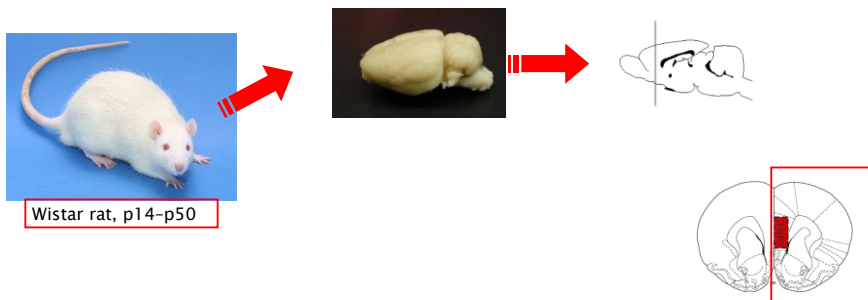
Figure 3-10. *In vitro* acute brain tissue slices were prepared. 300 µm thick tissue slices of the somatosensory cortex were cut by a vibratome.

MEAs replaced the chamber of an upright microscope (Figure 3-11). MEA microelectrodes were then employed to monitor non-invasively the extracellular electrical field of neuronal microcircuits in proximity with the substrate. An ad hoc commercial amplifier was employed - 1060BC, Multichannel Systems GmbH, Reutlingen (Germany) to acquire spontaneous electrical activity at 25 kHz/channel, after 1200x amplification. MC Rack software (Multichannel Systems, Reutlingen, Germany) was employed for disk storage of the digitized data. An acquisition computer with a PCI A/D board (MC Card, 64 channels A/D, 4 DIO, 16bits Multichannel Systems, Reutlingen, Germany), was employed in this experiment.
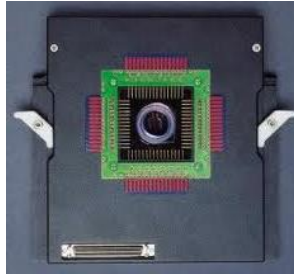
Figure 3-11. The MEA is mounted in the setup.

3.4 Results and Discussions

Surface characterization of MEAs. The Figure 3-12 shows the images of functional diamond MEAs fabricated on fused silica substrates. Microscope and SEM images confirmed the successful patterning of diamond and presence of diamond on the well-defined active sites. The final all diamond MEA is presented (Figure 3-13, Figure 3-14).
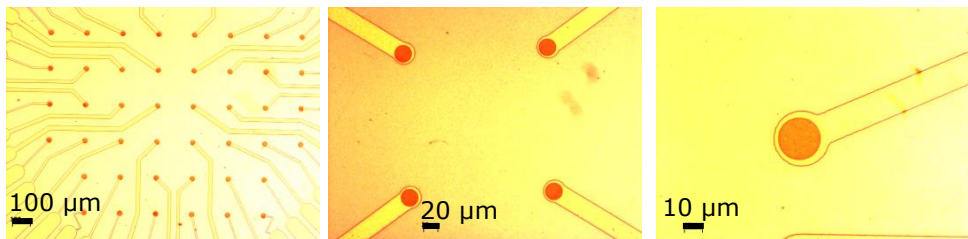
Figure 3-12. Microscope images of the patterned NCD layer on the BNCD electrode and metallic lines.
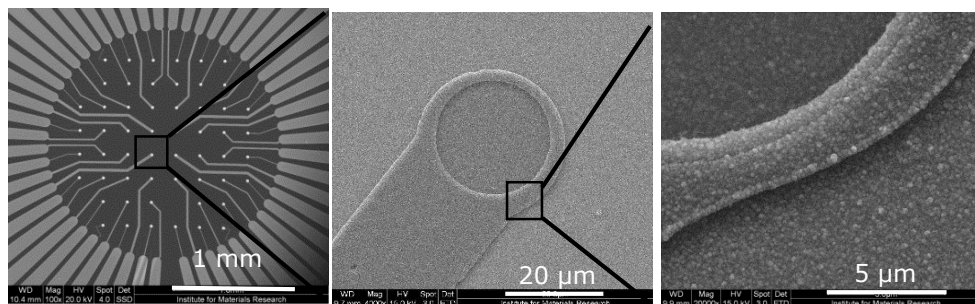
Figure 3-13. SEM results from the central part of the fabricated full diamond MEA. Left: zoomed on the central 2mm area of the MEA, showing all electrode contacts. Middle: zoomed on a single electrode, showing the fabricated area with NCD and BNCD. Right: zoomed on the edge of on electrode, illustrating the diamond coated surface.
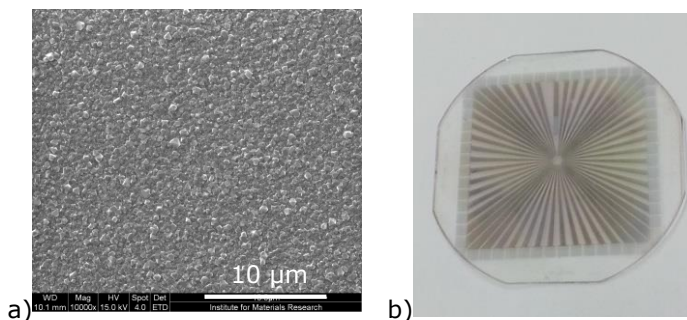
Figure 3-14. a) SEM image of BNCD film on the electrode, b) Full diamond MEAs fabricated on fused silica substrates.

To prepare the MEA for measurement in PBS, a ring was attached to the MEA to function as the PBS holder (Figure 3-15).

Figure 3-15. Flexible reusable cell culture silicone chamber (Greiner BioOne) was attached to MEA, creating a bath chamber required for electrochemical impedance measurement under PBS.

Surface termination and wettability of diamond. The oxygen terminated diamond surfaces yielded lower contact angle (< 20°) in comparison to the hydrogen terminated diamond surface with larger contact angle (>80°), representing hydrophilic and hydrophobic surfaces, respectively. This confirms that the wettability of the surface increases by oxygen treating the diamond [79], [80].

The contact angles of the substrates after treatment with medium with 10% FBS changed dramatically (Figure 3-16). For the H-treated, originally hydrophobic samples, the contact angle decreased to 60-65° and for the O-treated, originally hydrophilic samples, it increased to 55-60° after medium treatment. The results indicated that the wettability of the surfaces is significantly modified by the interaction of diamond surface with the cell medium containing 10% FBS. This can be due to the double layer effect [43]. Since the surface of hydrogen or oxygen terminated diamond exhibits downwards or upwards band bending respectively, the electrical charge close to the diamond surface can be compensated by ionic species originating from the environment. Once the surface came in contact with the FBS containing medium, the surface ions were exposed to the corona from the protein cocktail or opposite charged ions that compensate the original charge; equalizing the charge balance. We consider this as a reason for compensating the polarity of the surface in the biological conditions. This is confirmed by the fact that the water contact angle does not show the former wettability, suggesting that both positive and negative ions from the medium can attach to the surface to neutralize the surface charges. Interestingly, we see identical changes of contact angles for both BNCD and NCD for which we would expect different band bending. This suggest that the surface band bending changes occur in thin layer from the surface upon changing the termination due to large influence of the surface treatment on the surface conductivity in NCD and BNCD films. Findings confirm that BNCD and NCD surfaces interact by the same way with the cellular cultures and diamond MEAs composed of NCD and BNCD can provide a homogeneous interface to neural cultures.
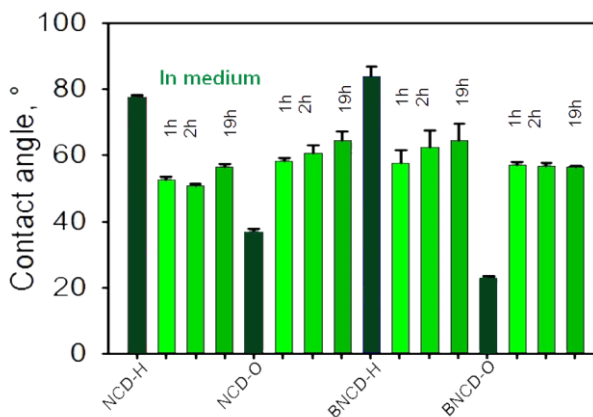
Figure 3-16. Contact angle measurement across differently terminated diamond surfaces, before and after (1-19h) incubation in medium with FBS.

Electrical characterization of diamond MEA. Electrical impedance spectroscopy was used to characterize the conductive diamond MEAs.

Impedance cross-talk data were plotted for a representative pair of conducting electrode lines (Figure 3-17). Impedance cross-talk of the diamond electrodes is measured in dry and in PBS buffer in a frequency range of 1MHz to 100Hz.
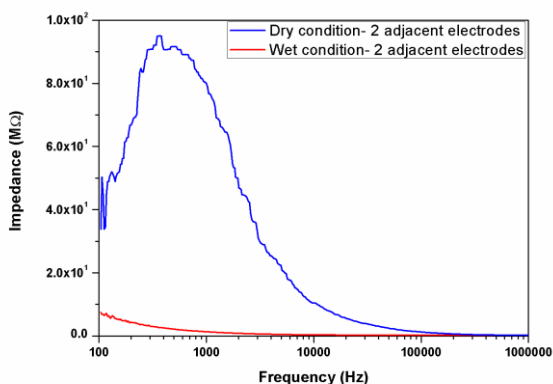
Figure 3-17. Cross-talk measurement in dry and wet conditions (in PBS).

In case of measurement in low frequencies (e.g. 1000 Hz) in PBS, the impedance cross talk shown between two adjacent electrodes can still be considered high (~1 MΩ), determined by the conduction through the buffer. From this, we could conclude that the capacitive cross-talk between electrodes was very low, confirmed by the formula:

$$\text{Capacitance (C)} = \varepsilon_r\, \varepsilon_r{'}\, \frac{A{'}}{d} \qquad\qquad\qquad (3\text{-}1)$$

$$\text{Impedance (Z)} = \rho\, \frac{L}{A}\, +\, \frac{1}{i\omega\, C} \qquad\qquad\qquad (3\text{-}2)$$

(Cross-talk impedance at 1 kHz):

$$\mathbf{10^6\, ohm} \sim \frac{1}{2\pi * 10^3 Hz * C} \rightarrow C \sim 10^{-10}\, F \qquad\qquad (3\text{-}3)$$

where $\varepsilon_r{'}$ and ε_r are relative permittivity of insulating diamond (which fills between the two capacitive areas~ 5.5) and the relative permittivity of air ~1, respectively. A' is the capacitive area, d is the distance between two electrodes, ρ is the resistivity of conductive diamond (~m Ω.cm) and L is the length of the line. The crosstalk in the PBS is also depending on the electrode size and the ionic conduction and diffusion processes in the electrolyte. A is the cross section of the line, (Figure 3-9), and ω represents the frequency. The cross talk is comparable to or lower than standard MEAs in electrolyte, because the diamond double layer capacity of BNCD in electrolyte is lower than metals [49], [81], [82]. The capacitive cross-talk for diamond MEAs is lower than other type of MEAs, for example with AlN insulation of the same thickness.
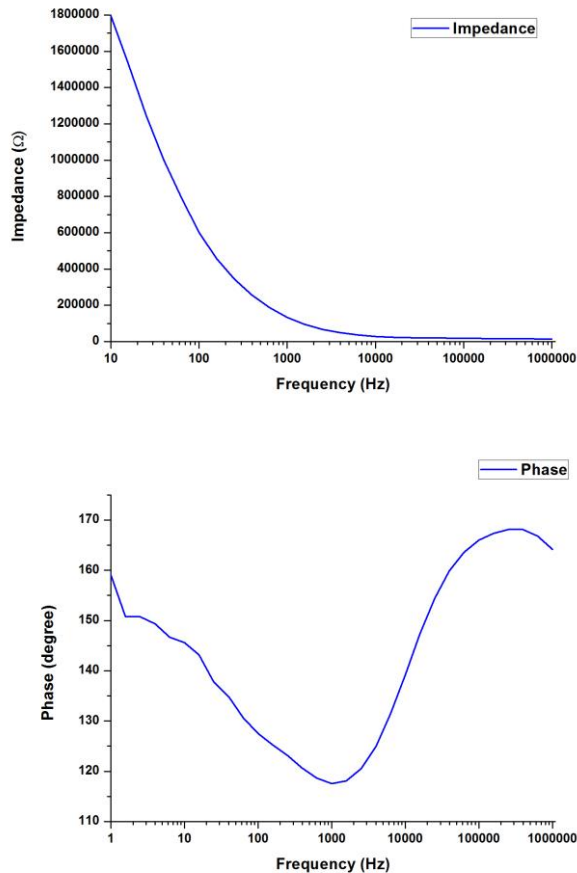
Figure 3-18. Impedance and phase vs frequency diagrams of an example electrode (circular channels of 20μm diameter).

The impedance and phase diagrams of the microelectrodes in PBS was measured as plotted and shown in Figure 3-18. The typical electrode showed an impedance of around 180 kΩ at 1 kHz. This value is comparable to commercial MEAs (~100-200 kOhms/ 1 kHz) and about factor 10 lower than the impedance for the cross talk in wet conditions.

Acute brain slice experiment on diamond MEAs. The diamond MEAs were further used for standard acute brain slice electrophysiological experiments as described in the Methods, under "submerged" conditions. Pharmacological disinhibition was then obtained by bath-applying 20μM of GABAzine (i.e., SR-

95531) in ACSF, as a competitive antagonist of GABA$_A$ receptors. This resulted in spontaneous episodic electrical (epileptiform) activity *in vitro*.

An A/D converter and a 60 channels analogue amplifier are used for recording the local electrical field potentials, corresponding to the excitable activity of neighbouring neurons. Raw electrical voltages were recorded under a monopolar configuration, i.e. with reference to a synthesized chlorinated silver pellet electrode, immersed in the bath chamber. Waveforms were acquired and plotted using MATLAB, showing Local Field Potentials during an epileptiform epoch (Figure 3-19), reflecting the synchronous activation of local subset of pyramidal neurons, spatially summated in close proximity of the MEA microelectrodes. Pharmacological disinhibition was necessary as somatosensory cortical slices display very low spontaneous activity.
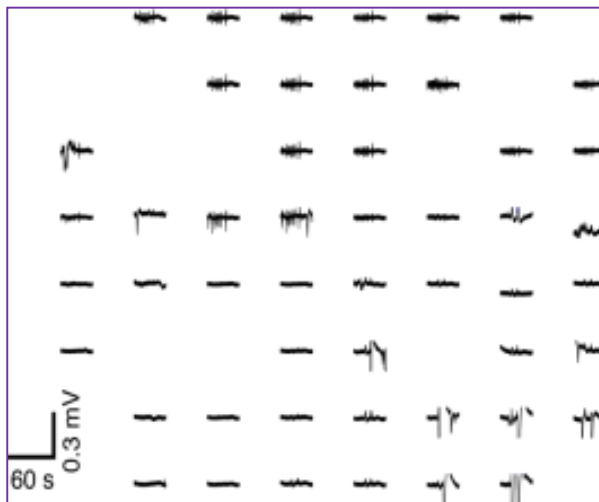
Figure 3-19. 50 microelectrodes, displayed simultaneously over 1min of recording, as a spatial map of the electrical activity across cortical layers (from top to bottom).

The overall level of noise associated to the diamond MEAs has also been measured by the same recording setup, without any brain tissue slice and under the identical conditions: under ACSF. The standard deviation of the voltages recorded from all the channels at 1 kHz are shown in Figure 3-20. The background electrochemical noise was found to be generally lower for diamond

microelectrodes, compared to the commercial Pt-microelectrodes arrays (from QWANE Bioscience, Lausanne, Switzerland).
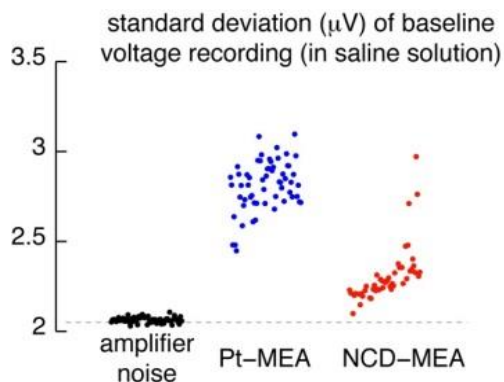
Figure 3-20. Quantification of the noise at the electrochemical interface between the NCD microelectrodes and the electrolyte, compared to control Pt-microelectrodes of commercial MEA, and to the intrinsic noise of the electronic amplifier.

3.5 Conclusions

Arrays of microelectrodes (MEAs) were successfully fabricated from diamond thin films. The diamond MEAs contain a monolithic diamond surface composed of B doped and un-doped diamond. This is an advantage compared to commercial MEAs of which surface is heterogeneous. The wettability of BNCD and NCD as differently terminated diamond surfaces were examined. The treated BNCD and NCD surfaces when exposed to a medium with FBS, showed a change in hydrophobicity, regardless of the prior oxygen or hydrogen treatment. However, for biological measurements the MEAs performed well.

The electrochemical impedance spectroscopy of diamond microelectrodes was analysed and the signal cross-talk between the neighbouring microelectrodes was found negligible. The diamond MEAs allowed detection of the local field potentials for acute rat brain slices, with an overall noise level of the diamond MEA generally lower than conventional MEAs. This all indicates that diamond MEAs have the potential to represent an advanced technology for long term electrical interfacing with neuronal systems.

4 Functional Diamond-Polyimide Electrodes for Electromyography (EMG) application

This Chapter is devoted to experimental results related to flexible diamond (BNCD) micro electrode arrays for Electromyography (EMG) applications. It deals with the fabrication methods used to engineer the EMG devices, and discusses the challenges in the path towards making a flaw-less flexible diamond MEA. The electrodes were designed according to specific functionality required for EMG experiments. In these electrodes, BNCD was used for the active conductive regions. To support and insulate the BNCD electrodes, Polyimide was used as a flexible, insulating and biocompatible material- which has already attracted a lot of attention for fabrication of sensors and multi-electrodes [83], [84]. This polymer is suitable for bio-application as less moisture adsorption occurs. It has low cytotoxicity and is used for implantable device fabrication. We accomplished the fabrications and characterization of 16-channel EMG electrodes of diamond and Polyimide for electromyography.

EMG electrodes can be used for recording electrical signals from muscles that arise as consequence of motor neuron actions initiated by the CNS commands. By using this technique, one can decode the measured neural signals patterns for driving artificial voluntary control prosthetic devices. Specifically, the read signals after the decoding can be used to control sensitive step-engines to drive and move prosthetic hands (Figure 4-1). The motivation behind this work was replacement of Pt-gold electrodes by diamond to achieved better stability *in vivo* as well as more favourable electrochemical and mechanical properties.

Here, I describe the technology how to develop the diamond EMG electrodes that were related to the EU project, MERIDIAN, and a significant part of my thesis. The design and development of the diamond-polyimide based electrodes were optimized to minimize the invasive surgical procedures for myoelectric recordings in humans.

Conducting diamond electrodes have been integrated with polyimide for this application, confirming the viability of the technology principles for fabricating flexible EMG diamond devices. The electrodes were to be further used in the

MERIDIAN project for multivariate intra-muscular signal detection. The property of having multiple electrodes allows to decompose the motor signals into individual motor unit firing patterns and robust event-triggered regression, to estimate muscle forces, which can be used as control signals for prosthetic devices. The proposed methods have the potential to overcome limitations related to reaction time and robustness in dynamic contractions. Therefore, they can significantly improve the usability of modern multifunctional hand-prostheses.

Figure 4-1. EMG Control of prosthetic devices such as Michelangelo-Ottobock hand for which the developed flexible electrodes were aimed.

4.1 Abstract

In this study, we have developed a micro-fabricated 16-channel and 64-channel diamond-polyimide microelectrode arrays for Electromyography purposes. The 6-cm electrodes are manufactured on Silicon/ Silicon dioxide platform and released from the substrate in the last stage. They contain elliptical-shaped diamond active areas with the thickness of 100nm, and polyimide insulating layers of ~24µm in total. The diamond conductive areas are connected to connector areas by means of metallic lines, which are sandwiched between two layers of polyimide. The electrodes are characterized in every step of fabrication, in order to mark and avoid any possible defects. The electrode flexibility testing was successfully carried out in the animal model. These electrodes hold the bases for further optimization for controlling the prosthetic devices.

4.2 Introduction

There are several approaches to study the central and peripheral nervous system (CNS and PNS) in the body. Methods such as functional Magnetic Resonance Imaging (fMRI) and Electroencephalography (EEG) are by far widely developed. However, a closer view of the neural communication and interaction between neurons can be achieved by *in vivo* implantation technology, which enables monitoring, measuring or using particular motor neuron signals. The material of the implant is a critical point of attention in fabrication of implants, since it is in close contact with an organ. In order to avoid inflammation of the tissue and other possible issues caused by the wear of the material, several factors must be taken care of. Ideally, the implanted material must respond with biocompatibility to hosting body environment, and should not initiate an unwanted reaction from the surrounding tissue. Therefore, the choices of material for the conductive and insulating parts of electrodes is of great importance. Investigating the category of biocompatible materials, diamond presents interesting physical and chemical characteristics in comparison to other materials. BNCD as a conductive material offers chemical and mechanical robustness in bio-sensing application studies which are already performed in animal models [53], [85].

The aim of this work was to fabricate BNCD micro electrode arrays (MEAs) for EMG purposes. Since the EMG electrodes are technically used to evaluate and record the electrical activity produced by skeletal muscles, these BNCD MEAs are designed in a way to allow *in vivo* measurement in muscles. In order to insulate and support the BNCD electrode sites, Polyimide is used. The fabrication plans, engineering and characterization of diamond-polyimide flexible electrodes are discussed in this chapter.

4.3 Experimental methods

The experimental methods are arranged as follows:

4.3.1 Design of the electrodes, fabrication plans and lithography masks

NCD–BNCD–Polyimide EMG electrodes. To start fabricating the flexible diamond electrodes, a complete fabrication plan was required. The plan was defined as the following micro fabrication steps in order to build the structure and pattern layers on silicon substrate (Figure 4-2). To define this plan, the materials' chemical and physical behaviour and structure in different conditions has been studied. NCD and Polyimide were used as insulating layers, while BNCD was used as the conductive parts of the electrodes. Several steps of photolithography, deposition, etching and annealing have been employed, which will be described in details in the following sections.
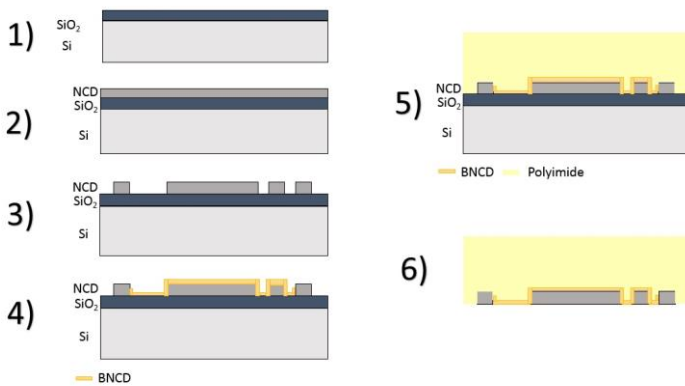
Figure 4-2. Fabrication plan for EMG electrodes. 1) Sacrificial SiO_2 layer is deposited on Si wafer. 2) NCD layer is grown. 3) NCD film is patterned. 4) BNCD is grown and patterned. 5) Polyimide layer covers the electrodes. 6) Electrodes are released from the substrates.

Three different photolithography masks were designed to be used at the UV exposure step in lithography. The first mask was applied to pattern the 'insulating' NCD parts of the electrodes:
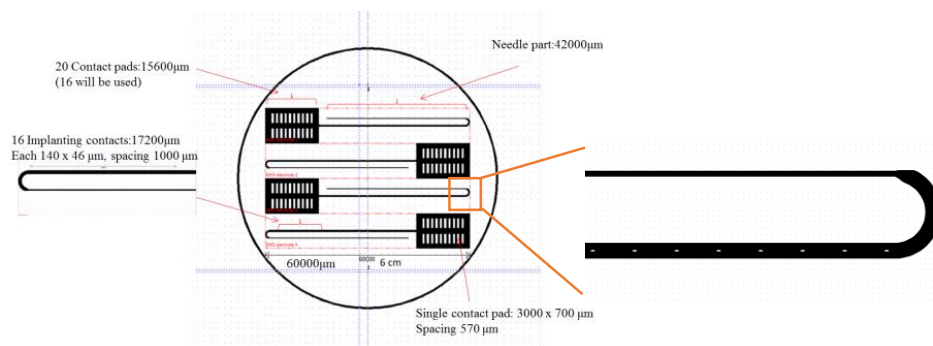
Figure 4-3. The photomask for insulating areas.

This photomask contained 4 defined electrodes as shown in Figure 4-3. Each of electrodes consisted of the active measurement areas, which were elliptical shape contacts, connected to 16 connectors with a long shank. 46 µm by 140 µm ellipses were defined with 1000µm spacing. Connector part consisted of 16 rectangles of 3000 µm by 700 µm with 570µm vertical and 1500 µm horizontal spacing. A narrow line/wire was defined to be served for a needle insertion to the tissue (see Figure 4-3).

This mask contained alignment marks (Figure 4-4), in order to enable patterning more structure on top of NCD in the following steps.
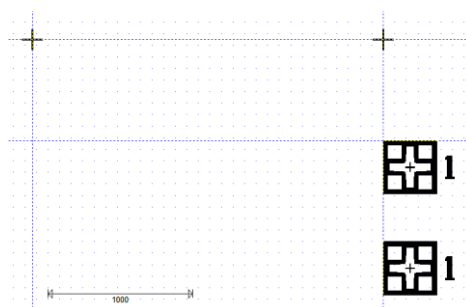
Figure 4-4. Alignment marks on the 'insulating' mask- Scale bar is 1000 µm.

The process followed by the fabrication of the conductive parts. Therefore, the second photo mask was used to pattern the BNCD 'conductive' areas of the electrodes (Figure 4-5).
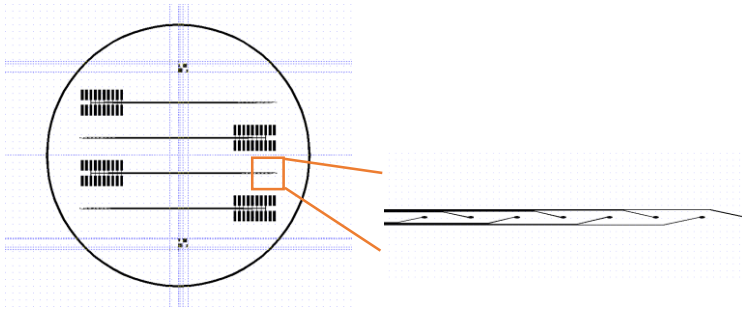
Figure 4-5. The photomask for Conductive areas.

This mask contained the patterns for conductive parts of the four electrodes, which included the rectangle contact areas connected by lines to the elliptical shapes. The lines had the thickness of 10µm with 10µm spacing. The structure on this mask defines the conductive structure as final BNCD layer in these flexible EMG electrodes. The photo-mask was aligned onto the NCD pattern by using the alignment marks.

The third photo mask was the 'PI' mask, which is used to insulate the electrodes by Polyimide (Figure 4-6). The design of this mask was made in a way to cover each whole electrode (conductive and insulating parts).
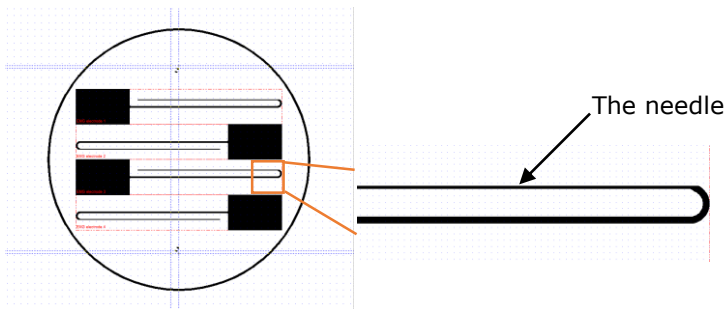
Figure 4-6. 'PI' photomask

When NCD-BNCD-PI electrodes were fabricated, some issues regarding the flexibility of the electrodes were observed. This led the project to define a new plan for fabrication of EMG electrode to overcome the issues.

New fabrication plan for BNCD-Polyimide EMG electrodes. A new scheme was developed for the diamond EMG electrodes to improve the flexibility of the electrodes. In the new design (see Figure 4-7), the NCD layer as insulator was replaced by polyimide. In addition, BNCD was designed to be on the conductive areas and the electrodes were embedded and insulated in polyimide from front and back side. A new fabrication plan was introduced in order to optimize the electrode functionality. According to this plan, the structure was first started with patterning of the conductive areas.
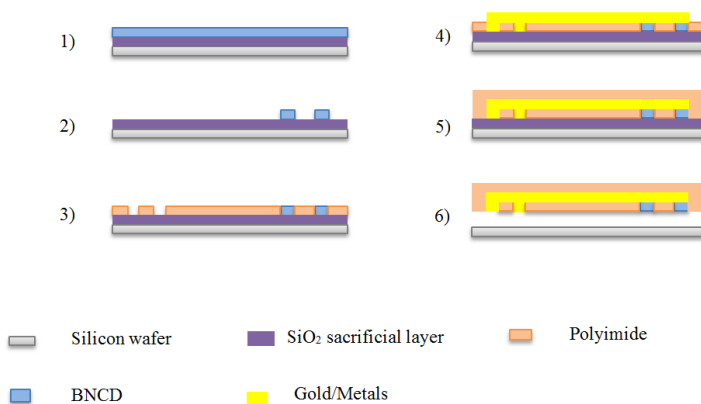
Figure 4-7. Schematic of the new process plan- 1)BNCD is grown on Si/SiO$_2$ substrate, 2)BNCD is patterned as active conductive sites, 3)Polyimide is coated and insulated the electrode, 4)Metallic tracks are patterned, 5) Polyimide is coated to insulate the metallic parts, 6) Electrode is released from the substrate by wet-etching of SiO$_2$.

Therefore, a new set of photolithography masks were designed and introduced to advance the quality and functionality of the final device. The new photo masks consisted of more electrodes with more channels, in order to increase the chance of having more successful results.

The photo masks were defined for 4inch silicon substrates, but a 3inch wafer could fit many electrodes as well. In the photomask for conductive areas (see Figure 4-8), the total of 22 electrodes (6cm long) were designed. From the 22

electrodes, 16 electrodes contained 16 channels (16 ellipses of 50µm by 150µm with 850µm spacing) and the other 6 electrodes contained 64 channels (64 ellipses of 40µm by 140µm with 360µm spacing). The reason for defining 64-channel electrodes was to take one step further to explore the possibilities of the ability to measure many channels at once *in vivo*.

To begin, BNCD layer was grown and patterned using the "conductive" photomask.
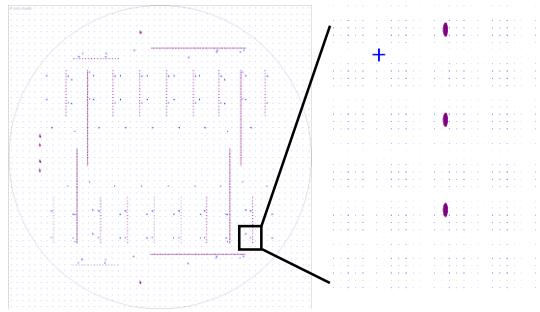
Figure 4-8. New photomask for BNCD patterning with enlarged ellipses.

The fabrication proceeded with insulating the BNCD with Polyimide. The photomasks for insulating areas consisted of 22 insulating parts for the electrodes (Figure 4-9). While keeping the ellipses open, it opens 2-columnar 16 connector pads (squares of 700µm by 700µm) for 16-channel and 64 connector pads (squares of 250µm by 250µm) for 64-channel electrodes. The sizes of the open ellipses were slightly smaller than the BNCD ellipses in order to assure the polyimide insulates the BNCD ellipses without a gap which can result from possible misalignment of the 'insulating' photomask.
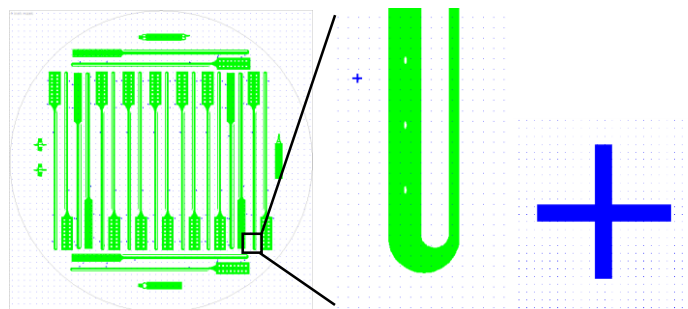
Figure 4-9. Patterning the first Polyimide layer with the photo mask for the first PI layer. The images shows enlarged area for ellipses and the alignment mark.

After fabricating the first insulating polyimide layer, the conductive connecting parts were patterned using the mask for the second conductive layer (Figure 4-10). This mask included 16-channel and 64-channel electrodes. For the 16-channel electrodes, 50μm by 150μm ellipses, 10μm lines with 10μm spacing and 16 square contacts were designed. For the 64-channel electrodes, 40μm by 140μm ellipses, 5μm lines with 5μm spacing and 64- square contacts were designed. For both types of the electrodes, the lines were connecting the ellipses to the square contacts (with the same sizes as in the previous mask). The square contacts and the wires -which would connect the ellipses to the square contacts- were designed to be made of metals such as Ti-gold or Cr-gold. The resulting electrodes were anticipated to be flexible without any stress.
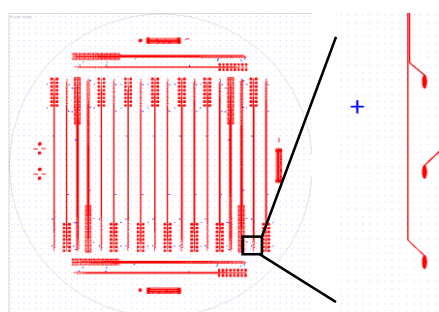
Figure 4-10. Photomask for metal patterning with enlarged connecting lines to the ellipses.

The process followed by complete insulating of the electrodes by a second layer of polyimide. The same processing step was implanted to coat and pattern the

PI layer, using the 'insulating' photomask#2 (Figure 4-11). This PI layer would cover each whole electrode.
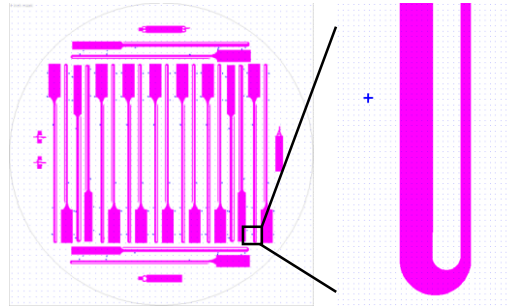
Figure 4-11. Second Polyimide layer photomask.

Although the new fabrication plan was more complicated and the process took longer, the resulting devices were promising.

4.3.2 Experimental procedure and technological steps for fabrication of NCD/BNCD/Polyimide flexible EMG electrodes

Substrate choice and diamond patterning. Two sets of substrates were used in these experiments. One set was (100) oriented Si wafer with a 1µm layer of thermal SiO_2. This silicon dioxide layer served as a sacrificial layer which was further removed to release the electrode. The sacrificial layer is a membrane or a layer that is used to deposit films or fabricate the electrodes on it. It is removed in the final step for releasing the patterned structure from the substrate.

The other set of Si substrates did not have the oxide layer except native oxide. Therefore, SiO_x was deposited in the house-built RF magnetron sputtering system, and then annealed ex-situ in a vacuum chamber at 1000° C for two hours in order to have stable and dominant SiO_2 form [86]. This SiO_2 layer also served as the sacrificial layer.

In order to fabricate flexible diamond electrodes, performing an initial flexibility test for dummy electrodes was needed. For that, an NCD layer was grown on Si/SiO$_2$ substrate. First, the substrate was seeded by spin coating a colloid of homogeneously dispersed nano diamonds in Milli-Q water, as described in the first experimental section of chapter 3. 250nm NCD was grown on seeded Si/SiO$_2$ substrate using the following conditions: 480 sccm H$_2$ and 20 sccm CH$_4$ (4%) as precursor gases in 30 Torr pressure and 3500 W power. It was patterned using photolithography and metal deposition: First, negative lift off photoresist NR9 was dispensed on NCD film and spin coated for 40 seconds with 3000rpm. Then it was baked on the hotplate at 150°C for a minute. After that, the photoresist was exposed to the UV light for 90 seconds using the photomasks for insulating areas (Figure 4-3).

After the photoresist was exposed to UV light of the mask aligner, the sample had a post-exposure bake at 100°C for a minute. The development took place in RD6 developer in ~17 seconds. Then 300nm of Cr was deposited (conditions described before) and lifted off by Acetone (Figure 4-12, a). The resulting Cr layer masked the NCD in the form of insulating mask of diamond layer. RIE with oxygen plasma was applied to remove the diamond outside of the insulating areas. 250nm of NCD was etched in less than half an hour (oxygen etching conditions described in previous chapter). Once O$_2$ etching of NCD was done, the masking Cr layer was removed using standard Cr etchant (Sigma Aldrich, Belgium). The result was the patterned NCD layer on the substrate (Figure 4-12, b).

a) b)
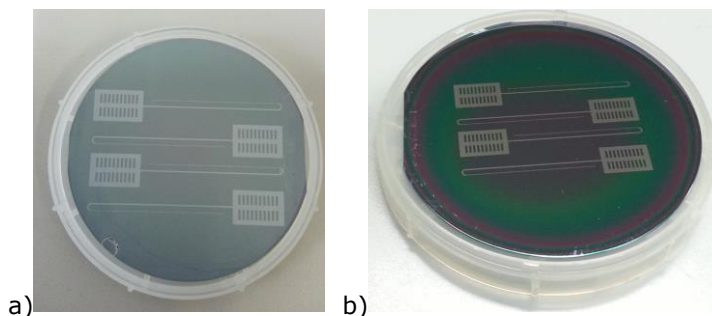
Figure 4-12. a) The substrate with grown NCD and coated Cr mask. b) The sample with etched/patterned NCD.

The choice of the polymer. The flexibility of the electrodes was achieved by using polymer layers on the surface of NCD. To choose the right polymer, one had to look into different options. For bio-application purposes, several polymers have already been studied in the literature [56]. In this research, Polyimide (PI) has been chosen for several reasons as follows. For EMG application, polyimide has quite good tensile strength [56]. It is insulating and has a relatively good thermal expansion coefficient. Our other collaborators in Switzerland and Italy (Microsystem Laboratories EPFL and Advanced Robotics Technology & Systems Lab, Pisa) used Polyimide, for the purpose of neural electrodes. Therefore, it was easy to discuss the issues. Consequently, Polyimide was used. However, there are different types of PI and one had to look into the processing steps for each product.

Among all polyimide types, PI-2574 was selected for few reasons that are explained as follows. For PI 2574 the processing steps were shorter and the required facilities were available in our lab. Also PI-2574 is self-priming and does not need an adhesion promoter. It is non-photo-definable and therefore much better for bio-application as less moisture adsorption would occur. It is biocompatible with low cytotoxicity and is used for implanting device fabrication. Therefore, PI-2574 was used for insulating part of these EMG electrodes. However, the patterning procedure is slightly different from most photoresists. The substrate needs to be clean and dry prior to coating. For that, normally the standard wafer cleaning procedure is followed by baking on the hotplate at 180°C for 5 minutes. Otherwise cleaning with Acetone can help before dehydration.

The process of PI-2574 coating. The coating of PI-2574 was followed as instructed in the manual. However, several initial test needed to be performed to optimize the thickness of the layer. The PI-2574 was spin coated on the surface in 2 steps: the first step consisted of 5 seconds spinning at 500rpm to have the material cover up to 80% of the surface; the second step consisted of 30 seconds spinning at 2500 rpm to get rid of the excess amount of polyimide and make a flat layer of around 12μm. 2500rpm is one of the slowest spin speeds that could be used for non-diluted Polyimide to make such thick layer. Also, an

acceleration was applied to let the polyimide cover the whole surface with the minimum stress introduced in the layer. Faster spinning speed gave thinner and more flat surface and slower spinning speed gave thicker but less homogeneous layer. Thus, edge beads around the edges with slow spinning were more pronounced than fast spinning.

When spin coating was executed, the substrate was baked on the hot plate in two steps: in the first step, it was baked for 30 seconds at 120°C and in the second step, it was baked for 30 seconds at 150°C. This baking with moderate temperature drives out the solvents partly, keeps the surface dry, yet solvable in the developer.

As the first test for polyimide coating on diamond, the layer of polyimide on NCD electrode patterns was cured without photolithography patterning. Therefore, after the soft bake of PI, the substrate went through the curing procedure (or the hard bake). Curing of PI-2574 was executed on the hotplate up to 300° C in the Nitrogen atmosphere. First the temperature ramped from room temperature to 200° C with the rate of 4° C/min (for 50 minutes). The temperature stayed at 200°C for 30 minutes. Then it ramped up to 300° C with the rate of 2.5° C/min (for 40 minutes). The sample was kept at 300°C for one hour and then it was cooled down to room temperature gradually. The cured polyimide is resistant to different variety of solvents and chemicals.

The resulting diamond and cured polyimide layer were then released in diluted HF for a test to see if diamond patterns are transferred onto the polymer (Figure 4-13). In the releasing step, the SiO_2 sacrificial layer was chemically etched in diluted HF. The released polymer layer showed good flexibility and microscope images and SEM results confirmed that the pattern is transferred on the backside of the polyimide (Figure 4-14).
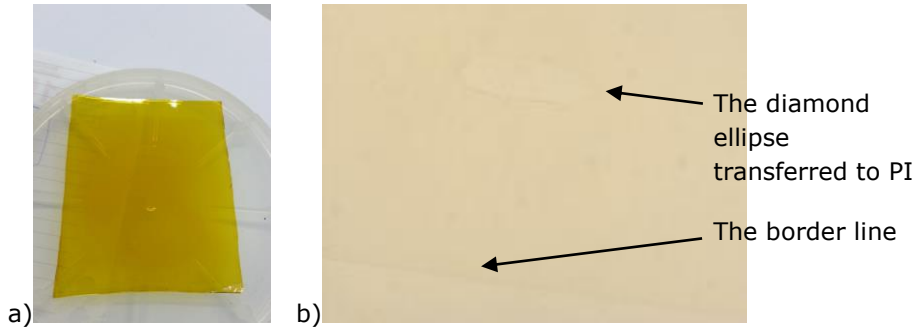
Figure 4-13. a) The released polymer, b) Optical microscope image of the backside, which shows the presence of diamond pattern.
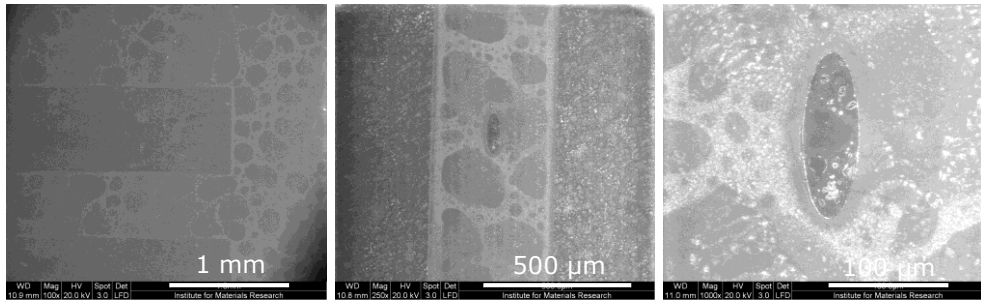
Figure 4-14. SEM images show NCD patterns transferred onto the polyimide layer.

Fabrication steps for the EMG electrodes. After the initial tests proved the presence of diamond on polymer, the fabrication of actual flexible diamond electrodes was carried out. Referring to the previous studies on diamond implantable neuro electrodes [54], [87], ~1µm of NCD was grown on the substrate to make the insulating part of the electrodes. Subsequently, the photolithography step and Cr deposition were preceded to mask the NCD by means of the insulating mask. After O_2 etching of NCD was carried out, the masking Cr layer was removed by Cr etchant. However, the alignment marks made by Cr-NCD needed to be protected prior to Cr etching (Figure 4-4, Figure 4-15), since an alignment step on the NCD pattern was following required.

This protection of the alignment marks was achieved by an extra step of photo lithography using positive photoresist S1818 (Microposit, Germany). The photoresist was spin coated for 30 seconds with 3000 rpm and baked on the hot plate at 115°C for one minute. Then it was exposed to the UV light (i-line) for 8 seconds while the alignment marks were just covered with a small piece of silicon wafer. After the exposure, the substrate was developed in 2 baths, each bath containing a mixture of Milli-Q water and the developer 351 (Microposit, Germany) (ratios. 5:1) for 15 seconds each. Then it was rinsed and dried. By this lithography, a layer of photoresist covered the alignment marks for the step of Cr etching.
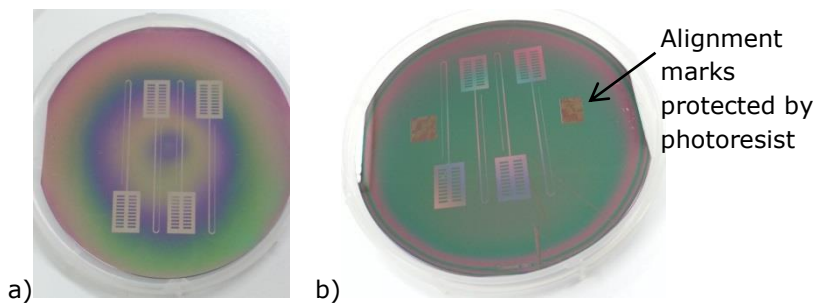
Figure 4-15. a) Before protection of alignment marks and etching the diamond. b) After etching the diamond, protection of alignment marks and removing the masking Cr

Optical microscopy images showed the diamond patterned as insulating layer of the electrodes (Figure 4-16). After Cr etching, the photoresist on the alignment marks was then removed by Acetone.
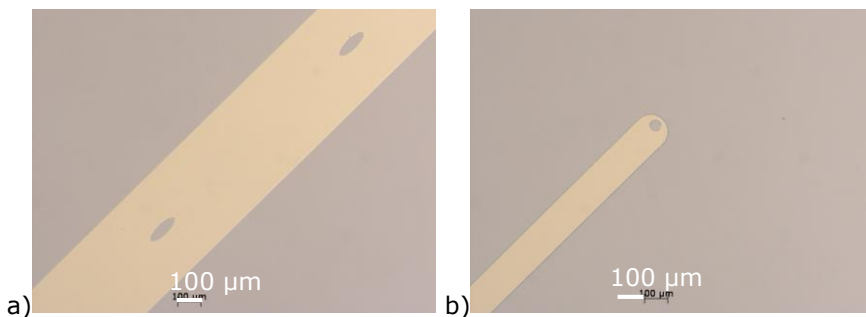
Figure 4-16. a, b) Patterned NCD shown under the optical microscope. b) The end of the needle area.

To fabricate the conductive layer of the electrodes, BNCD film was employed. It is a challenging approach to grow BNCD directly on NCD and then mask it by metal layer in order to pattern it. Because during RIE etching of BNCD, the NCD layer underneath could also be attacked by the plasma after BNCD was etched. To avoid this problem, another approach was proceeded; one step of photolithography and metal deposition was employed to pattern a stop-etch layer on the electrodes to protect the NCD layer in the following RIE process. For that, first a bi-layer stack lift off photolithography was executed on the substrate. The substrate was dehydrated at 180 °C on the hotplate for 5 minutes. The positive lift-off resist LOR 3B (MicroChem, Germany) was spin coated on the surface in 2 steps; first for 5 seconds at 500rpm and then for 40 seconds at 4000 rpm. Then it was baked for one minute at 180 °C. LOR3B needed an extra positive imaging resist to be defined. Therefore, S1818 was coated on the surface and baked as explained before. Then the substrate was exposed to the UV light for 8 seconds, using the 'conductive' photomask (Figure 4-5).

Once the photoresist was exposed, it was developed for one minute in a mixture of Milli-Q water and Thetramethylamuniumhydroxide (TMAH) (25%) (Ratio 10:1) to produce ~2.3-5% of TMAH concentration. Once the bi-layer stack photoresist was developed, it was ready for material deposition. To explore possibilities for the etch-stop layer, different depositions were performed. Either 300nm of Cr/AlN or 100nm of Cr + 200nm of Aluminium Nitride (AlN) were deposited. AlN was deposited using Aluminium target and a plasma with the mixture of 39sccm of Ar and 11sccm of N_2 as gas mixture and 300W power in few mTorr. The rate of the deposition of AlN (~2nm/min) was slower than chromium or tungsten (~10-20nm/min). Once the masking material was deposited, it was lifted off in Acetone. With AlN deposition, the lift-off process could take longer than normal, as the photoresist might have experienced temperatures higher than room temperature during the long run depositions. In this case, ultra-sonication of the substrate in acetone could help dissolving the resist in acetone in order to process further. The resulting mask covers everywhere on the surface but the parts for conductive diamond electrodes (Figure 4-17, a).

Further on, the substrate was seeded by nano diamonds and loaded in ASTEX reactor for BNCD growth. The growth of diamond on AlN has, however, shown to be very much depending on the surface termination of AlN, as the seeding process is challenging [77]. Therefore, the thickness of the diamond layer was measured *in situ* by laser light on a small piece of Si that was seeded and placed in the centre of the sample (where there is no pattern), from which surface the laser light was reflected to the detector. 100 nm of BNCD was grown on the substrate surface to coat the electrode areas using 395 sccm H_2, 5 sccm CH_4 and 100 sccm TMB as gas mixture with 3500W in 20Torr (Figure 4-17, b). After the growth, the stop etch layer was removed. In case Cr+ AlN was deposited, it was removed by standard Cr etchant. If there was only AlN deposited, 20% KOH solution was used to remove the stop etch layer. After the stop etch layer was removed, the BNCD layer remained on the conductive parts of the electrodes (Figure 4-17, c).
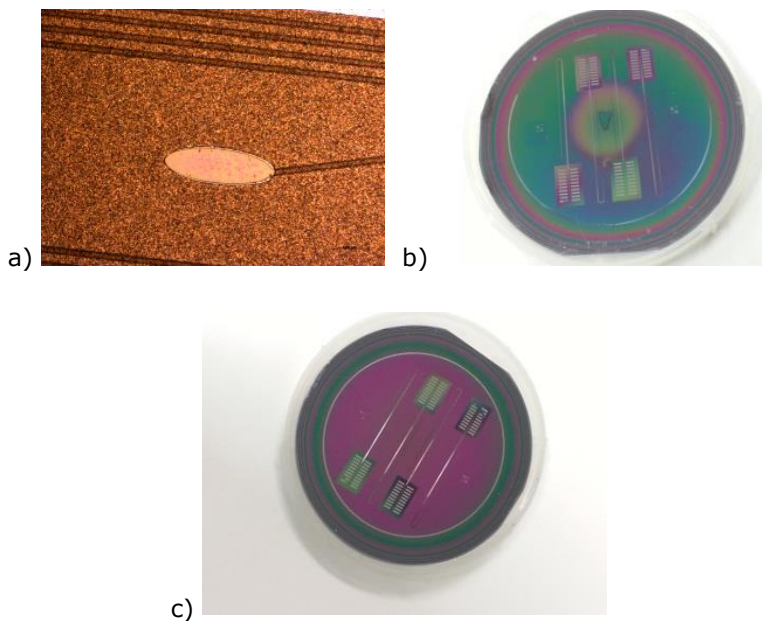
Figure 4-17. a) Stop-etch layer patterned on NCD. b) BNCD grown on the sample. c) BNCD patterned on the electrodes.

The sample was afterwards ready to be coated with insulating PI layers, using the 'PI' photomask (Figure 4-6).

Approaches to coat a thick PI layer. Substrate was cleaned by Acetone and dehydrated on the hotplate at 180°C for 5 minutes. To have a thick PI layer, several approaches were tried, as summarized in table 4-1. Method 'A' was PI spin coating for 5 seconds at 500rpm and then 2500rpm for 30 seconds. This resulted in a layer of about 11µm. Method 'B' was PI spin coating for 5 seconds at 500rpm and then 2000rpm for 30 seconds. This led to a layer of about 13µm. As a test, two samples were coated 3 times by method A, and another two samples were coated 3 times by method B. They were baked at 100°C and 120°C to see if the layers would damage by developing or stay clean. It was estimated that the resulting layers would be around 33 µm and 39 µm, respectively.

After coating and baking, the positive imaging resist S1818 was spin coated on the surfaces. The layer was baked at 90°C for one minute. Then it was exposed to the UV light for 8 seconds using the PI photomask. The PI photomask was aligned on the surfaces using the alignment marks. Then the layers were developed in ma-D 532 S developer (Microresist technology GmbH, Germany). One step of development with ma-D 532 S was employed to develop the photoresist and etch the underlying polyimide. It took 1-2 minutes to develop the layers completely. Since the coated PI layer was thick, warming the developer up to 25°C could help speeding up the PI development with minimal effect on the imaging photoresist. From all the samples, only sample#1 and #4 were successful at this step and other layers were damaged. In both cases the developer was refreshed once.

Table (4-1): Conditions for thick PI coating #1

	Sample# 1 Method B	Sample# 2 Method B	Sample# 3 Method A	Sample#4 Method A
Layer thickness	3x 13µm	3x 13µm	3x 11µm	3x11µm
Bake T for 2min	120°C	100°C	120°C	100°C
Developing T	~25°C	~25°C	~25°C	~25°C

Developing t	1:30 sec	1:22 sec	1:55 sec	1:20 sec
Successful	Yes	No	No	~ Yes

However, after cleaning the photoresist by Acetone, only sample#1 survived this procedure and PI layer on sample#4 was damaged. Sample#1 was cured to proceed with the releasing step. After the cure, the layer thickness was measured by DekTak and it came out to be less than 20µm. As a result of this experiment, spin coating several layers at once without intermediate baking does not produce a relevant thick PI layer. Therefore, the coating tests proceeded with baking intervals, i.e. layers coated with method B were baked on the hotplate, using 3 different conditions (Table 4-2).

Table (4-2): Conditions for thick PI coating #2

	Coating	Baking t	Baking T
Sample 1	2000 rpm, 5x	15 sec	@ 120°C
Sample 2	2000 rpm, 5x	15 sec	@ 100°C
Sample 3	2000 rpm, 5x	15 sec	@ 90°C

After 5 times coating and baking, samples were baked for 1 min at the same temperatures. Imaging resist S1818 was coated and baked for 1 min at 90°C. However, when exposing to the UV, the samples got stuck to the PI photo mask which means that the top surfaces were not dry enough. Therefore, the alignment was difficult. Development was done quickly (at 23°C), but all the layers were dissolved. In most cases, the needle part (shown in Figure 4-6) started to dissolve completely already before the rest of the polymer was developed. The reason could be that the top layers were not baked enough.

Baking the PI layers after every coating was not easy. In case of having several layers, the first layer would have been baked several times already until the last layer was baked. Baking in the oven was also tried instead of hotplate and the results were not positive. Therefore, finding an optimized condition with the baking time and temperature for every step was challenging.

The final strategy was to make a thick (~50µm) layer of PI by repeating the whole coating/curing procedure several times after each other. However, for this purpose one needed to align the PI photo mask onto the previously patterned Polyimide, each time. Since the thickness of the first layer was already several microns (>3µm), it was not possible to perfectly focus on the surface of PI as well as the substrate by the microscope of the mask aligner. Above that, it was impossible to have an alignment with the precision of 1µm (i.e. the resolution of Mask aligner). Therefore, due to the thickness of the layer, an error of ±few µm (i.e. human eyes error + set up error + the resolution of the mask aligner) was predictable.

To try the new strategy, the first dummy PI electrodes were fabricated with the thicknesses between 35 to 55µm. PI was coated for 5 seconds at 500rpm and then for 30 seconds at 2500 rpm. Then it was baked at 120°C and then at 150°C for 30 seconds each. S1818 was coated on the surface for 5 seconds at 500rpm and then for 30 seconds at 3000rpm. Then it was baked at 90°C for a minute. Next, the layer was exposed to UV light for 8 seconds using the PI mask, and then developed. The sample was checked carefully while developing; it was rinsed and dried to check how far it was developed to estimate the remaining time.

After curing the first patterned PI, the thickness of the PI layer was measured by DekTak to be around 12µm. This procedure was performed 3 times and finally the releasing of the dummy electrodes (i.e. the etching of SiO_2) was performed in a diluted mixture of Milli-Q water and HF: H_2O: HF (Ratio 10:1). Thus, a Teflon beaker was used for etching. The diluted HF had the minimal effect on the cured polyimide. The dummy electrodes were finally released successfully (Figure 4-18).
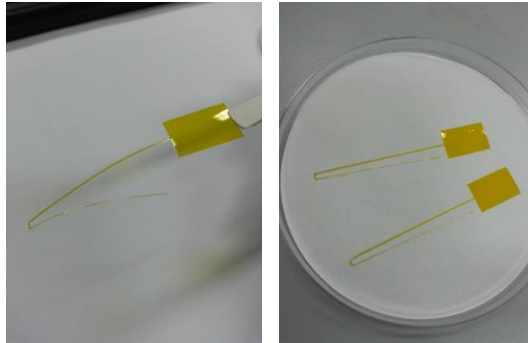
Figure 4-18. The first successful released dummy PI electrdoes.

4.3.3 Releasing of the NCD/BNCD/PI EMG electrodes and their integration.

Final coating of PI on diamond. The important step was releasing of electrodes from the sacrificial layer after the full patterning procedure. Therefore, when the MEA was fabricated with NCD and BNCD, the thick PI layer was coated (Figure 4-19, a). The final thickness of the layer to be released was ~55μm (i.e. PI thickness + the diamond layers).

a)   b)
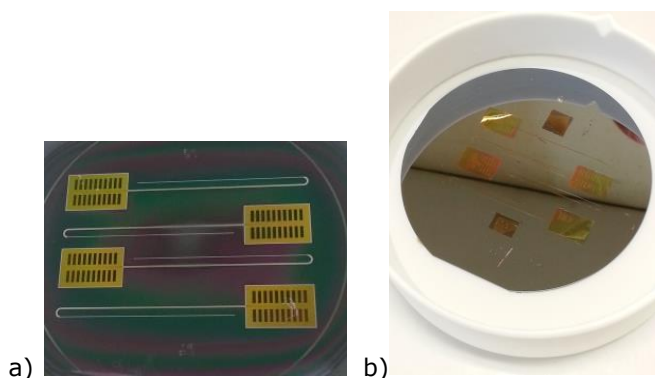
Figure 4-19. a) Several layers of PI, coated on the electrodes, b) Electrodes being released in the diluted HF in a Teflon beaker.

The electrodes were released in the Teflon beaker, same as for dummy electrodes (Figure 4-19, b). It took the electrodes several days to release completely from the substrate. Once an electrode was released, it floated on the surface of the HF solution. The electrode was then transferred carefully to the first water bath for cleaning. In some cases the needle part broke in this step because it was attached loosely to the electrode and it became thinner at the developing step. The most important reason was the design of the needle where it was attached to the electrode.

Figure 4-20. Weak attachment of needle to the electrode which caused losing the needle in releasing process. The fragile attachment of the needle in the design is shown.

As shown in Figure 4-20, the connection part of the needle is fragile, which makes the lack of strength when being released.

The diamond-PI electrodes which survived the first cleaning bath were transferred to the second water bath and then taken out and kept on a clean room tissue for drying. However, after drying, they started to bend and curl (Figure 4-21).
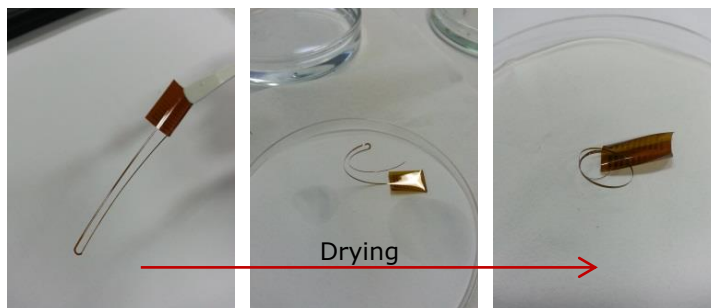
Figure 4-21. Released diamond-PI electrodes tend to curl after drying.

The reasons for bending of the electrodes were explored. For that the curing step for polyimide was studied. This step was to harden the polyimide material by cross-linking the chains in the structure. Heat causes the rings to close or 'Imidize' [88] while driving out all the solvents. Only after curing, the polyimide will perform with the best mechanical and electrically isolating properties [89]. This curing step is found to be a critical step for the PI layer. Bending of electrodes was often observed on the released NCD-BNCD-polyimide electrodes. The difference in the thermal expansion coefficients of the two materials (CTE diamond $\sim 10^{-6}K^{-1}$, polyimide$\sim$30-60 $*10^{-6}K^{-1}$ at 20°C) induced some stress built at the interface which might cause the curling of the diamond-polyimide electrodes.

However, several dummy PI and diamond-PI electrodes were prepared and released and the dummy PI electrodes were already sent to the university hospital in Göttingen to be used as test electrodes for biological *in vivo* experiments to prepare for the diamond-PI electrodes (Figure 4-22).

a)   b)
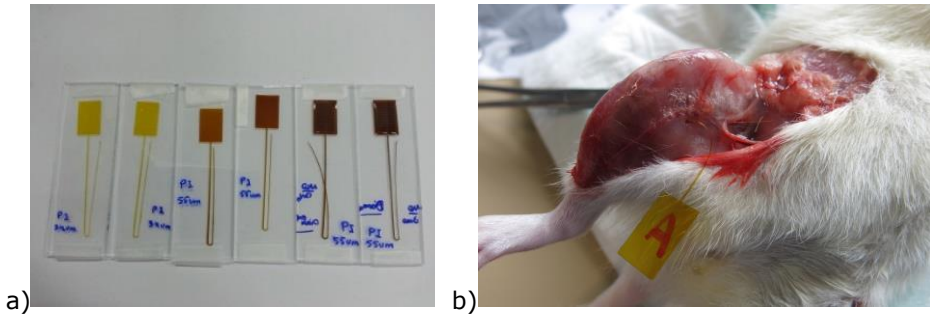
Figure 4-22. a) Successfully released electrodes. b) A test with dummy PI electrode in the animal model.

Released diamond-PI electrodes were attached to the corresponding 16-pin connectors (Farnell) by means of a z- axis conductive tape (Farnell), because soldering or wire bonding was not possible on polyimide and diamond. These electrodes were polyimide on one side and fully diamond on the other side. NCD and BNCD formed the insulating and conductive parts of the electrode, while soldering and wire bonding was possible only for (some) metals.

Once the NCD-BNCD-PI electrodes were attached to the connectors, they were sent for biological *in vivo* tests. However, after measurement at University of Göttingen, it was established that the electrodes did not perform well. First of all, the electrodes curled once they dried. Second, they were fragile, so opening the curls caused damages to the electrodes some times. Third, the attachment of the electrode to the connector by the conductive tape (as the best possible approach by far) was not successful (Figure 4-23). Also, the size of the connector part was found to be un-necessarily big and the connection of the connector to the wire and the wire to the needle was not designed attentively. All these issues resulted in moving towards a new design for fabrication of diamond-PI EMG electrodes to improve the functionality of the devices.

Figure 4-23. Conductive tape peeling off from the electrode and the connector due to curling of the electrode.

4.3.4 BNCD electrodes fully embedded in Polyimide- New design and technological steps

New design scheme for diamond polyimide EMG MEAs. In the new design, a new fabrication process plan was defined (Figure 4-7). BNCD was used to engineer the active conductive areas on the electrodes, using a 'BNCD' photomask (Figure 4-8). This photo mask consisted of ellipses as channels of electrodes that would be fabricated by BNCD. Theses electrodes would be insulated by a layer of Polyimide 2574 (Figure 4-9). After that, each channel or contact area would be eventually connected to a connector pad by a 10µm wide metallic connecting line (second conductive mask, Figure 4-10), while insulated from each other by a second polyimide layer (second PI mask, Figure 4-11). Altogether, the diamond electrode arrays insulated by polyimide, were comprised of the measurement area, the needle and the connector part, which connected the electrode to the measurement device. The contact areas on the shank were meant to be inserted in the tissue by means of a needle which was fabricated along the shank.

Since there were only two layers of polyimide included in this design, it would result in a thinner PI layer (comparing the previous scheme). In order to confirm the flexibility and functionality of such thickness, a test electrode pattern was

made with two PI layers. The successful release of these dummy electrodes confirmed the good flexibility and strength of layers.

4 inch Si wafers with thermal or deposited silicon dioxide layer were used as substrate. The SiO_2 layer was served as a sacrificial layer and was removed in the last step of the fabrication.

Fabrication steps of new EMG electrodes. In the first step, the Si/SiO_2 substrates were cleaned according to the standard wafer cleaning procedure, RCA1, RCA2 [76]. Afterwards, the substrates were seeded with nano diamond particles in order to activate the surface for the following diamond growth procedure [90]. They were immersed into a water-based colloid of nano diamonds for a minute. In this colloid, detonation nano diamonds (NanoAmando®B from NanoCarbon Research Institute Ltd., Nagano, Japan) were dispersed in Milli-Q water by ultra-sonication, to make a homogeneous seeding solution. The seeded substrates were spin dried for 40 seconds at 4000 rpm. The surface was flushed with Milli-Q water for the first 10 seconds of spinning in order to remove extra number of nano diamonds and leave a monolayer dispersed on the surface. The monolayer of nano diamonds adhered to the substrate surface by means of Van der Waals forces. The seeded substrates were transferred to ASTeX 6550 series diamond reactor where the growth of BNCD took place.

For fabrication of flexible diamond MEAs, BNCD was used as the active conductive layer. 100nm BNCD film was grown with MWPECVD method using 2750W and 22Torr in 570°C, 3% Methane and 10000ppm boron concentration. The acquired BNCD thickness was sufficient to cover the area which comes to contact with the tissue in the biological experiment. The measured resistance of the film varied from ~1 kΩ to ~50 kΩ across the substrate. To pattern the BNCD film into the elliptical shaped contact areas, a photolithography step was used with a new negative photoresist. An adhesion promoter (for photoresist), MCC primer 80/20 (Micro resist technology, GmbH) was spin coated on the BNCD surface for 30 seconds in 4000 rpm and baked on the hotplate at 110° C for 2 minutes. Then, the negative lift off photoresist ma-N 1420 (Micro resist technology, GmbH) was spun onto the surface for 30 seconds in 3000rpm and

baked at 100° C for 2 minutes. Subsequently, the sample was exposed to the UV light (i-line: 365nm) of Karl Suss MA55mask aligner for 40 seconds using the desired photomask (Figure 4-8). Once the photoresist was exposed, the sample was developed in ma-D 533 S developer (Micro resist technology, GmbH) for 150 seconds. The remaining photoresist covered the whole surface of substrate but the ellipses. After rinsing and drying, the substrate was next ready for metal deposition. In this step, the choice of the metal as a mask was important. The metal layer needed to adhere well to diamond. Similarly, resistance to diluted HF (H_2O: HF ratio 10:1) solution was a must, regarding the last step of the processing. That is why Cr was selected. Thus, about 300nm of Cr was deposited on the surface and then lifted off in Acetone. Finally, Cr ellipses covered the diamond film, then oxygen plasma was employed to etch the un-masked diamond by means of RIE process, using 300W and 50 sccm of oxygen in few mTorr pressure. After the etching was done, the BNCD ellipses masked with Cr were pattered on the substrate and checked under SEM (Figure 4-24).
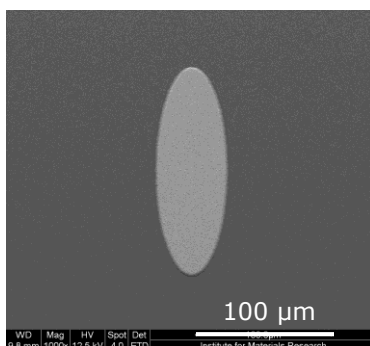
Figure 4-24. SEM image of the BNCD ellipses coated with Cr.

PI coating and challenges. The coating and patterning of Polyimide PI2574 as the insulating layer was challenging, because finely structured definition of the polyimide was required. One step of Acetone cleaning and dehydration on the hot plate (at 180°C for 5 minutes) was performed to prepare the surface for PI coating. A relatively thick layer (~12μm) of Polyimide 2574 was coated on the surface and patterned to insulate the diamond electrode arrays masked with Cr. For that, PI was spin coated on the substrate for 5 seconds at 500rpm and then for 30 seconds at 2500 rpm, and baked on the hotplate at 120°C and 150°C for

30 seconds each. Since PI2574 is not photosensitive, the positive photoresist S1818 was spin coated on the sample for 30 seconds at 3000 rpm and baked at 90°C for a minute. The sample was exposed to the UV light for 8 seconds using the 'PI-1 insulating' photomask shown in Figure 4-9.

After exposure, the Polyimide was developed. For the developing step, besides ma-D 532 S, ma-D 533 S could also be used as dip-development. Both developers are TMAH-based and contain surfactant, however, ma-D 532 has lower concentration of TMAH than ma-D 533 S. Polyimide 2574 is, however, generally supposed to be best-developed in NaOH-based developers; yet, experiencing with patterning thick PI by dip-developing showed that the two chosen developers worked better. Both developers have been used in this project for PI development. For the beginning, ma-D 532 S was chosen because of lower TMAH concentration. However, our practice indicated that ma-D 532 S damaged the surface since it took longer to develop the thick polyimide (Figure 4-25). After developing, the photoresist still needed to be cleaned by Acetone, and that also affected the surface.
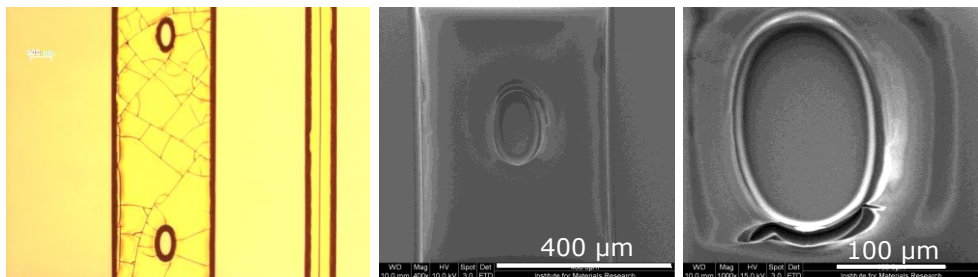
Figure 4-25. Unsuccessful patterning of Polyimide in long developing time with ma-D 532 S.

Since there were fine structures to be patterned by PI, SEM was used to investigate how polyimide appeared after curing. Since the structures in the new designs were finer, it was extremely difficult to get a clear cut end in the structure with ma-D 532 S developer. Developing took several minutes. The resulting PI surface was shown to be useless to process further and the ellipses seemed to be over developed. It was because the dip-development or 'wet etching' of PI in microfabrication occurs 'isotropic'. In this case the development

happened in all directions, i.e. horizontally as well as vertically. Horizontal development causes unavoidable results in side walls of the pattern which initiates significant undesirable changes in further processing steps (Figure 4-25).

To solve this issue, some conditions needed to be checked and adjusted. The UV exposure time was adjusted for the S1818+PI patterning to be 16 seconds instead of 8, because the lamp was too old to produce light with required intensity. Also the use of the other developer was necessary. Polyimide was developed in ma-D 533 S for ~50 seconds and then immediately transferred to a water bath. This additional step prior to rinsing by DI water was found to be essential to the surface of PI because rinsing cannot remove the developer from the whole surface at once. Thus, the developer might still work in some areas while being washed in other areas. Working longer means starting to over-develop or damage the surface. Since the polyimide was only baked shortly at moderate temperature, it was not fully resistant to the developer. So the parts that were even masked by the photoresist could also be attacked by the developer at some point. That is why the developing time was critical as well as cleaning and washing steps. After cleaning the substrate in the water bath, the substrate was then rinsed well with water and dried. Our experiences indicated that sometimes the surface needed longer cleaning and rinsing with DI water. It could also need few more seconds of development to fully develop the layer without damaging the surface. In the last step, the photoresist was removed by acetone for 5 seconds. Then the surface was rinsed well with DI water and blow-dried.
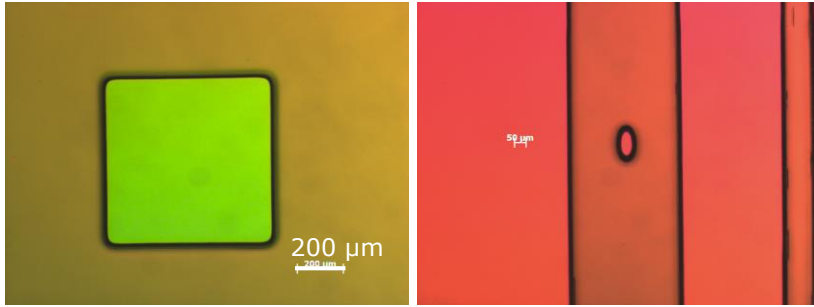
Figure 4-26. Successful patterning of Polyimide using stronger developer and shorter developing time.

Finally, the Polyimide layer was ready to go under curing step, which was a necessary step to drive out all the solvents in the layer and transfer the polyimide precursor to the polyimide. By adjusting several conditions, successful patterning of polyimide 2574 by dip-development was achieved (Figure 4-26).

The cured polyimide is resistant to different variety of solvents and chemicals. Therefore, the microfabrication was preceded. To progress with the patterning, one must have the clean sidewalls of polyimide and a film surface without disconnections and cut-offs. Although the curing step was a stressful step for polyimide film, it was still possible to get a continuous film and clean sidewall with wet development. With some other types of polyimide such as PI-2600 series, only dry etch (plasma etch) is possible as developing step, using CF_4 plasma for etching. The advantage of dry etching is that the resulting structure is very clean and the surface is not damaged. However, as plasma etch is anisotropic, therefore the resulting structure will have sharp and straight sidewalls, despite the present method which gives round sidewalls. So one might conclude that dry etch was preferred in order to avoid the round sidewalls, while round sidewall was actually beneficial for our purpose. Because in the following steps, photolithography needed to be executed, a round sidewall would let the photoresist coat, get exposed and pattered nicely on the polyimide layer. Patterning the photoresist on the sharp straight walls seems to be problematic.

Once the PI was cured, it was ready for further microfabrication procedure. Following, connecting lines and contacts were defined to connect the ellipses to

the connectors using photolithography and metal deposition. In the lithography step, the negative lift off photoresist was applied and exposed to the UV light using the photomask shown in Figure 4-10. The ellipses in this mask were patterned as big as the BNCD ellipses to make sure they cover the whole active conductive area, even with a probable misalignment (as explained earlier due to the thickness of PI).

The surface was exposed for 40 seconds with the aligned 'conductive' mask and then developed in the ma-D 533 S for 75 seconds. After the lithography, chromium and gold were deposited. 100nm of gold was sputtered on the surface of substrate. Prior to that, a very thin layer of chromium was deposited to improve the adhesion of gold to the polymer and BNCD. However, after lift-off in acetone, most of the metal layer peeled off from the surface of wires, ellipses and square contacts. Investigating about the issue, SEM images showed that the metal layer was removed from the areas, which most probably had photoresist residues. This means the photoresist was not developed completely in the lithography step (Figure 4-27). Thus, there has been leftovers of the resist in areas where should not be, and consequently lifted off the metal layer undesirably.
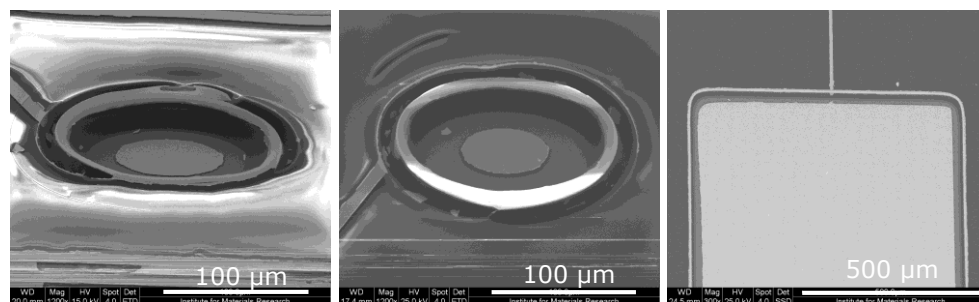
Figure 4-27. Disconnected metal areas due to poor definition of the photoresist. It is obvious from the SEM images that the narrow line shape is not connected to the elliptical or square shape. Also, there is no continuous film inside the ellipses and squares.

For patterning the metal by lift off method, one needed a clear defined side wall photoresist structure, otherwise when the metal was deposited (also) on the walls, after the lift off, it would be lifted off and may damage the area next to

them. As a test, the same photoresist was coated on a test sample, baked and exposed, but developed in different timings. SEM results showed that the best result came from developing the resist for 150 seconds in order to get finest definition for the structure.
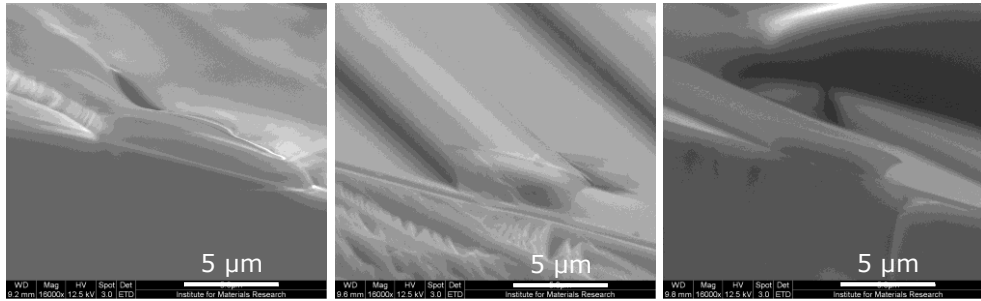
Figure 4-28. The negative photoresist developed with different timing. Left: 75s, Middle: 120s, Right: 150s.

Once the developing time for the photoresist was adapted (150 seconds), photolithography was performed to pattern the metal on polyimide structures. The photoresist lines were indeed patterned with ~2μm sidewalls (i.e. the horizontal distance between the lower edge and higher edge of the photoresist layer, as visible in Figure 4-28) and that seemed to be enough to have a clean straight line. However, transmission optical microscopy images showed that there was excess amount of photoresist 'pooled' inside the ellipses and around the squares (Figure 4-29). The leftover of the photoresist showed that it was not fully developed in 150s, although the lines were finely defined and developed. The cause of this issue could be the topography of the polyimide surface. As the PI layer was defined with a certain thickness, the spin coated photoresist tended to pool inside the ellipses [91] and did not get out of the ellipses by such spin speed. This formed a thicker layer of resist inside the ellipses which could not be developed in the defined time. This was one of the disadvantages of the spin coating technique for the negative photoresist.
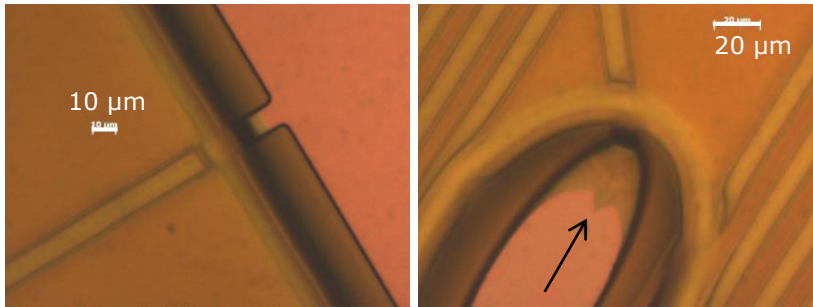
Figure 4-29. The photoresist thickens around the edges and pools inside the deep ellipses.

Also as visible in Figure 4-29, it is not easy to determine by optical microscopy where the polyimide ellipse top and down part was, and one could not say what happened in the darker areas in the ellipses.

One solution for this issue was to develop the photo resist longer. However, by increasing the developing time, the narrow patterned lines disappeared as all the photoresist developed completely. Another solution was spinning at higher speeds. To overcome the issue, an extra spinning step was added after the final spin coating, which introduced the spinning at 6000 rpm for 5 seconds. By this fast accelerated spinning, it was possible to get rid of the bulk of the photoresist that was pooled in the ellipses and consequently define them correctly.

SEM measurement helped looking precisely onto the structure and determining the regions (Figure 4-30). A successful photoresist patterning was finally achieved on polyimide structure.
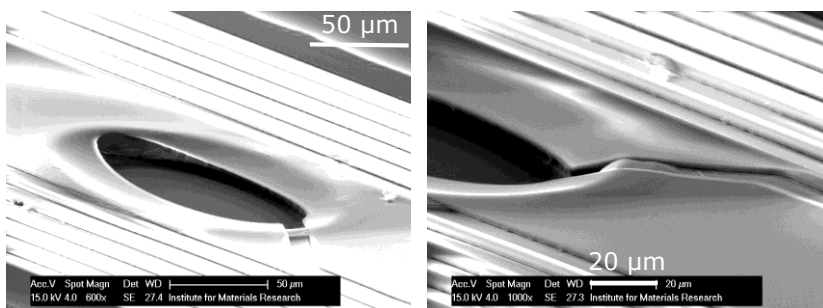
Figure 4-30. Negative photoresist patterned correctly on the polyimide structure.

Once the photoresist patterning issue was solved, the adhesion of metal to polyimide was examined. Since the metallic patterns peeled off in the first try, it became clear that the polyimide surface was naturally passive and the adhesion to metal did not occur easily. The surface of polyimide needed some pre-treatments to activate the surface with functional groups and help adhesion to novel or non-novel metals [92]–[94]. Therefore, a step of surface pre-treatment was done prior to lithography for metal patterning. This step included oxygen treatment of the surface in a RF plasma reactor, using 100W and 35 sccm of O_2 for 5 minutes. Testing with scotch tape showed that a layer of chromium and gold (Cr/Au) would not detach from the PI after surface treatment.

Finally, performing the pre-treatment on the actual sample, the resulting conductive structure was formed in Cr-Au and showed a perfect patterning of metal lines as well as ellipses and square contacts on PI without any disconnections. These metal parts were responsible to connect the BNCD ellipses to the defined squares to attach to the measurement device.

The process followed by complete insulating of the electrodes by polyimide. The same processing step was implanted to coat and pattern the PI layer, using the 'insulating' photomask#2 (Figure 4-11).

In this step, the development could also be done with ma-D 532 S developer; since PI covered the whole electrodes and no fine structure definition was needed. As the topography of the walls was not critical, a lower concentration of TMAH could also be used with longer developing time. After the development, the masking positive photoresist was cleaned by acetone and then sample was ready for curing (Figure 4-31).
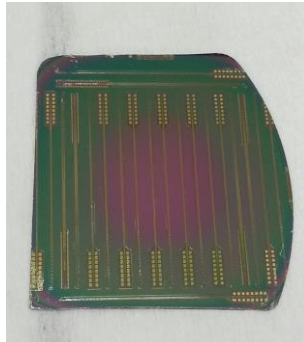
Figure 4-31. BNCD-polyimide electrodes fabricated on Si wafer, ready for curing the PI.

Releasing of the electrodes and issues. Once the curing was done, the electrodes were ready to be released. The releasing of the electrodes (i.e. the etching of SiO_2) was done in a diluted mixture of Milli-Q water and HF (H_2O: HF ratio 10:1) in a Teflon beaker. Depending on the thickness of the SiO_2 to be etched, it took a day to several days for electrodes to be released one by one.
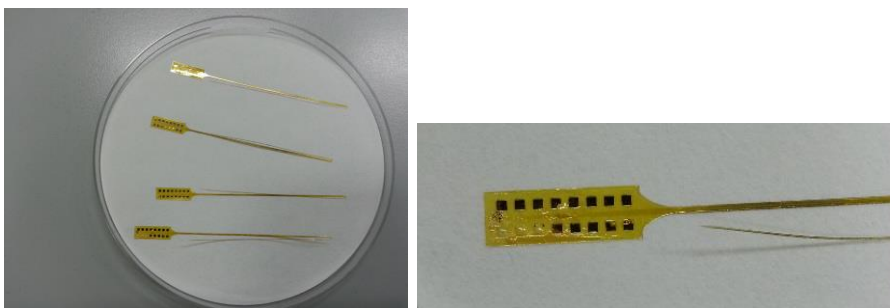
Figure 4-32. First set of the released electrodes: some square contacts are detached due to weak adhesion to polyimide.

Once these electrodes were released, it was observed that some metallic squares detached from the electrode (Figure 4-32). Investigating the causes, it was revealed that the last polyimide layer did not have a good adhesion to the metallic patterns. The metallic wires and ellipses were sandwiched between polyimide and diamond layers, but the square contacts were only coated with polyimide on one side, and were exposed on the other side.

To solve the issue of detaching metal squares from the electrode, at the stage of metal deposition, another thin Cr layer was coated after the gold layer. Then the metallic top surface was pre-treated by oxygen plasma and prepared for polymer coating. Therefore, the same oxygen surface treatment was performed to enable successful coating of PI on metal. With such strategy, the attachment of the metal to the PI layer was guaranteed. Therefore, new samples were prepared and for metal contacts, 15nm of Cr, 100nm of Au and again 15nm of Cr were deposited and treated with O_2 plasma as explained above. At the end, sample was insulated with PI layer and cured. The electrodes were released and finally, the resulting released electrodes were transferred to a water bath for cleaning and dried on clean room tissue. There were no issues during the releasing procedure and the contacts showed excellent adhesion to the polyimide. The final electrodes had the total thickness of ~25μm, which are presented in the result section.

4.3.5 Characterization of the EMG electrodes

Surface characterization of the electrodes. Several techniques were employed to investigate the patterning of the electrodes on the substrate. Scanning electron microscopy (SEM) technique (using Fei Quanta 200 F setup) and optical microscopy were used in every step of fabrication to assure the correct definition of the structure and assess if there were defects. Raman spectroscopy (using HORIBA Jobin Yvon T64000 spectrometer) was performed on the BNCD area of the electrodes to confirm the presence of diamond. Atomic Force Microscopy (AFM) studied the topography of BNCD film from the seeding sites by means of a Bruker Multimode 8 with a V series controller setup in the tapping mode. AFM and Raman spectra were measured after the electrodes were released. The Polyimide layer thickness was measured finally by dektak ST3 profilometer.

Preparation for measurements *in vivo*. A set of customized-designed PCB boards were received from university hospital in Göttingen to attach the electrodes. These PCB boards were used to connect the electrodes to the

measurements devices. The electrodes were glued to the PCB boards using Digi-Key, CircuitWorks CW2460 conductive epoxy, and were sent back for biological measurements (Figure 4-33).
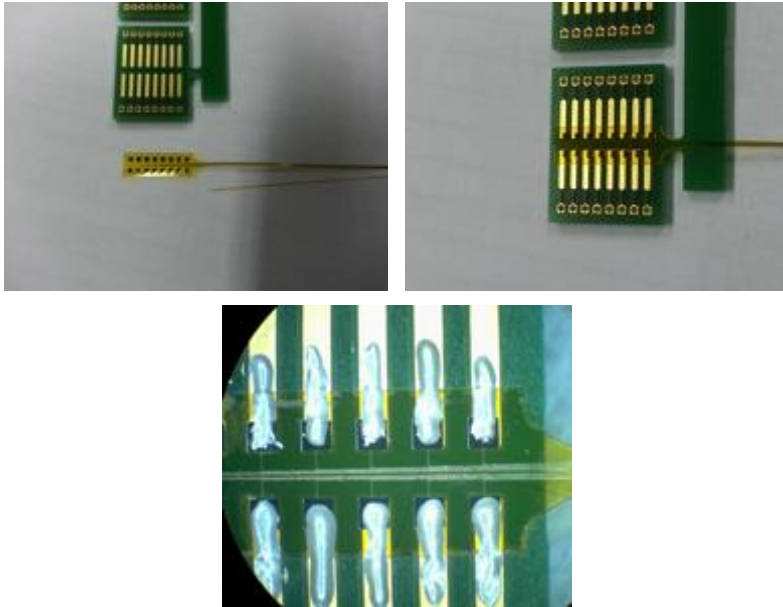
Figure 4-33. Final diamond-polyimide EMG electrodes were glued to the customized PCB board.

4.4 Results and Discussions

Flexibility of diamond/polyimide electrodes. The final diamond- polymer electrodes with the thickness of ~25um were successfully fabricated (Figure 4-34) and released in diluted HF, by etching the sacrificial layer.
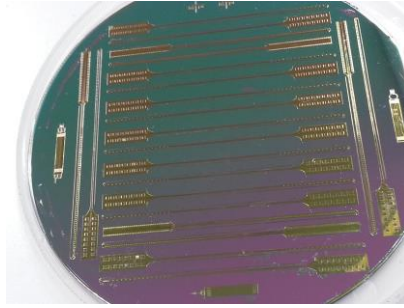
Figure 4-34. Final fabricated electrodes on Si/SiO$_2$ substrate.

The released diamond- polymer electrodes were excellently flexible and suitable for implantation (Figure 4-35).
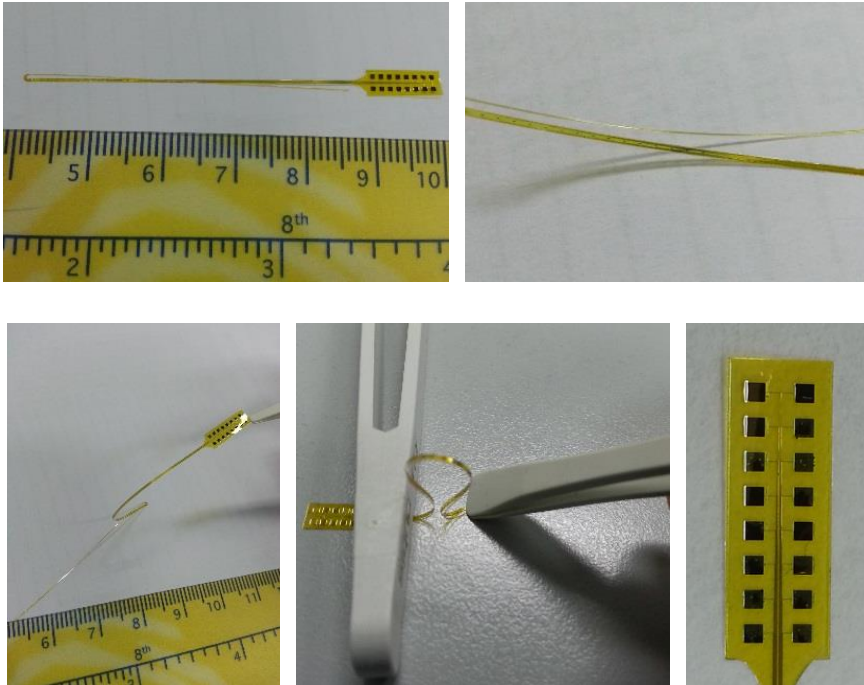
Figure 4-35. Successful releasing of flexible diamond- polymer EMG electrodes.

Characterization of EMG electrodes. Optical microscopy as a preliminary enquiry of the fabrication steps, as well as SEM imaging, proved that BNCD ellipses were defined correctly (Figure 4-36). Moreover, the first insulating polyimide layer was patterned in accurate alignment with the BNCD ellipses

(Figure 4-37). Likewise, metallic connecting lines were shown to connect the ellipses to the squares well (Figure 4-38).
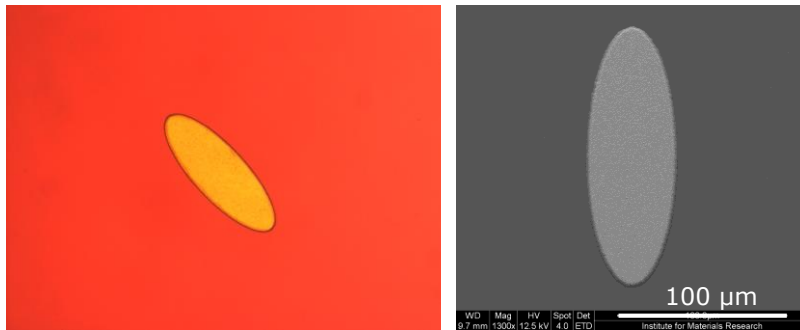
Figure 4-36. Successfully fabricated BNCD ellipses shown by microscope and SEM images.
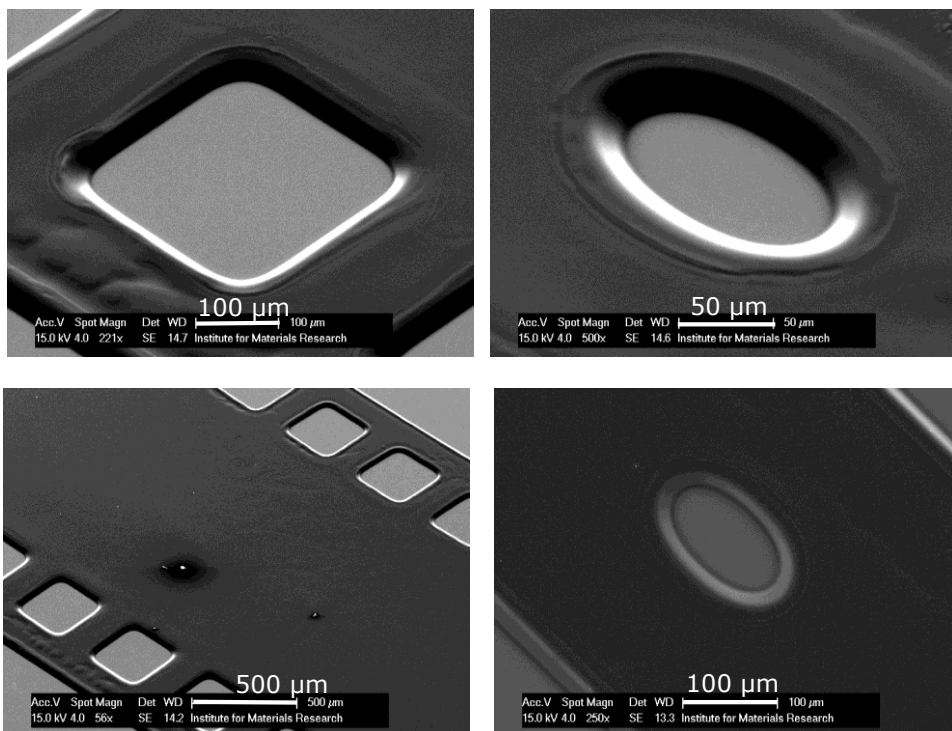
Figure 4-37. Successfully patterned and cured Polyimide with adapted conditions. Correctly defined areas for elliptical and square contacts are visible.
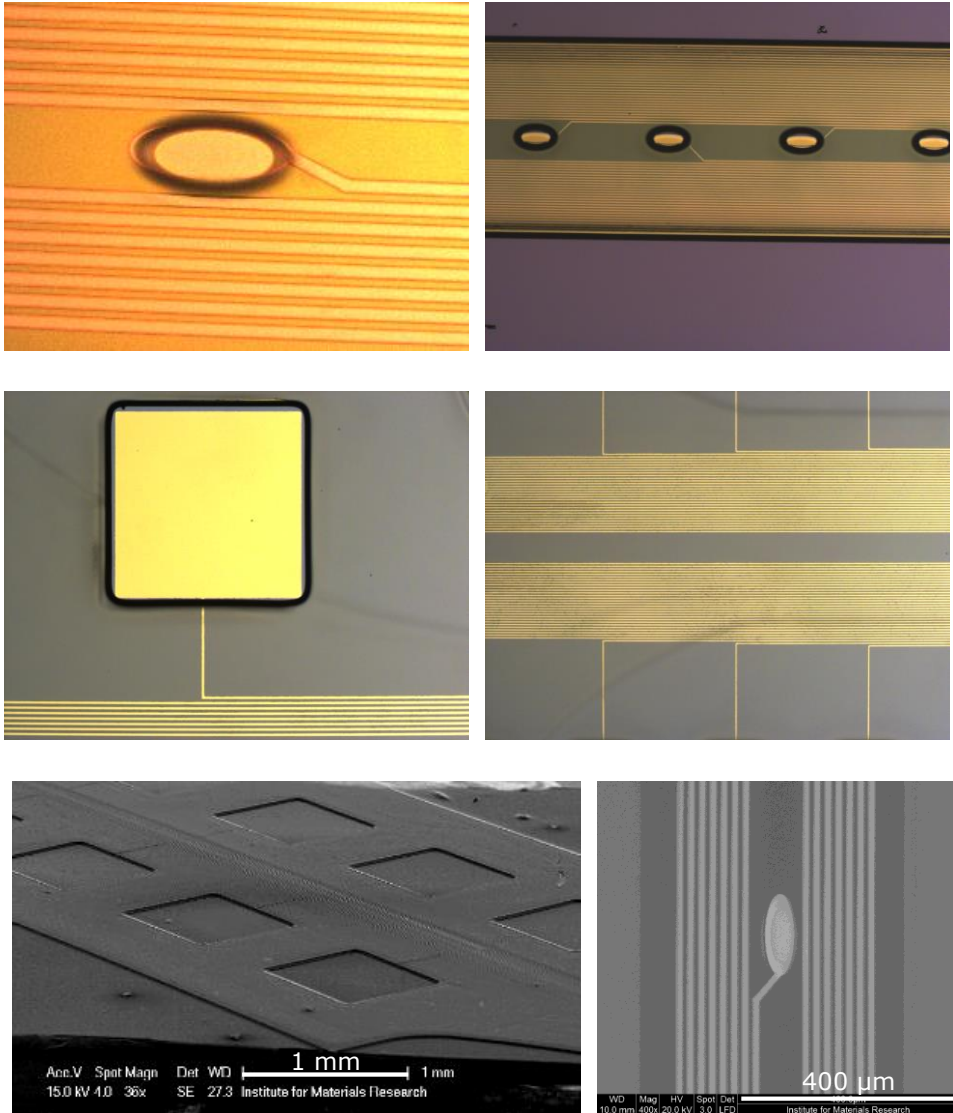
Figure 4-38. Microscopic and SEM images of successful Patterned metallic structure on polyimide and BNCD.

The final electrodes have been examined under SEM to make sure the connections between the ellipses and wires or the squares and the wires were decent after coating the PI and releasing. However, since the lines were covered with a layer of ~12um polyimide, they were not visible very well. Yet, one could see the connections were established (Figure 4-39).
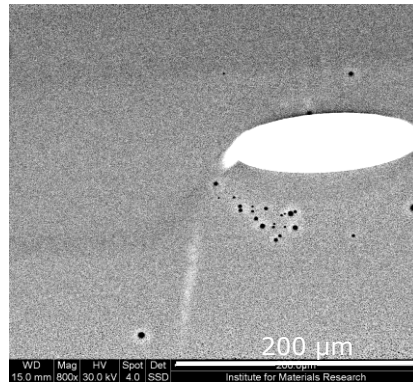
Figure 4-39. SEM study showed the connection of the lines were established to the ellipses.

Once the electrodes were released, the diamond sites were examined with Raman spectroscopy to confirm the presence of diamond (Figure 4-40). The diamond film was, however, already checked after the growth of BNCD layer, by SEM technique, looking at the grown surface of BNCD. Yet, after releasing of the electrodes, the top side of BNCD which was coated with metal and polymer, was not visible anymore. Therefore, Raman spectroscopy was used to acquire information about the presence of BNCD on the released electrodes.
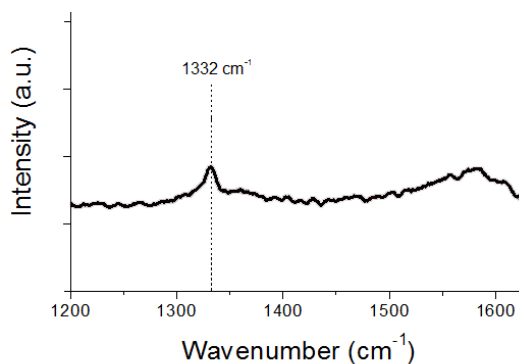
Figure 4-40. Raman spectroscopy of BNCD nucleation sites on the released electrodes, confirms the presence of diamond on the electrodes.

The diamond peak at 1332 cm^{-1} is visible in Raman spectra. The side broad band on the right is related to disordered carbon and graphitic impurities in the layer [30].

We performed several SEM measurements on the backside of BNCD film on the released electrodes. However, since the film starts to grow on an extremely smooth Si/SiO$_2$ surface, the nucleation sites look very smooth as well. That is the reason acquiring the morphology of BNCD nucleation sites in SEM was not useful. The nucleation sites of diamond (BNCD) grown on Si/SiO$_2$ were then examined by AFM. AFM results showed that seeding sites of BNCD look totally different from the grown surface of the film (Figure 4-41). It can be concluded that diamond seeding site looks more like UNCD surface [75], [95].
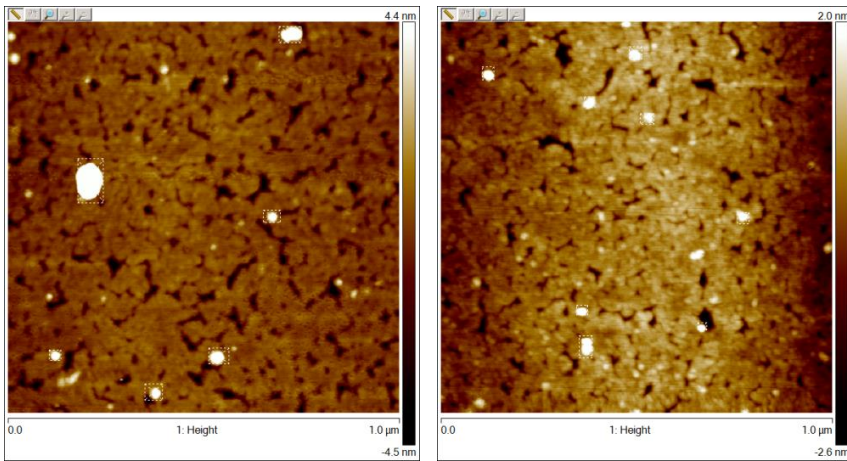
Figure 4-41. AFM images of the BNCD nucleation sites on the released electrodes.

After these investigations, it was confirmed that diamond-polyimide EMG electrodes were successfully fabricated.

Impedance measurement of the electrode. An in-house impedance analyser was used to measure the impedance of the BNCD electrodes of the flexible MEAs. For that purpose, the electrodes sites were placed in PBS solution together with a gold wire as a reference electrode to be measured. The measurement contact areas of the electrodes were kept outside of the PBS to connect to measurement probe of the analyser.
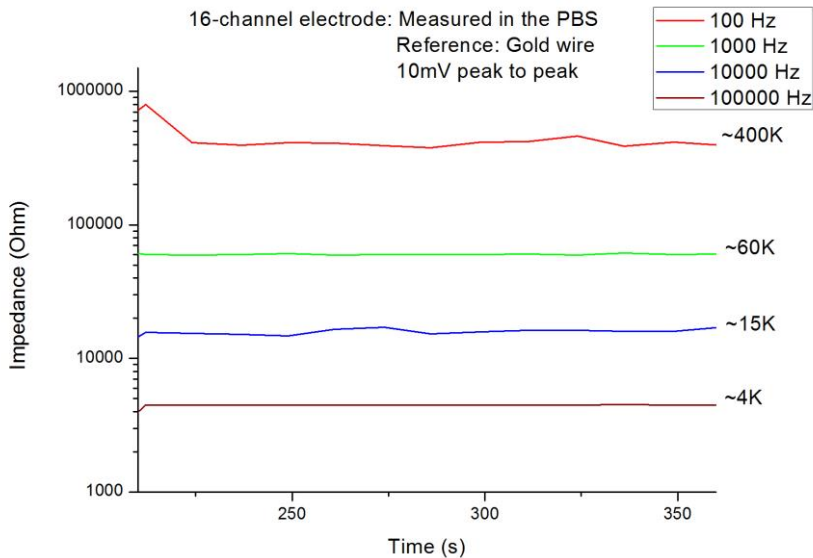
Figure 4-42. The impedance of the BNCD electrodes in different frequencies across time. Impedances are shown in different colours for different frequencies. The measurements seem to be stable across time.

10mV potential difference was applied between the electrode contact and the reference electrode. The impedance of the channels were measured in a time frame at different frequencies, ranging from 100 kHz to 100Hz (Figure 4-42). The description of the analyser setup can be found in an article from the Material research group of Hasselt university [96]. The impedance measurements of the flexible diamond electrodes confirmed the functionality of the fabricated EMG electrodes.

4.5 Conclusion

We have demonstrated step-by-step microfabrication technology leading to successful preparation of multichannel electrode arrays made solely of diamond and polyimide. The resulting electrodes are flexible, and the sizes and thickness of them are suitable for the EMG implantation. Raman measurements confirmed the presence of diamond in the active measurements areas of the electrodes.

Optical microscopy, AFM and SEM were used to characterize the surfaces in each step and confirmed the well-defined structures of the MEAs. The impedance measurements presented acceptable impedance of the diamond-polyimide EMG electrodes. In frequencies ranging from 100 kHz to 100Hz, the electrodes showed impedances below 400 kOhms. In the frequency range of biological measurements (i.e. 1000Hz) the electrodes showed impedance of around 60 kOhms which is comparable or better with similar type of electrodes used for EMG.

These EMG electrodes will be used in the future works to drive artificial prosthetic devices and to measure the EMG signals in muscles. The EMG signals can be analysed to detect medical problems or abnormalities, as well as diagnose the neuromuscular diseases and other EMG applications.

5 Functional Bio-molecular Monolayers on Diamond using PEI:
A novel paradigm for construction of Man-Machine Interface

This Chapter is devoted to experimental results related to using Polyethyleneimine (PEI) polycationic polymer coating on the diamond films as a promoter for neuron growth. Whilst in the third and fourth chapters we have developed MEA technology for *in vitro* and *in vivo* application, in the present chapter we attempted to find such surface functionalization that would enable to use electrodes without inducing any cellular toxicity. We present the development of original technique to overcome the cell toxicity issue of neuron-device interface based on PEI monolayer interfaces. We have found that diamond surface properties enable formation of such PEI monolayer that is strongly chemically bound to the diamond surface. Due to this chemical bonding, the released of cell toxic PEI molecules can be avoided and functional neural coatings can be developed on diamond. Electrochemical properties have been studied on the PEI–coated diamond electrodes and have shown favourable characteristics for construction of neural interfaces. Along with this research, we refer to the following article in preparation for submission to 'advanced functional materials':

Farnoosh Vahidpour, Kathleen Sanen, Matthew McDonald, Zuzana Vlčková Živcová, Elena Gjorgievska , Yaso Balasubramaniam, ,Ken Haenen, Ladislav Kavan, Marcel Ameloot, Anitha Ethirajan , Hans-Gerd Boyen & Milos Nesládek; *Functional Bio-molecular PEI Monolayers on Diamond- A Novel Approach for Construction of Man-Machine Interface.*

Abstract

Boron doped Diamond (BDD) is anticipated to serve as highly performing electrode material for applications to bioelectronics exploiting its unique

electrochemical potential window of 3.5 V, biocompatibility and excellent chemical stability. In this work, we report on a method for creating strongly bonded atomically-thin monolayers of poly-cationic PEI organic polymer on BNCD that is used as a promoter for neuron growth. PEI is widely used for biomedical applications; however, its drawback is the toxicity. Here, we demonstrate a technique for stripping PEI to atomic monolayer that is strongly chemically bound to diamond surface. PEI further upgrades the diamond electrochemical performances, such as the value of double layer capacitance, while keeping the width of the electrochemical potential window. We demonstrate that BNCD thin films coated with the PEI monolayers solve the toxicity problem due to strength of PEI bond to diamond that is enabled by electronic band bending at the diamond surface. This enables using PEI coatings in the wide range of biomedical applications involving the biological cell adhesion. We discuss in detail the mechanism of formation of PEI monolayers on Boron doped diamond, monitored by X-ray Photoelectron Spectroscopy (XPS). Further on, we study electrochemical properties of BNCD- PEI hybrids. We use PEI – diamond hybrid structure for engineering neural – solid state interfaces and demonstrate successful neuron culturing on such surface. The adhesion of neural cell is enhanced by electrical charge attachment of extracellular matrix (ECM) components on the PEI surface.

5.1 Introduction

The interface between living neural cell and man-made artificial electrode is the key component in brain-machine devices. Micro/nano electrode arrays (M/NEA) for studying neuron cultures *in vitro* or *in vivo* as prosthetic or therapeutic implants are examples of such interfaces. Recent works of nano-scale interfaces allow coupling single neurons to single electrodes [97] and assure transferring the neural signal to MEA with a high fidelity and high signal/noise ratio [17], [97].

Due to its largest known electrochemical potential window of 3.5 V, man-made synthetic boron doped diamond was suggested to be ideal material for capacitive

coupled MEAs [27], [50] with no faradic electrical current component in biological buffers. Diamond surface can be nano-engineered, providing large surface with high electrochemical capacity [98], [99] and thus provide high double layer capacitance. Diamond has an additional advantage in very high chemical stability and it is highly biocompatible [36], [48].

However, despite reported biocompatibility in cellular environment, it has been shown that diamond surface does not provide a permissive surface for neural growth [63], [100]. An important step for making diamond a permissive substrate for neurons is functionalizing diamond surface with ECM molecular promoters such as Poly-L-Lysine (PLL) or Polyethyleneimine to encourage culturing primary neural to adhere and outgrow [15], [16].

PEI has been commonly used in neuro-engineering to enable neural growth on MEAs for *in vitro* cultures promoting the adhesion of neurons on the surface of various metallic alloys, for example in TiN-based MEAs [12]. The positively charged PEI allows stimulating the attachment of Cell Adhesion Molecules (CAMs) and assists the neural growth. Nevertheless, it is known that PEI has also toxic effects for various types of cells, including the neural cells, and is not suitable for *in vitro* cultures. PEI can disrupt the cell membrane if it is not used in the right concentrations [35], [65], [101]–[103].

Here, we present a method that can be used for constructing highly stable neuro-electrical interfaces on diamond based on fabrication of PEI poly-cationic polymer monolayers that are very strongly adhered by chemical bonds to the diamond surface. We demonstrate that the diamond surface has a unique capability for forming such monolayers, with specific advantage of serving as neuron adhesion promoter and at the same time preserving the unique electrochemical properties of diamond electrodes. We show that by using diamond in combination with PEI, the problem of cellular toxicity can be solved; PEI is strongly bound to the diamond surface and practically irremovable, even in very harsh chemical environment. By chemically stripping PEI to monolayer, no PEI can be released to the cellular environment, insuring no toxicity. Functional PEI monolayers on diamond are studied by XPS and by electrochemical Impedance Spectroscopy (EIS). We evaluate the band bending

at the diamond surface and establish that it is essential for enabling a strong bonding of PEI to diamond. Rat's cortical neurons are cultured on PEI monolayer coated diamond thin films to demonstrate the usability of the procedure for constructing of neuron interfaces.

5.2 Experimental Methods

Substrate preparation for XPS study. Different types of substrates were used in this study: BNCD thin film grown on Fused Silica substrates and epitaxial boron doped diamond films grown on un-doped diamond single crystals (BSCD).

Prior to the CVD epitaxial growth, the [100] oriented single crystal diamond substrates were treated for 20 minutes with 1:1:10 mixture of H_2SO_4, HNO_3 and bi-distilled Milli-Q water, while heated until fuming. Then, each sample was rinsed thoroughly with bi-distilled Milli-Q water and then blow-dried.

The B-doped epitaxial films on single crystals (BSCDs) were grown in an in-house diamond reactor using 1% CH_4, 10000-20000 ppm TMB, 200W and 56 Torr in 960°C. The following growth conditions [Table 5-1] were used to grow epitaxial boron doped diamond on the single crystals:

Table 5-1. Boron doped epi-layer growth conditions for Single crystals

Conditions	Sample:1	Sample:2	Sample:3
CH_4 (sccm)	0.1 %	0.1 %	0.1 %
B-doping (ppm)	10000	15000	20000
Temperature	960°C	960°C	960°C
Pressure (mBar)	75	75	75
Surface Roughness	4.84 nm	5.51 nm	6.26 nm
Resistance	5 – 6 KΩ	3 – 4 KΩ	5 – 6 KΩ
Layer thickness	280 nm	280 nm	280 nm

For BNCD growth, the fused silica substrates were cleaned by standard wafer cleaning procedure method, RCA1,2 [76], to prepare for diamond growth. Next,

150nm BNCD film was grown on these substrates in ASTEX 6550 MPECVD system, using 1% Methane (CH_4), 5000 ppm TMB, 3000W, 37 Torr in 700°C [Table 5-2].

Table 5-2. Growth conditions for BNCD grown on fused silica substrates.

Conditions	CH_4	B-doping	Temperature	Pressure	Power	Layer thickness
BNCD film	1%	5000 ppm	700°C	37 Torr	3000 W	150nm

After the diamond growth, all the samples were treated with the same procedures as explained, i.e 20 minutes cleaning with 1:1:10 mixture of H_2SO_4, HNO_3, and H_2O to remove any possible graphitic impurities from the diamond surface and to oxidize. These samples were kept in clean and closed boxes until PEI treatment. The oxidation procedure is found to be a key prerequisite for the PEI treatment of diamond films.

PEI treatment for EIS and XPS measurements. (Procedure I). After the cleaning step**,** all the samples were soaked in 0.1% PEI solution (w/v – weight per volume) of PEI (Sigma-Aldrich) in bi-distilled Milli-Q water for overnight treatment. After that, the solution was removed and samples were rinsed 4 times, each time by 1,5ml bi-distilled Milli-Q water and blow-dried. The full protocol used for PEI coating of diamond surface, is mentioned below.

Detailed protocol for PEI coating on diamond surface. The samples (for example MEA surfaces) are flushed with fresh bi-distilled water, then the wet MEAs are autoclaved. Next, they are coated with Polyethyleneimine solution using standard PEI protocol below. The surface is initially cleaned by the described cleaning procedure, to have ultraclean and oxidized surface.

1- *The PEI concentration that is normally used is 0.1 % w/v in sterile Milli-Q water. Few microliter of PEI was measured by normal plastic pipettes, (Since the stock PEI cannot be precisely measured into a thin pipette, an approximate measured amount is acceptable). An example dilution to 1% was based on stock solution at 50% w/v, by diluting 20 microliters*

> of stock PEI in 9.98mL or ~10mL of sterile water. Beakers should be used very clean and dry, to minimize the exposure to un-sterile conditions.
>
> 2- Dilution was further processed in ultra-sonicated bath for about 30 minutes to form a homogenous dispersion.
>
> 3- After that, the diamond grown substrates were placed in a clean and dry beaker/ petri dish with this diluted PEI solution, and the beaker is covered (e.g. with Para film). The surface of substrates has to be covered completely with the PEI solution.
>
> 4- Samples stayed covered in the solution for the minimum of ~8 hours (or overnight), and after that, the solution was removed.
>
> 5- The substrates were rinsed 4 times; each time ~1.5 ml Milli-Q water was poured on the samples and then removed (by pipette) to refresh again.
>
> 6- After rinsing, the substrates were dried completely by blow -drying.
>
> 7- Finally, a very thin but full coverage of the surface with PEI molecules is obtained.

Water washing of PEI. (Procedure II). To reduce the thickness of PEI layer we have developed following procedure based on washing in Milli-Q water. For this purpose, the PEI coated sample was rinsed with Milli-Q water by means of a microfluidic device as a flow cell (with the volume of 30µl/min) to perform "striping" of PEI layer, for 16 hours (overnight). When the process is finished and the sample is dried, it is finally measured in the XPS set up to investigate the coating and evaluate the strength of PEI bonding to the diamond surface.

SDS washing of PEI. (Procedure III). To further reduce the thickness of PEI layer, Sodium dodecyl sulphate (SDS) with the concentration of 2mM is used. The PEI coated sample is rinsed with SDS by means of the same setup as used in procedure II, for 16 hours. Afterwards, it is rinsed again with Milli-Q water in the same flow cell for 3 hours to remove the residues of the SDS on the surface. The sample is finally dried and measured by XPS to investigate the strength of PEI bonding to the diamond surface.

XPS survey scan. Immediately after adsorption of the PEI layers on top of the diamond films followed by careful rinsing with Milli-Q water (Procedure I), the

samples were transferred to a Physical Electronics (PHI) 5600LS electron spectrometer setup equipped with a small-spot X-ray source providing monochromatized Al-K$_\alpha$ photons (1486.6 eV). The binding energy scale of the hemispherical energy analyser was calibrated by means of an independent Au reference sample, setting the Au-4f$_{7/2}$ core level position to 84.00 eV. For comparison, we have made XPS also on samples stripped by water and SDS (Procedure II, III).

Substrate preparation for neuron culture sterilization: The BNCD Substrates were immersed for 2 h in a 70% EtOH (ethanol) solution. After air-drying in a laminar flow hood, substrates were coated with PEI solution as explained previously, prior to cell seeding.

Primary cortical neuron cultures preparation: E18 Wistar rat embryo brains were isolated and collected in 7 mM HEPES buffered Hanks balanced salt solution (HBSS). Meninges were removed and dissected cerebral cortex were treated in pre-heated HBSS containing trypsin (0.05%) for 15 min at 37°C. After that three times washing with minimal essential medium (MEM) supplemented with 10 % heat-inactivated normal horse serum (Invitrogen) and 0.5% glucose (further referred to as MEM-horse medium) was proceeded. A fire-polished Pasteur pipette was used to mechanically dissociate the cortex tissue that was suspended in MEM-horse medium. The resulting homogenate was filtered through a 70 μm cell strainer and centrifuged at 1000 rpm and 12°C for 5 min. Cells were seeded at a density of 30.000 cells/cm² on the BNCD substrates. 24 hours later, medium was replaced to Neurobasal medium (ThermoFisher Scientific) containing 2% B27 (Invitrogen) and 1% glucose. Cells were grown in a humidified environment of 37°C and 5% CO_2.

Electrochemical impedance spectroscopy (EIS) measurements. The Cyclic Voltammetry (CV) and EIS measurements were performed using a three electrode system in aqueous phosphate buffer solution pH 7.00 (PBS, Sigma Aldrich). The boron doped diamond films with or without PEI was employed as a working electrode (Ag contact with Au wire insulated by epoxy coating), platinum mesh was used as counter electrode and Ag/AgCl electrode (sat. KCl) was used as a reference. The electrochemical impedance spectra were measured

in the frequency range from 100 kHz to 0.1 Hz and in the bias voltage range from 0 V to 0.9 V using AUTOLAB PGSTAT128N potentiostat with the frequency response analyser (EcoChemie). The measurement was controlled by the GPES4 and FRA software. All electrochemical measurements were carried out in Argon (Ar) atmosphere. The equivalent circuit (Figure 5-1) used for our BNCD MEA electrodes consisted of four components: R_s is ohmic resistance of the electrolyte solution, electrodes, contacts etc. is in series with the parallel combination of the space charge capacitance (BDD/electrolyte interface) represented by constant phase element (CPE) and its associated resistance (R_1) in series with diffusion impedance Z_w, the so-called Warburg element regarding slow adsorption / desorption of ions at the interface [52].

The impedance of a CPE equals:

$$Z_{CPE} = B(i\omega)^{-\beta} \tag{5-1}$$

Where ω is the EIS frequency and B, β are the frequency-independent parameters of the CPE ($0 \leq \beta \leq 1$). The value of capacitance, C is obtained from Z_{CPE} as follows:

$$C = \frac{(R_2 \cdot B)^{1/\beta}}{R_2} \tag{5-2}$$

An obvious advantage of this evaluation protocol is that it removes the virtual 'frequency dispersion' of Mott-Schottky plots [104], [105]. This dispersion was often pronounced also on diamond electrodes [53], [52], [109], [110].
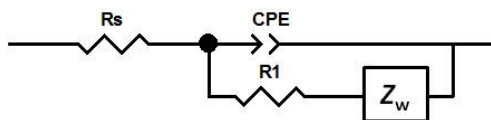
Figure 5-1. Equivalent circuit. Equivalent circuit used to fit the electrochemical impedance spectra for pure BNCD/BSCD and for BNCD/BSCD with PEI on the surface. R_s is ohmic serial resistance, *CPE* is constant phase element, R_1 is the associated charge transfer resistance and Z_w is the Warburg element.

5.3 Results and Discussions

The principle of formation of PEI. PEI in its nature is an electrically isolating cationic polymer material with the band gap of 6.2 eV, i.e. slightly larger than that of diamond (5.4 eV). Providing that PEI layer is chemically stable in electrolyte [108], we estimated that the electrochemical properties of the surface will not change by a substantial manner due to the fact that the PEI has a larger band-gap than diamond. PEI dipolar moments of amine groups in poly-cationic PEI polymers can lead to existence of electrical charged layer at the surface to which PEI is bonded [108]. Recently, in another application, Poly-Ethylene-Imine Ethoxylated (PEIE) or PEI coatings have been used to lower the electrode work function of metals for application to photovoltaics [82], [108].

Boron doped diamond is a p-type semiconductor with Eg ~ 5.5 eV. Boron acceptor level and E_F in semiconducting diamond is at about 0.36 eV from the valence band (E_{VB}). Upon the metallic doping, the E_F shifts towards the valence band of diamond. The oxidization of diamond groups leads to a surface termination with carboxyl or hydroxyl groups with large dipolar moment. By attaching such molecular species with electrical dipole as COOH-, OH-, one anticipates that holes from the Ev of diamond compensate for the negative charge at the surface leading to downwards band banding, i.e. holes from the bulk of B-doped diamond are transferred to the surface, compensating for the dipolar moments. However, as the layer is boron-doped with B- concentration ~ 1×10^{21} cm^{-3}, the surface bending for the full coverage (~ 1×10^{15}) would lead

only to very mild band bending. Upon forming the contact with PEI, it is anticipated that the positive charge present at the amino groups of PEI molecules (as a polycationic polymer) will lead to a strong ionic binding to the diamond surface and force the holes at the diamond surface to deplete, restoring thus the charge balance. By stripping the PEI layer to monolayer, we anticipate that the majority of the positive charge will be removed from the surface leading the surface again practically neutral with a strong bond formed between PEI and oxidized diamond.

To elucidate the surface state of diamond and bonding of PEI to the diamond surface, we have carried out C1s XPS measurements of oxidized diamond surface, diamond with standard PEI coating (procedure I) and with further thinned PEI coating after extensive water and SDS washing (procedure II+ III) to remove residual PEI chains as well as using SDS to strip PEI to monolayers. The thickness of PEI layer is an extremely important parameter of the functionality of the PEI-electrode. When in contact with neural cells, any residual PEI molecules released to the cellular environment are expected to be highly toxic [35], [65], [101]–[103]. In another type of experiments in the solar cell field, PEI was used to match the work function, the thickness was about 10 nm [108]. Such thickness would be, however, too large for biological application due to PEI toxicity. In our case, we have developed an extensive washing procedure (procedure III) to reduce the thickness of the PEI layer to practically monolayers, to provide a non-toxic interface.
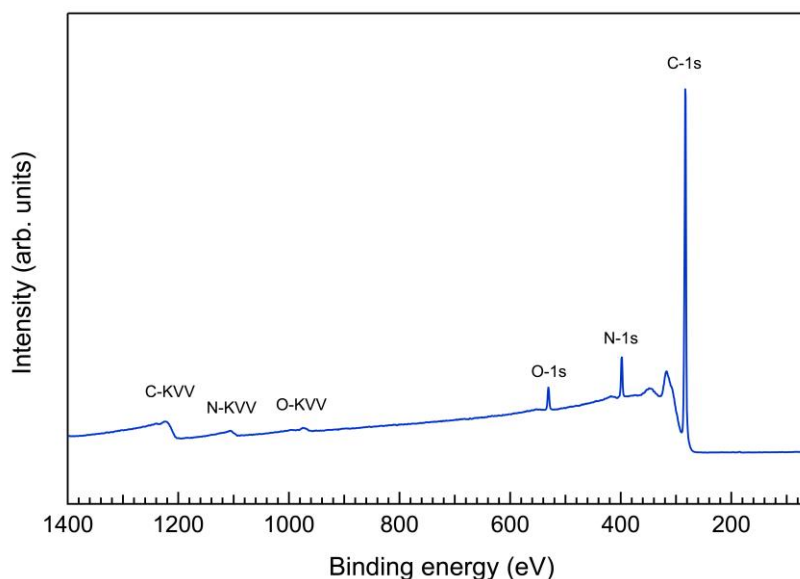
Figure 5-2. XPS survey scan of a PEI treated diamond sample.

Figure 5-2 shows an XPS survey scan acquired immediately after the deposition of a PEI layer on top of a clean diamond film. Clearly, the spectrum is dominated by the C-1s core line (binding energy 284 eV) representing contributions emitted from the diamond substrate as well as from carbon atoms residing in the PEI layer. The successful deposition of a PEI layer at the sample surface can be concluded from the existence of a N-1s peak observed at a binding energy of about 398 eV. The O-1s signal visible at around 531 eV can be assigned to the adsorption of water molecules during rinsing the sample in deionized water. The occurrence of the three elements C, N, and O can also be inferred from the corresponding Auger lines (C-KVV, N-KVV, O-KVV). Besides the (unavoidable) presence of oxygen in the spectrum, no further contaminations can be detected in Figure 5-2. Normalization on residual boron content that is present in epitaxial B-doped diamond and using the B-1s peak intensity (too small to be visible in the Figure 5-2) before and after PEI water washing (procedure I), points toward the thickness of PEI layer of $\sim$ 2- 3 nm.

The corresponding XPS survey scan and C1s peak is shown in Figure 5-3. A clear shift of the C1s peak of diamond surface toward higher energy can be established after PEI coating. XPS measurements after procedure (I) confirms an XPS spectra C1s peak shift of about 0.2 eV to higher energies, i.e. positive charging of the surface. The water washing had no significant influence on the position of C1s peak. However, the procedure III, i.e SDS stripping led to narrowing the C1s peak and shifting of the C1s peak back to lower energies, reflecting the fact that the amount of the positive charge on the diamond surface is reduced by washing out the excess of the PEI polymer. The detailed study of N-1s peak confirmed that after SDS stripping, the PEI is still present at the diamond surface. While the washing with H_2O procedure leads to the PEI thickness reduction as determined by XPS to ~ 3 nm, further extensive SDS stripping (procedure III) leads to the PEI further reduction to ~ 1.2 nm (as determined from XPS), which is practically one single monolayer. Thus, as results of these measurements, it can be confirmed that PEI monolayer is formed and strongly bonded to the surface of diamond and not removable even after very radical washing in SDS detergent. Such PEI – diamond interface layer is anticipated to provide extremely stable interface for neural interfacing.
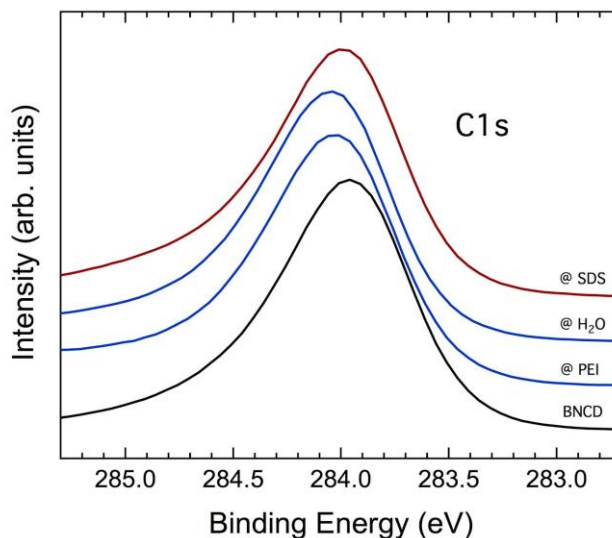
Figure 5-3. C1s peak from diamond, shifting backward and forward, before and after washing procedures.

These data agree with the band model presented above, where by attaching the PEI layer the C1s peak shifted at about 0.6 eV.

EIS measurements. To investigate the electrochemical performances of the PEI–diamond surface (Procedure I, II, III), the diamond electrodes (BNCD), and Boron doped single crystalline Diamond (BSCD) with and without PEI layer, were tested in aqueous phosphate buffer solution pH 7.00 (PBS, Sigma Aldrich) by CV and EIS measurement. We used both BNCD and BSCD films to compare the behaviour of both types of diamond films and to eliminate influence of sp^2 carbon on electrochemical characteristics that is present on BNCD surface [109].

Figure 5-4 shows the cyclic voltammograms of boron doped diamond films (BNCD, BSCD) with oxygen terminated surface and of the same boron doped diamond films modified with the PEI on the surface (BNCD-PEI, BSCD-PEI). The anodic and cathodic currents of water decomposition are slightly larger in the case of boron doped diamond surfaces with PEI (BNCD-PEI and BSCD-PEI), than for pure B-doped diamond surface (BNCD and BSCD). For both cases of B-doped diamond (BNCD, BSCD), it can be concluded that the presence of PEI on the diamond surface does not significantly change its potential window of water stability. This is an important result for the construction of neural electrodes, confirming that the capacitive coupling and low background current as well as large potential window are attained. Additionally, in the case of BNCD and BNCD-PEI (Figure 5-4, left) enhancement of both anodic and cathodic currents have been observed, prior to the water decomposition at the potential of approximately 1 V anodic vs. Ag/AgCl for BNCD-PEI and 1.2 V (anodic) vs. Ag/AgCl for BNCD, and 1.3 for BNCD-PEI cathodic vs. 1. 4 eV Ag/AgCl for BNCD. This can be assigned to the redox and oxidation processes associated with surface oxide functionalities at the sp^2 carbon phase present at the grain boundaries of polycrystalline diamond [110], [111]. The corresponding reduction current localized at functional groups appears at ca. -0.3 V.
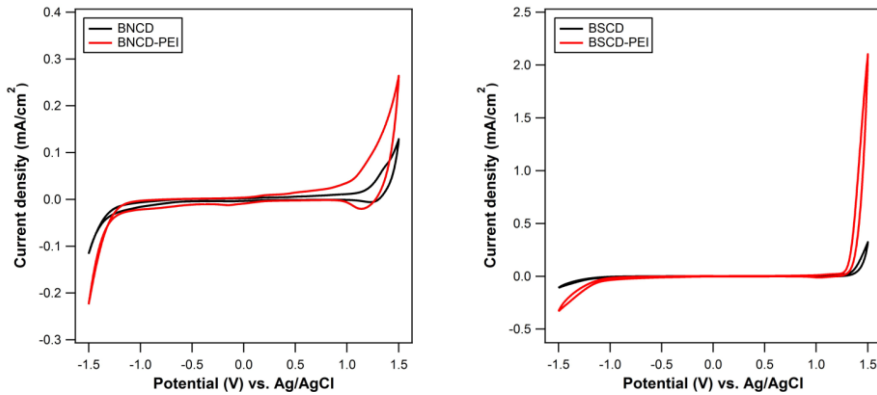
Figure 5-4. Cyclic voltammetry. Cyclic voltammograms of Boron doped NanoCrystalline Diamond (BNCD – left) and Boron doped SingleCrystalline Diamond (BSCD – right) films with PEI (red line)/without PEI (black line) on the oxygen terminated surface. Electrolyte solution PBS (pH 7); Scan rate 100 mV/s. Electrode potentials are given vs. the Ag/AgCl electrode.

The electrochemical impedance spectra were fitted to the equivalent circuit shown in

Figure 5-1 [52], [81], [112]. This equivalent circuit provided the best fits to experimental spectra.

Figure 5-5 shows the Mott-Schottky plots for BSCD and BNCD, with and without PEI coating. The Mott-Schottky equation used to analyse the data is:

$$\frac{1}{C_{sc}^{2}} = \left(\frac{2}{e\varepsilon_0\varepsilon_r N_A}\right)\left(\phi - \phi_{FB} - \frac{kT}{e}\right) \tag{5-3}$$

where C_{sc} is the capacitance of the space-charge (depletion) region normalized to the electrode area, e is the electron charge, ε_0 is the permittivity of free space, ε_r is the dielectric constant of the semiconductor, N_A the number of acceptor per unit volume, φ the applied voltage, φ_{FB} is the flat band potential, k is Boltzmann's constant and T is the temperature.

This plot allows to determine the acceptor concentration (N_A) which is $9.4*(10^{20})$ cm^{-3} for pure single crystalline boron doped diamond (BSCD). For single

crystalline diamond with PEI (BSCD-PEI) on the surface is N_A decreased to a value $4.7 \cdot 10^{20}$ cm^{-3}. The flat band potentials were determined from intercept of the linear part of $1/C^2$. It equals 1.4 V for BSCD while in the case of BSCD-PEI, this value decreased to 0.8 V vs. Ag/AgCl (Figure 5-5). This shift would correspond to upwards band bending. However, we should keep in mind that there are various complicating factors which influence the capacitance measurements and the Mott-Schottky plots. In the case of polycrystalline boron doped diamond (BNCD, BNCD-PEI) containing the sp^2 carbon impurities at diamond grain boundaries, the impedance measurements showed another surface behaviour based EIS data, see Figure 5-5 left. Although the Mott Schottky analysis is feasible even on heavily doped diamonds by providing correct N_A values, the flat band potentials can exhibit a significant alterations due to double-layer and the other second-order effects [109].
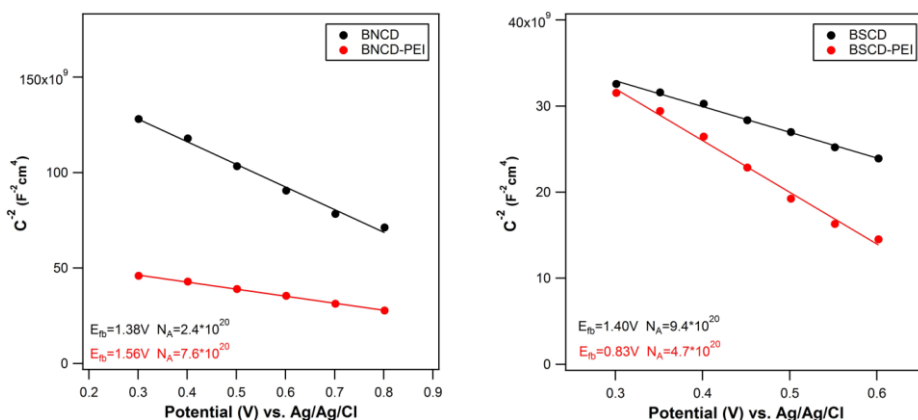
Figure 5-5. Mott-Schottky plot. The Mott Schottky plot (C_{sc}^{-2} vs. E) for Boron doped NanoCrystalline Diamond (BNCD – left) and Boron doped SingleCrystalline Diamond (BSCD – right) films with PEI (red symbols)/without PEI (black symbols) on the oxygen terminated surface. The acceptor concentration ($N_{A\ (BNCD)} = 2.4 \cdot 10^{20}$, $N_{A\ (BNCD\ PEI)} = 7.6 \cdot 10^{20}$, $N_{A\ (BSCD)} = 9.4 \cdot 10^{20}$, $N_{A\ (BSCD\ PEI)} = 4.7 \cdot 10^{20}$) was determined from the slope. The flat band potentials for pure BNCD and BSCD are 1.4V vs. Ag/AgCl. The flat band potential for BNCD with PEI is 1.6V and BSCD with PEI is 0.8V vs. Ag/AgCl.

Biocompatibility of diamond substrates, with and without PEI coating.
One fundamental problem for the construction of brain-machine interfacing are poor adhesive properties and limited viability for extended neuron culturing on

foreign substrates [39], [59], which suggests a lack of binding sites on the substrate surfaces. To facilitate neuronal densities capable of exploitation for *in vitro* use, we employed PEI monolayers. Our data clearly demonstrates marked improvement in neuronal density on BNCD in the presence of a PEI monolayer (Figure 5-6). Neuronal density values were significantly higher across all time points for diamond substrates pre-treated with PEI (procedure I) compared to those lacking PEI treatment (as control). A trend of decreasing densities with elapsed cell culture seeding time was present with the no PEI coated substrates. However, that trend was absent with PEI treated substrates. It can be concluded that PEI pre-treatment significantly increases neuronal density compared to BNCD substrates alone. On the contrary, BNCD substrates without PEI coating show a continual decline in neuronal numbers across one week, while those cultured in the presence of PEI maintain similar densities at 7 DIV. It is important to note that some neuronal adhesion was possible on bare BNCD substrates, however, our results illustrate the higher numbers of both neuronal and non-neuronal cell types in the presence of PEI.
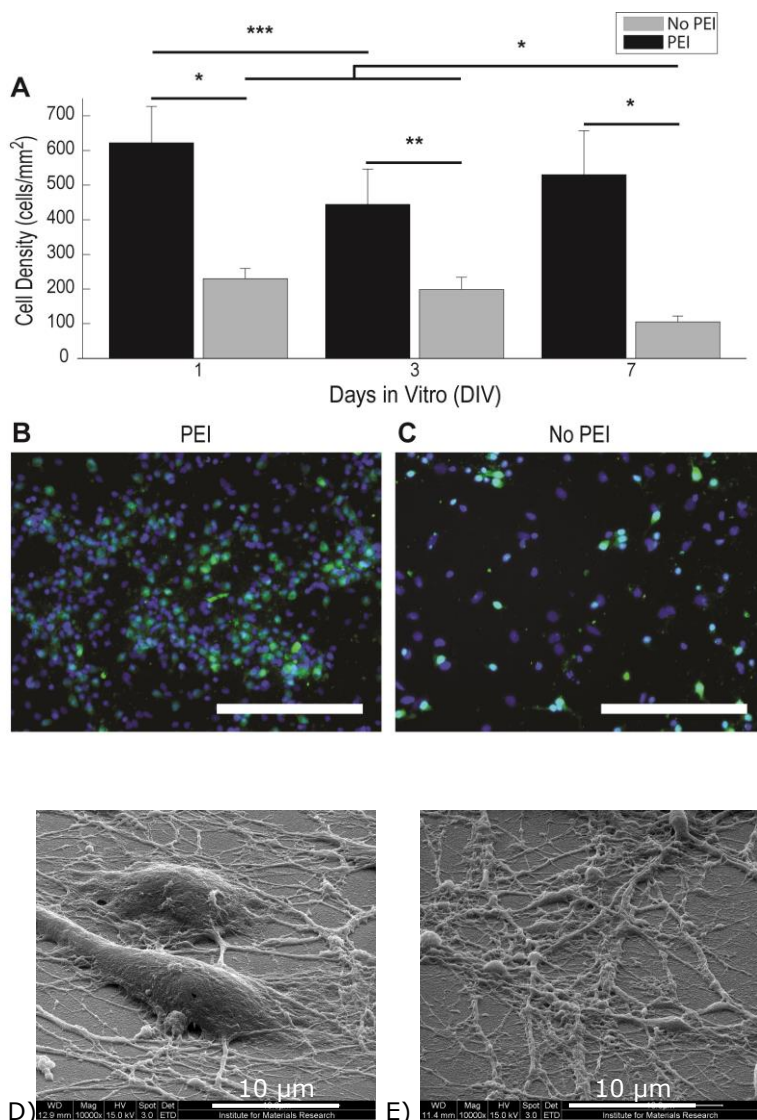
Figure 5-6. Increased neuronal density with PEI monolayers on diamond. A) Neuron density on PEI treated BNCD substrates was significantly higher at all time-points versus untreated BNCD substrates (control). A small but significant decrease occurred between 1 and 3 DIV with PEI treatment, though no further decrease was seen at DIV 7. Without PEI treatment, the presence of neurons decreased significantly at DIV 7. The levels for significant statistical differences are indicated as * $p < 0.0005$, ** $p<0.005$, *** $p<0.05$ (n=6). B, C) Immunofluorescent staining for cell nuclei (DAPI, blue), neuronal nuclei (NeuN, green), was performed 7 days after cell seeding (horizontal calibration bars: 200μm). Only cells stained for both DAPI and NeuN (blue-green in overlay) were considered neuronal. Without PEI treatment significantly fewer cells overall, and neuronal

cells specifically, were observed. D, E) SEM images show successful and dense growth of neurons on PEI monolayer coated diamond surfaces.

5.4 Conclusion

The presented work demonstrates that diamond with monolayers of PEI, prepared by SDS stripping, can be used very effectively for construction of neural interfaces. Diamond has major advantages over classical metallic electrodes by having significantly large electrochemical potential window [49] and providing capacitive coupling with very low Faradic components. The presented method for coating diamond with PEI shows that PEI can be efficient as neural adhesion promoter on diamond surfaces. Further on, PEI molecules form uniquely strong bonding on oxidized diamond surface by forming an ionic bond as shown by the presented electrical band diagram scheme. Bonding PEI to diamond surface leads to highly stable and practically unmovable PEI monolayer (in biologic conditions), that is extremely adherent to diamond and resistant to washing, achieved by stripping detergent treatment such as SDS. Therefore, it is anticipated that using PEI in cellular culture will not lead to cell-toxicity. The PEI monolayer has beneficial influence on surface of the diamond electrode that is anticipated to provide better performance for construction of brain-machine interfaces.

6   General Conclusions and outlook

This thesis demonstrated successful development of diamond MEAs on fused silica substrates as well as flexible MEAs for application in cell culture and for Electromyography measurements. Diamond films were employed for construction of well performing neuron-device interfaces by using one single material for fabrication of functional surfaces. BNCD was used as the conductive electrode material and NCD was used as the insulating material of the electrodes. A novel and precise coating method was developed to produce PEI monolayers on diamond surface and applied to treat the surface of diamond for preparation of neural cultures.

Fabrication of all diamond flat MEAs. Benefiting from the interesting properties of insulating and conductive films of diamond, flat diamond mono-surface micro electrode arrays have been fabricated on fused silica substrates. MEAs were prepared by using set of micro-fabrication steps such as photolithography, deposition and etching.

Due to differences in thermal expansion coefficients of diamond and fused silica, only less than 200nm of diamond could be coated, due to the presence of diamond film delamination for thicker layers and the strain. Nevertheless, such thickness showed to be sufficient for electrochemical and biological *in vitro* experiments. NCD and BNCD grown on fused silica were hydrogen and oxygen treated by means of plasma and UV-Ozone lamp. The wettability of these surfaces was then assessed using contact angle measurement by water droplet. The oxygen treated surfaces (NCD –BNCD) were hydrophilic and hydrogen treated surfaces were hydrophobic. According to our findings, when these surfaces were treated with physiological medium with FBS, the wettability of hydrophobic and hydrophilic surfaces showed a dramatic change. After observing this effect, the impact of the ionic solution on the hydrophilic and hydrophobic surfaces was studied and found to be the reason for the changes on the surface wetting.

The diamond MEAs were fabricated by patterning diamond in well-defined electrodes on the fused silica substrates. The microelectrodes were characterized for capacitive cross talk measurements and the result presented negligible signal cross talk between the neighbouring electrodes. The impedance measurements showed an acceptable impedance of the electrodes ~180 kΩ.

The diamond MEAs were used in biological measurements and local field potentials of rat's brain slice were measured. The overall noise level of diamond MEAs was found generally lower than the commercial-made MEAs under identical measurement conditions. As the result of this work, an article is submitted to PSS a: *All-diamond functional surface micro-electrode arrays for brain-slice neural analysis.*

Fabrication of flexible diamond-polyimide electrodes. Flexible diamond electrodes were fabricated to function as Electromyography (EMG)*.* In the first design, NCD was used as top insulating material. However, the NCD-BNCD-Polyimide electrodes had flexibility issues. Therefore, in a new design BNCD was used as active conductive electrodes sites and Polyimide was used as the biocompatible support and insulating material. The issues regarding flexibility of NCD-BNCD-Polyimide MEAs were solved by a novel fabrication plan. The connection lines (which were sandwiched between two polyimide layers) were made of metal and only BNCD electrodes were exposed. Such electrodes showed excellent flexibility and good integration of diamond with PI. The electrodes were characterized by optical microscopy, Raman spectroscopy, AFM and SEM step by step to optimize the technical issues during the fabrication and to solve them.

Construction of PEI monolayers on diamond. The application of PEI on diamond surface plays a key role as a neural adhesion promoter, to yield a high density of neurons on the surface. However, because PEI is generally toxic to cells, we have developed a novel technique for PEI coatings on diamond that were bonded chemically to the diamond surface. This phenomenon, based on the charge interaction at the diamond surface, enabled a strong ionic bonding of the PEI to diamond. Further on, we have used SDS washing to strip PEI coating to monolayers. XPS measurements on PEI stripped diamond surfaces confirmed the presence of the PEI monolayer at the surface. It was shown that the formed

monolayer of PEI on the surface is extremely adherent and resistant. The PEI monolayer has the benefit of non-toxicity and favourable influence on the capacitive characteristics of the diamond electrode that will provide better performance for construction of brain-machine interfaces. These findings resulted in an article which is in preparation for submission: *Functional Biomolecular PEI Monolayers on Diamond- A Novel Approach for Construction of Man-Machine Interface.*

Future outlook and applications

Fabrication of all diamond flat MEAs. Regarding the planar diamond MEAs, further optimization of coupling parameters such as roughness, capacitance, and impedance can be beneficial. One can also use higher Boron doping levels to avoid presence of metallic tracks. More challenging is further integration of the planar electrodes with 3D structured designs, in order to assess the attachment of cells in details.

Fabrication of flexible diamond-polyimide electrodes. The flexible diamond electrodes were fabricated for EMG applications. The final tests and long-term studies of the flexibility and the functionality of NCD-BNCD-polyimide electrodes are to be executed *in vivo* for EMG measurements, to demonstrate the benefit of BNCD and NCD as electrode materials for *in vivo* applications [40], [53].
Such experiments use EMG electrodes for several purposes, such as control of prosthetic devices or measure electrical signals from muscles.
In order to be able to measure from higher number of channels simultaneously, the current electrodes can be further improved by using the 64-channel electrodes.

Construction of PEI monolayers on diamond. Benefiting from PEI monolayer coatings on diamond films, long term *in vitro* experiments can be performed. This will allow examination of the quality and functionality of the PEI 'monolayer' on diamond, after a longer period of time exposure in biological environment. More challenging will be *in vivo* experiments inspired by the PEI monolayer

coated diamonds. In this regime, biomedical diamond implants are to be implemented benefiting from diamond films coated with PEI monolayers.

References

[1]   M. Bonnauron, S. Saada, C. Mer, C. Gesset, O. a. Williams, L. Rousseau, E. Scorsone, P. Mailley, M. Nesladek, J.-C. Arnault, and P. Bergonzo, "Transparent diamond-on-glass micro-electrode arrays for ex-vivo neuronal study," *Phys. Status Solidi*, vol. 205, no. 9, pp. 2126–2129, Sep. 2008.

[2]   Y. Y. Hui, B. Zhang, Y. Chang, C. Chang, H. Chang, J. Hsu, K. Chang, and F. Chang, "Two-photon fluorescence correlation spectroscopy of lipid-encapsulated fluorescent nanodiamonds in living cells," vol. 18, no. 6, pp. 2135–2143, 2010.

[3]   F. Neugart, A. Zappe, F. Jelezko, C. Tietz, J. P. Boudou, A. Krueger, and J. Wrachtrup, "Dynamics of diamond nanoparticles in solution and cells.," *Nano Lett.*, vol. 7, no. 12, pp. 3588–91, Dec. 2007.

[4]   J. Pine, "Advances in Network Electrophysiology: Using Multi-Electrode Arrays," M. Taketani and M. Baudry, Eds. Boston, MA: Springer US, 2006, pp. 3–23.

[5]   I. L. Jones, P. Livi, M. K. Lewandowska, M. Fiscella, B. Roscic, and A. Hierlemann, "The potential of microelectrode arrays and microelectronics for biomedical research and diagnostics," *Anal. Bioanal. Chem.*, vol. 399, no. 7, pp. 2313–2329, 2011.

[6]   J. T. Robinson, M. Jorgolli, A. K. Shalek, M.-H. Yoon, R. S. Gertner, and H. Park, "Vertical nanowire electrode arrays as a scalable platform for intracellular interfacing to neuronal circuits," *Nat. Nanotechnol.*, vol. 7, no. 3, pp. 180–184, 2012.

[7]   A. Hai, J. Shappir, and M. E. Spira, "In-cell recordings by extracellular microelectrodes.," *Nat. Methods*, vol. 7, no. 3, pp. 200–2, Mar. 2010.

[8]   A. Hai, A. Dormann, J. Shappir, S. Yitzchaik, C. Bartic, G. Borghs, J. P. M. Langedijk, and M. E. Spira, "Spine-shaped gold protrusions improve the adherence and electrical coupling of neurons with the surface of micro-electronic devices.," *J. R. Soc. Interface*, vol. 6, no. 41, pp. 1153–1165, 2009.

[9]   G. W. Gross, E. Rieske, G. W. Kreutzberg, and a Meyer, "A new fixed-array multi-microelectrode system designed for long-term monitoring of extracellular single unit neuronal activity in vitro.," *Neurosci. Lett.*, vol. 6, no. 2–3, pp. 101–105, 1977.

[10]   G. W. Gross, W. Y. Wen, and J. W. Lin, "Transparent indium-tin oxide electrode patterns for extracellular, multisite recording in neuronal cultures.," *J. Neurosci. Methods*, vol. 15, no. 3, pp. 243–252, 1985.

[11]   H. Oka, K. Shimono, R. Ogawa, H. Sugihara, and M. Taketani, "A new planar multielectrode array for extracellular recording: Application to hippocampal acute slice," *J. Neurosci. Methods*, vol. 93, no. 1, pp. 61–67, 1999.

[12] D. a Wagenaar, J. Pine, and S. M. Potter, "Effective parameters for stimulation of dissociated cultures using multi-electrode arrays.," *J. Neurosci. Methods*, vol. 138, no. 1–2, pp. 27–37, Sep. 2004.

[13] G. Gholmieh, W. Soussou, M. Han, A. Ahuja, M. C. Hsiao, D. Song, A. R. Tanguay, and T. W. Berger, "Custom-designed high-density conformal planar multielectrode arrays for brain slice electrophysiology," *J. Neurosci. Methods*, vol. 152, no. 1–2, pp. 116–129, 2006.

[14] N. S. Baek, J.-H. Lee, Y. H. Kim, B. J. Lee, G. H. Kim, I.-H. Kim, M.-A. Chung, and S.-D. Jung, "Photopatterning of Cell-Adhesive-Modified Poly(ethyleneimine) for Guided Neuronal Growth.," *Langmuir*, pp. 2717–2722, Feb. 2011.

[15] H. K. Kleinman, L. Luckenbill-Edds, F. W. Cannon, and G. C. Sephel, "Use of extracellular matrix components for cell culture.," *Anal. Biochem.*, vol. 166, no. 1, pp. 1–13, Oct. 1987.

[16] H. K. Kleinman, R. J. Klebe, and G. R. Martin, "Role of collagenous matrices in the adhesion and growth of cells.," *J. Cell Biol.*, vol. 88, no. 3, pp. 473–85, Mar. 1981.

[17] M. E. Spira and A. Hai, "Multi-electrode array technologies for neuroscience and cardiology.," *Nat. Nanotechnol.*, vol. 8, no. 2, pp. 83–94, Feb. 2013.

[18] P. Fromherz, "Three levels of neuroelectronic interfacing: silicon chips with ion channels, nerve cells, and brain tissue.," *Ann. N. Y. Acad. Sci.*, vol. 1093, pp. 143–60, Dec. 2006.

[19] P. Bergonzo, a. Bongrain, E. Scorsone, a. Bendali, L. Rousseau, G. Lissorgues, P. Mailley, Y. Li, T. Kauffmann, F. Goy, B. Yvert, J. a. Sahel, and S. Picaud, "3D shaped mechanically flexible diamond microelectrode arrays for eye implant applications: The MEDINAS project," *Irbm*, vol. 32, no. 2, pp. 91–94, 2011.

[20] L. Bacakova, L. Grausova, J. Vacik, a. Fraczek, S. Blazewicz, a. Kromka, M. Vanecek, and V. Svorcik, "Improved adhesion and growth of human osteoblast-like MG 63 cells on biomaterials modified with carbon nanoparticles," *Diam. Relat. Mater.*, vol. 16, no. 12, pp. 2133–2140, 2007.

[21] M. Bevilacqua, S. Patel, A. Chaudhary, H. Ye, and R. B. Jackman, "Electrical properties of aggregated detonation nanodiamonds," *Appl. Phys. Lett.*, vol. 93, no. 13, p. 132115, 2008.

[22] C. Gaillard, G. Cellot, S. Li, F. M. Toma, H. Dumortier, G. Spalluto, B. Cacciari, M. Prato, L. Ballerini, and A. Bianco, "Carbon Nanotubes Carrying Cell-Adhesion Peptides do not Interfere with Neuronal Functionality," *Adv. Mater.*, vol. 21, no. 28, pp. 2903–2908, Jul. 2009.

[23] T. N. Rao and A. Fujishima, "Recent advances in electrochemistry of diamond," *Diam. Relat. Mater.*, vol. 9, no. 3–6, pp. 384–389, Apr. 2000.

[24] M. Nesladek, J. J. Mares, and P. Hubik, "Superconductivity and low-

dimensional electrical transport in nanocrystalline diamond," *New Diam. Front. Carbon Technol.*, vol. 16, no. 6, pp. 323–336, 2006.

[25]   F. Bouamrane, A. Tadjeddine, J. E. Butler, R. Tenne, and C. Lévy-Clément, "Electrochemical study of diamond thin films in neutral and basic solutions of nitrate," *J. Electroanal. Chem.*, vol. 405, no. 1–2, pp. 95–99, Apr. 1996.

[26]   S. F. Cogan, "Neural stimulation and recording electrodes.," *Annu. Rev. Biomed. Eng.*, vol. 10, pp. 275–309, Jan. 2008.

[27]   A. Kraft, G. Gmbh, and K. Str, "Doped Diamond : A Compact Review on a New , Versatile Electrode Material," vol. 2, pp. 355–385, 2007.

[28]   P. K. Ang, K. P. Loh, T. Wohland, M. Nesladek, and E. Van Hove, "Supported Lipid Bilayer on Nanocrystalline Diamond: Dual Optical and Field-Effect Sensor for Membrane Disruption," *Adv. Funct. Mater.*, vol. 19, no. 1, pp. 109–116, Jan. 2009.

[29]   K.-K. Liu, C.-L. Cheng, C.-C. Chang, and J.-I. Chao, "Biocompatible and detectable carboxylated nanodiamond on human cell," *Nanotechnology*, vol. 18, no. 32, p. 325102, Aug. 2007.

[30]   J. V. Macpherson, "A practical guide to using boron doped diamond in electrochemical research," *Phys. Chem. Chem. Phys.*, vol. 17, no. 5, pp. 2935–2949, 2015.

[31]   Y.-C. Chen, D.-C. Lee, C.-Y. Hsiao, Y.-F. Chung, H.-C. Chen, J. P. Thomas, W.-F. Pong, N.-H. Tai, I.-N. Lin, and I.-M. Chiu, "The effect of ultra-nanocrystalline diamond films on the proliferation and differentiation of neural stem cells.," *Biomaterials*, vol. 30, no. 20, pp. 3428–35, Jul. 2009.

[32]   T. Lechleitner, F. Klauser, T. Seppi, J. Lechner, P. Jennings, P. Perco, B. Mayer, D. Steinmüller-Nethl, J. Preiner, P. Hinterdorfer, M. Hermann, E. Bertel, K. Pfaller, and W. Pfaller, "The surface properties of nanocrystalline diamond and nanoparticulate diamond powder and their suitability as cell growth support surfaces," *Biomaterials*, vol. 29, no. 32, pp. 4275–4284, 2008.

[33]   a. Voss, H. Wei, C. Müller, C. Popov, W. Kulisch, G. Ceccone, C. Ziegler, M. Stengl, and J. P. Reithmaier, "Influence of the surface termination of ultrananocrystalline diamond/amorphous carbon composite films on their interaction with neurons," *Diam. Relat. Mater.*, vol. 26, pp. 60–65, 2012.

[34]   Y.-C. Chen, D.-C. Lee, T.-Y. Tsai, C.-Y. Hsiao, J.-W. Liu, C.-Y. Kao, H.-K. Lin, H.-C. Chen, T. J. Palathinkal, W.-F. Pong, N.-H. Tai, I.-N. Lin, and I.-M. Chiu, "Induction and regulation of differentiation in neural stem cells on ultra-nanocrystalline diamond films.," *Biomaterials*, vol. 31, no. 21, pp. 5575–87, Jul. 2010.

[35]   X. Q. Zhang, M. Chen, R. Lam, X. Xu, E. Osawa, and D. Ho, "Polymer-functionalized nanodiamond platforms as vehicles for gene delivery," *ACS Nano*, vol. 3, no. 9, pp. 2609–2616, 2009.

[36] V. N. Mochalin, O. Shenderova, D. Ho, and Y. Gogotsi, "The properties and applications of nanodiamonds.," *Nat. Nanotechnol.*, vol. 7, no. 1, pp. 11–23, Jan. 2012.

[37] O. Faklaris, V. Joshi, T. Irinopoulou, P. Tauc, M. Sennour, Ḱ. H. Girard, J. Arnault, A. Thorel, Ḱ. J. Boudou, and P. a Curmi, "Nanoparticles for Cell Labeling : Study of," vol. 3, no. 12, pp. 3955–3962, 2009.

[38] M. F. Weng, B. J. Chang, S. Y. Chiang, N. S. Wang, and H. Niu, "Cellular uptake and phototoxicity of surface-modified fluorescent nanodiamonds," *Diam. Relat. Mater.*, vol. 22, pp. 96–104, 2012.

[39] A. Thalhammer, R. J. Edgington, L. a Cingolani, R. Schoepfer, and R. B. Jackman, "The use of nanodiamond monolayer coatings to promote the formation of functional neuronal networks.," *Biomaterials*, vol. 31, no. 8, pp. 2097–104, Mar. 2010.

[40] J. M. Halpern, S. Xie, G. P. Sutton, B. T. Higashikubo, C. a. Chestek, H. Lu, H. J. Chiel, and H. B. Martin, "Diamond electrodes for neurodynamic studies in Aplysia californica," *Diam. Relat. Mater.*, vol. 15, no. 2–3, pp. 183–187, Feb. 2006.

[41] P. Ariano, A. Lo Giudice, A. Marcantoni, E. Vittone, E. Carbone, and D. Lovisolo, "A diamond-based biosensor for the recording of neuronal activity.," *Biosens. Bioelectron.*, vol. 24, no. 7, pp. 2046–50, Mar. 2009.

[42] M. Dankerl, S. Eick, B. Hofmann, M. Hauf, S. Ingebrandt, A. Offenhäusser, M. Stutzmann, and J. a. Garrido, "Diamond Transistor Array for Extracellular Recording From Electrogenic Cells," *Adv. Funct. Mater.*, vol. 19, no. 18, pp. 2915–2923, Sep. 2009.

[43] M. Dankerl, M. V. Hauf, M. Stutzmann, and J. a. Garrido, "Diamond solution-gated field effect transistors: Properties and bioelectronic applications," *Phys. Status Solidi*, vol. 209, no. 9, pp. 1631–1642, Sep. 2012.

[44] M. Cottance, S. Nazeer, L. Rousseau, G. Lissorgues, A. Bongrain, R. Kiran, E. Scorsone, P. Bergonzo, A. Bendali, S. Picaud, and S. Joucla, "Diamond Micro-Electrode Arrays (MEAs): a new route for in-vitro applications .," no. April, pp. 16–19, 2013.

[45] V. Maybeck, R. Edgington, A. Bongrain, J. O. Welch, E. Scorsone, P. Bergonzo, R. B. Jackman, and A. Offenhäusser, "Boron-doped nanocrystalline diamond microelectrode arrays monitor cardiac action potentials," *Adv. Healthc. Mater.*, vol. 3, no. 2, pp. 283–289, 2014.

[46] J. Park, Y. Show, V. Quaiserova, J. J. Galligan, G. D. Fink, and G. M. Swain, "Diamond microelectrodes for use in biological environments," *J. Electroanal. Chem.*, vol. 583, no. 1, pp. 56–68, 2005.

[47] B. A. Patel, X. Bian, V. Quaiserová-Mocko, J. J. Galligan, and G. M. Swain, "In vitro continuous amperometric monitoring of 5-hydroxytryptamine release from enterochromaffin cells of the guinea pig ileum.," *Analyst*, vol. 132, no. 1, pp. 41–47, 2007.

[48] L. Tang, C. Tsai, W. W. Gerberich, L. Kruckebeu, and D. R. Kania, "Biocompatibility of chemical-vapour- deposited diamond," vol. 16, no. 6, pp. 483–488, 1995.

[49] Z. V. Živcová, O. Frank, V. Petrák, H. Tarábková, J. Vacík, M. Nesládek, and L. Kavan, "Electrochemistry and in situ Raman spectroelectrochemistry of low and high quality boron doped diamond layers in aqueous electrolyte solution," *Electrochim. Acta*, vol. 87, pp. 518–525, Jan. 2013.

[50] R. Kiran, L. Rousseau, G. Lissorgues, E. Scorsone, A. Bongrain, B. Yvert, S. Picaud, P. Mailley, and P. Bergonzo, "Multichannel boron doped nanocrystalline diamond ultramicroelectrode arrays: design, fabrication and characterization.," *Sensors (Basel).*, vol. 12, no. 6, pp. 7669–81, Jan. 2012.

[51] G. Pastor-moreno and D. J. Riley, "Electrochemical studies of moderately boron doped polycrystalline diamond in non-aqueous sol v ent," vol. 47, pp. 2589–2595, 2002.

[52] J. a Garrido, S. Nowy, A. Härtl, and M. Stutzmann, "The diamond/aqueous electrolyte interface: an impedance investigation.," *Langmuir*, vol. 24, no. 8, pp. 3897–904, Apr. 2008.

[53] J. M. Halpern, M. J. Cullins, H. J. Chiel, and H. B. Martin, "Chronic in vivo nerve electrical recordings of Aplysia californica using a boron-doped polycrystalline diamond electrode," *Diam. Relat. Mater.*, vol. 19, no. 2–3, pp. 178–181, Feb. 2010.

[54] A. E. Hess, D. M. Sabens, H. B. Martin, C. a Zorman, and S. Member, "Diamond-on-Polymer Microelectrode Arrays Fabricated Using a Chemical Release Transfer Process," vol. 20, no. 4, pp. 867–875, 2011.

[55] D. J. Garrett, A. L. Saunders, C. McGowan, J. Specks, K. Ganesan, H. Meffin, R. a. Williams, and D. a. X. Nayagam, "In vivo biocompatibility of boron doped and nitrogen included conductive-diamond for use in medical implants," *J. Biomed. Mater. Res. Part B Appl. Biomater.*, p. n/a–n/a, 2015.

[56] C. Hassler, T. Boretius, and T. Stieglitz, "Polymers for neural implants," *J. Polym. Sci. Part B Polym. Phys.*, vol. 49, pp. 18–33, 2011.

[57] A. Mercanzini, K. Cheung, D. L. Buhl, M. Boers, A. Maillard, P. Colin, J.-C. Bensadoun, A. Bertsch, and P. Renaud, "Demonstration of cortical recording using novel flexible polymer neural probes," *Sensors Actuators A Phys.*, vol. 143, no. 1, pp. 90–96, May 2008.

[58] B. Rubehn and T. Stieglitz, "In vitro evaluation of the long-term stability of polyimide as a material for neural implants," *Biomaterials*, vol. 31, no. 13, pp. 3449–3458, 2010.

[59] P. Ariano, O. Budnyk, S. Dalmazzo, D. Lovisolo, C. Manfredotti, P. Rivolo, and E. Vittone, "On diamond surface properties and interactions with neurons.," *Eur. Phys. J. E. Soft Matter*, vol. 30, no. 2, pp. 149–56, Oct.

2009.

[60]   S. M. Ojovan, M. McDonald, M. McDonald, N. Rabieh, N. Shmuel, H. Erez, M. Nesladek, and M. E. Spira, "Nanocrystalline diamond surfaces for adhesion and growth of primary neurons, conflicting results and rational explanation.," *Front. Neuroeng.*, vol. 7, no. June, p. 17, 2014.

[61]   K. F. Chong, K. P. Loh, S. R. K. Vedula, C. T. Lim, H. Sternschulte, D. Steinmüller, F.-S. Sheu, and Y. L. Zhong, "Cell adhesion properties on photochemically functionalized diamond.," *Langmuir*, vol. 23, no. 10, pp. 5615–5621, 2007.

[62]   C. G. Specht, O. a. Williams, R. B. Jackman, and R. Schoepfer, "Ordered growth of neurons on diamond," *Biomaterials*, vol. 25, no. 18, pp. 4073–4078, 2004.

[63]   P. W. May, E. M. Regan, a. Taylor, J. Uney, a. D. Dick, and J. McGeehan, "Spatially controlling neuronal adhesion on CVD diamond," *Diam. Relat. Mater.*, vol. 23, pp. 100–104, 2012.

[64]   H. Sorribas, D. Braun, L. Leder, P. Sonderegger, and L. Tiefenauer, "Adhesion proteins for a tight neuron – electrode contact," vol. 104, pp. 133–141, 2001.

[65]   B. I. Florea, C. Meaney, H. E. Junginger, and G. Borchard, "Transfection efficiency and toxicity of polyethylenimine in differentiated Calu-3 and nondifferentiated COS-1 cell cultures.," *AAPS PharmSci*, vol. 4, no. 3, p. E12, 2002.

[66]   A. Schurr, "Editor ' s Column," vol. i, 1981.

[67]   D. Kensall and B. James, "Integrated-Circuit Microelectrodes," no. 3, pp. 238–247, 1970.

[68]   W. L. C. Rutten, "Selective electrical interfaces with the nervous system.," *Annu. Rev. Biomed. Eng.*, vol. 4, pp. 407–52, Jan. 2002.

[69]   "MEA-IT Manual."

[70]   J. F. Rizzo, "Methods and Perceptual Thresholds for Short-Term Electrical Stimulation of Human Retina with Microelectrode Arrays," *Invest. Ophthalmol. Vis. Sci.*, vol. 44, no. 12, pp. 5355–5361, Dec. 2003.

[71]   J. D. Weiland, D. J. Anderson, and M. S. Humayun, "In vitro electrical properties for iridium oxide versus titanium nitride stimulating electrodes," *IEEE Trans. Biomed. Eng.*, vol. 49, no. 12 I, pp. 1574–1579, 2002.

[72]   A. Grill, "Diamond-like carbon coatings as biocompatible materials — an overview," vol. 12, pp. 166–170, 2003.

[73]   Y.-C. Lin, E. Perevedentseva, L.-W. Tsai, K.-T. Wu, and C.-L. Cheng, "Nanodiamond for intracellular imaging in the microorganisms in vivo.," *J. Biophotonics*, vol. 5, no. 11–12, pp. 838–47, Nov. 2012.

[74]   M. Allen and N. Rushton, "Diamond-like," vol. 6605, no. 94, 1994.

[75] R. J. Nemanich, J. a. Carlisle, A. Hirata, and K. Haenen, "CVD diamond—Research, applications, and challenges," *MRS Bull.*, vol. 39, no. 06, pp. 490–494, 2014.

[76] W. Kern, "The Evolution of Silicon Wafer Cleaning Technology," *J. Electrochem. Soc.*, vol. 137, no. 6, p. 1887, 1990.

[77] P. Pobedinskas, G. Degutis, W. Dexters, W. Janssen, S. D. Janssens, B. Conings, B. Ruttens, J. D'Haen, H.-G. Boyen, a. Hardy, M. K. Van Bael, and K. Haenen, "Surface plasma pretreatment for enhanced diamond nucleation on AlN," *Appl. Phys. Lett.*, vol. 102, no. 20, p. 201609, 2013.

[78] H. Köndgen, C. Geisler, S. Fusi, X. J. Wang, H. R. Lüscher, and M. Giugliano, "The dynamical response properties of neocortical neurons to temporally modulated noisy inputs in vitro," *Cereb. Cortex*, vol. 18, no. 9, pp. 2086–2097, 2008.

[79] A. Krueger and D. Lang, "Functionality is key: Recent progress in the surface modification of nanodiamond," *Adv. Funct. Mater.*, vol. 22, no. 5, pp. 890–906, 2012.

[80] S. D. Janssens, S. Drijkoningen, M. Saitner, H.-G. Boyen, P. Wagner, K. Larsson, and K. Haenen, "Evidence for phase separation of ethanol-water mixtures at the hydrogen terminated nanocrystalline diamond surface.," *J. Chem. Phys.*, vol. 137, no. 4, p. 044702, 2012.

[81] Z. Vl, V. Petrák, O. Frank, and L. Kavan, "Diamond & Related Materials Electrochemical impedance spectroscopy of polycrystalline boron doped diamond layers with hydrogen and oxygen terminated surface," vol. 55, pp. 70–76, 2015.

[82] H. Krysova, Z. Vlckova-zivcova, J. Barton, V. Petrak, M. Nesladek, P. Cigler, and L. Kavan, "Visible-light sensitization of boron-doped nanocrystalline diamond through non-covalent surface modification," *Phys. Chem. Chem. Phys.*, vol. 17, pp. 1165–1172, 2014.

[83] S. Metz, a Bertsch, D. Bertrand, and P. Renaud, "Flexible polyimide probes with microelectrodes and embedded microfluidic channels for simultaneous drug delivery and multi-channel monitoring of bioelectric activity.," *Biosens. Bioelectron.*, vol. 19, no. 10, pp. 1309–18, May 2004.

[84] Y. X. Kato, S. Furukawa, K. Samejima, N. Hironaka, and M. Kashino, "Photosensitive-polyimide based method for fabricating various neural electrode architectures.," *Front. Neuroeng.*, vol. 5, no. June, p. 11, Jan. 2012.

[85] A. Ramanaviciene, K. Sanen, and M. Ameloot, "Impact of Diamond Nanoparticles on Neural," no. January 2016, 2014.

[86] X. Y. Chen and Y. Lu, "Annealing and oxidation of silicon oxide films prepared by plasma-enhanced chemical vapor deposition," 2004.

[87] H. Chan, D. M. Aslam, J. Wiler, and B. Casey, "A NOVEL DIAMOND MICRO PROBE FOR NEURO-CHEMICAL AND -ELECTRICAL RECORDING IN NEURAL PROSTHESIS."

[88] R. L. Hubbard and L. Technologies, "Reduced Stress and Improved with Stable Polyimide Dielectrics Stress and Warpage in Polymer Dielectrics."

[89] P. Details and S. Bake, "Pi-2525, pi-2555& pi-2574," no. November, 2012.

[90] M. D. Faculty, S. U. Prof, W. U. Prof, V. K. U. L. Prof, G. Tu, M. Prof, B. Prof, and M. K. U. L. Prof, "No Title."

[91] K. Cooper, C. Hamel, B. Whitney, and S. MicroTec, "Conformal photoresist coatings for high aspect ratio features," *Proc. Int. Wafer-Level Packag. Conf.*, 2007.

[92] Y. Nakamura, Y. Suzuki, and Y. Watanabe, "Effect of oxygen plasma etching on adhesion between polyimide films and metal," *Thin Solid Films*, vol. 290–291, no. 1996, pp. 367–369, 1996.

[93] D. L. Pappas, "Studies of adhesion of metal films to polyimide," *J. Vac. Sci. Technol. A Vacuum, Surfaces, Film.*, vol. 9, no. 1991, p. 2704, 1991.

[94] S. J. Park, E. J. Lee, and S. H. Kwon, "Influence of surface treatment of polyimide film on adhesion enhancement between polyimide and metal films," *Bull. Korean Chem. Soc.*, vol. 28, no. 2, pp. 188–192, 2007.

[95] O. a. Williams, M. Nesladek, M. Daenen, S. Michaelson, a. Hoffman, E. Osawa, K. Haenen, and R. B. Jackman, "Growth, electronic properties and applications of nanodiamond," *Diam. Relat. Mater.*, vol. 17, no. 7–10, pp. 1080–1088, 2008.

[96] P. S. Solidi, J. Broeders, and N. Oceanography, "pss," no. January 2016, 2011.

[97] N. a. Kotov, J. O. Winter, I. P. Clements, E. Jan, B. P. Timko, S. Campidelli, S. Pathak, A. Mazzatenta, C. M. Lieber, M. Prato, R. V. Bellamkonda, G. a. Silva, N. W. S. Kam, F. Patolsky, and L. Ballerini, "Nanomaterials for Neural Interfaces," *Adv. Mater.*, vol. 21, no. 40, pp. 3970–4004, Oct. 2009.

[98] "Mater. Res. Soc. Symp. Proc. Vol. 1203 © 2010 Materials Research Society 1203-J17-01," vol. 1203, 2010.

[99] a. F. Azevedo, M. R. Baldan, and N. G. Ferreira, "Nanodiamond Films for Applications in Electrochemical Systems," *Int. J. Electrochem.*, vol. 2012, pp. 1–16, 2012.

[100] Y. Sun, Z. Huang, W. Liu, K. Yang, K. Sun, S. Xing, D. Wang, W. Zhang, and X. Jiang, "Surface coating as a key parameter in engineering neuronal network structures in vitro.," *Biointerphases*, vol. 7, no. 1–4, p. 29, Dec. 2012.

[101] Y. Bledi, a J. Domb, and M. Linial, "Culturing neuronal cells on surfaces coated by a novel polyethyleneimine-based polymer.," *Brain Res. Brain Res. Protoc.*, vol. 5, no. 3, pp. 282–9, Jul. 2000.

[102] A. R. Vancha, S. Govindaraju, K. V. L. Parsa, M. Jasti, M. González-

García, and R. P. Ballestero, "Use of polyethyleneimine polymer in cell culture as attachment factor and lipofection enhancer.," *BMC Biotechnol.*, vol. 4, p. 23, Oct. 2004.

[103] M. Wang, P. Lu, B. Wu, J. D. Tucker, C. Cloer, and Q. Lu, "High efficiency and low toxicity of polyethyleneimine modified Pluronics (PEI–Pluronic) as gene delivery carriers in cell culture and dystrophic mdx mice," *J. Mater. Chem.*, vol. 22, no. 13, p. 6038, 2012.

[104] L. Kavan, M. Zukalova, O. Vik, and D. Havlicek, "Sol-gel titanium dioxide blocking layers for dye-sensitized solar cells: electrochemical characterization.," *Chemphyschem*, vol. 15, no. 6, pp. 1056–61, Apr. 2014.

[105] L. Kavan, N. Te, T. Moehl, and M. Gra, "Electrochemical Characterization of TiO 2 Blocking Layers for Dye- Sensitized Solar Cells," 2014.

[106] M. D. Krotova, Y. V. Pleskov, a. a. Khomich, V. G. Ralchenko, D. N. Sovyk, and V. a. Kazakov, "Semiconductor properties of nanocrystalline diamond electrodes," *Russ. J. Electrochem.*, vol. 50, no. 2, pp. 101–107, Feb. 2014.

[107] L. Boonma, "Observation of Photocurrent from Band-to-Band Excitation of Semiconducting p-Type Diamond Thin Film Electrodes," *J. Electrochem. Soc.*, vol. 144, no. 6, p. L142, 1997.

[108] Y. Zhou, C. Fuentes-Hernandez, J. Shim, J. Meyer, A. J. Giordano, H. Li, P. Winget, T. Papadopoulos, H. Cheun, J. Kim, M. Fenoll, A. Dindar, W. Haske, E. Najafabadi, T. M. Khan, H. Sojoudi, S. Barlow, S. Graham, J.-L. Brédas, S. R. Marder, A. Kahn, and B. Kippelen, "A universal method to produce low-work function electrodes for organic electronics.," *Science*, vol. 336, no. 6079, pp. 327–32, Apr. 2012.

[109] L. Kavan, Z. Vlckova, V. Petrak, O. Frank, P. Janda, H. Tarabkova, M. Nesladek, and V. Mortet, "Electrochimica Acta Boron-doped Diamond Electrodes : Electrochemical , Atomic Force Microscopy and Raman Study towards Corrosion-modi fi cations at Nanoscale," *Electrochim. Acta*, 2015.

[110] J. Foord and J. P. Hu, "Electrochemical oxidation and reduction processes at diamond electrodes of varying phase purity," vol. 3127, no. 12, pp. 3121–3127, 2006.

[111] H. B. Martin, A. Argoitia, J. C. Angus, and U. Landau, "Voltammetry Studies of Single-Crystal and Polycrystalline Diamond Electrodes," vol. 146, no. 8, pp. 2959–2964, 1999.

[112] M. R. Baldan, A. F. Azevedo, A. B. Couto, and N. G. Ferreira, "Journal of Physics and Chemistry of Solids Cathodic and anodic pre-treated boron doped diamond with different sp 2 content : Morphological , structural , and impedance spectroscopy characterizations," *J. Phys. Chem. Solids*, vol. 74, no. 12, pp. 1830–1835, 2013.

Publications

- **Farnoosh Vahidpour**, Kathleen Sanen, Matthew McDonald, Zuzana Vlčková Živcová, Elena Gjorgievska , Yaso Balasubramaniam, ,Ken Haenen, Ladislav Kavan, Marcel Ameloot, Anitha Ethirajan , Hans-Gerd Boyen & Miloš Nesládek; Functional Bio-molecular PEI Monolayers on Diamond- A Novel Approach for Construction of Man-Machine Interface- In preparation.

- **Farnoosh Vahidpour**, Lowry Curley, István Biró, Matthew McDonald, Dieter Croux, Paulius Pobedinskas, Ken Haenen, Michele Giugliano, Miloš Nesládek; All-diamond functional surface micro-electrode arrays for brain-slice neural analysis; submitted to PSSA (Physica Status Solidi a)

- Antonina M Monaco, Anastasiya Moskalyuk, Jaroslaw Motylewski, **Farnoosh Vahidpour,** Andrew M H Ng, Kian Ping Loh, Miloš Nesládek · Michele Giugliano; Coupling (reduced) Graphene Oxide to Mammalian Primary Cortical Neurons *in Vitro*; AIMS Material Science, 2015, 2(3): 217-229. DOI: 10.3934/matersci.2015.3.217

- Ieva Baleviciute, Vilma Ratautaite, Almira Ramanaviciene, Zigmas Balevicius, Jeroen Broeders, Dieter Croux, Matthew Mcdonald, **Farnoosh Vahidpour**, Ronald Thoelen, Ward De Ceuninck, Ken Haenen, Miloš Nesládek, Alfonsas Reza, Arunas Ramanavicius; Evaluation of Theophylline Imprinted Polypyrrole Film; Synthetic Metals, 08/2015; DOI:10.1016/j.synthmet.2015.07.021

- Aida Vaitkuviene, Matthew McDonald, **Farnoosh Vahidpour**, Jean-Paul Noben, Kathleen Sanen, Marcel Ameloot, Vilma Ratautaite, Vytautas Kaseta, Gene Biziuleviciene, Almira Ramanaviciene, Miloš Nesládek, Arunas Ramanavicius; Impact of differently modified nanocrystalline diamond on the growth of neuroblastoma cells; N Biotechnol. DOI: 10.1016/j.nbt.2014.06.008.

- Aida Vaitkuviene, Vilma Ratautaite, Almira Ramanaviciene, Kathleen Sanen, Rick Paesen, Marcel Ameloot, Vladimira Petrakova, Matthew McDonald, **Farnoosh Vahidpour**, Vytautas Kaseta, Giedre Ramanauskaite, Gene Biziuleviciene, Miloš Nesládek, Arunas Ramanavicius; Impact of diamond nanoparticles on neural cells; Molecular and Cellular Probes, DOI:10.1016/j.mcp.2014.10.005

Abstracts

Oral presentations

- <u>Antonina Monaco</u>, Anastasiya Moskalyuk, Jaroslaw Motylewski, **Farnoosh Vahidpour**, Andrew M. H. Ng, Kian Ping Loh, Miloš Nesládek, Michele Giugliano; Graphene Oxide and reduced Graphene Oxide as novel nanostructured materials for neuronal growth; 11th National Congress of the Belgian Society for Neuroscience, May 2015; DOI:10.3389/conf.fnins.2015.89.00082

- **Farnoosh Vahdipour**, Matthew McDonald, Elena Gjorgievska, Zuzana Vlčková Zivcová, Ladislav Kavan, Hans-Gerd Boyen, Ken Haenen, Miloš Nesládek, Functional biomolecular monolayers on diamond: a novel platform for the construction of artificial neural interfaces, SBDD workshop: Surface and Bulk Defects in Diamond, Hasselt, Belgium, Feb 2014

- **Farnoosh Vahidpour**, Matthew McDonald, Istvan Biro, Weng Siang Yeap, Ken Haenen, Michele Giugliano, <u>Miloš Nesládek</u>, Functional Characteristics of All Diamond Microelectrode Arrays and Neural Adhesion Study, NDNC, Singapore, May2013

- **Farnoosh Vahidpour**, Paulius Pobedinskas, Istvan Biro, Michele Giugliano, Ken Haenen, Miloš Nesládek, All-carbon diamond micro-electrode arrays for neural interfacing, MRS Spring Meeting, Material Research Society, San Francisco, USA, May2013

- **Farnoosh Vahidpour**, Matthew McDonald, Lowry Curley, Istvan Biro, Weng Siang Yeap, Ken Haenen, Michele Giugliano, Miloš Nesládek, Highly Functional All- Diamond Microelectrode Arrays for Neural Interfacing, SBDD workshop: Surface and Bulk Defects in Diamond, Hasselt, Belgium Feb 2013

- **Farnoosh Vahidpour**, Paulius Pobedinskas, Aida Vaitkuviene, Istvan Biro, Michele Giugliano, Ken Haenen, Miloš Nesládek, Fabrication and Characterization of Novel Diamond Micro-electrode Arrays
ACIN Meeting, IMEC, Leuven, Belgium, Dec 2012

- **Farnoosh Vahidpour**, Aida Vaitkuviene, I.Biro, Michele Giugliano, Miloš Nesládek, Fabrication and Characterization of Novel Diamond Micro-electrode Arrays ,MERIDIAN Meeting, Pisa, Italy, Oct 2012

- **Farnoosh Vahidpour**, Matthew Mcdonald, Istvan Biro, Paulius Pobedinskas, Ken Haenen, Michele Giugliano, Miloš Nesládek; Fabrication and Characterization of novel Diamond Microelectrode Arrays, CITA Meeting, Cell Interfacing Technology and Applications, IMEC, Leuven, Belgium, Oct 2012

- **Farnoosh Vahidpour**, Paulius Pobedinskas, Jules John Vandersarl, Ken Haenen, Michele Giugliano, Miloš Nesládek, Novel approaches for fabrication of diamond-based neuronal probes developed on flexible substrates, CDCM, Granada, Spain: International Conference on Diamond and Carbon Materials, ***Paper selected for the finale of the Young Scholar award competitions***; Sep2012

Poster presentations

- <u>Marie Jakl Krečmarová</u>, Michal Gulka, Mehran Khorshid, Patricia Losada-Pérez, Matthew MacDonald, **Farnoosh Vahidpour**, Emilie Bourgeois, L. Fekete, Vincent Mortet, Miloš Nesládek, Novel concept NV centre - electrochemical diamond trace element chemosensors, SBDD workshop in Hasselt, Belgium: Surface and Bulk Defects in Diamond, Feb 2016

-
- **Farnoosh Vahidpour**, Ali Parsapour, Matthew McDonald, Ken Haenen, Miloš Nesládek, Diamond – Myoelectric Interface Devices: Concept and Demonstration, SBDD workshop in Hasselt, Belgium: Surface and Bulk Defects in Diamond, Feb 2015

- **Farnoosh Vahdipour**, Matthew McDonald, Elena Gjorgievska, Zuzana Vlčková Zivcová, Ladislav Kavan, Hans-Gerd Boyen, Ken Haenen, Miloš Nesládek, Functional biomolecular monolayers on diamond: a novel platform for the construction of artificial neural interfaces, ENFI workshop, Jülich, Germany: Engineering of Functional Interfaces, July 2014

- **<u>Farnoosh Vahdipour</u>**, Lowry Curley, Matthew McDonald, Weng Siang Yeap, Michele Giugliano, Ken Haenen, Miloš Nesládek, All-carbon diamond micro-electrode arrays for neural interfacing, ENFI workshop, Jülich, Germany: Engineering of Functional Interfaces, ***Winner of the Best Poster Presentation Award,*** July 2013

- <u>Lowry Curley</u>, **Farnoosh Vahidpour**, Matthew McDonald, Istvan Biro, Anastasiya Moskalyuk, Andy Taylor, Miloš Nesládek, Michele Giugliano, Nanocrystalline Diamond Substrates as a Neuronal Interfacing Material, BSN, Belgian Society of Neuroscience, Brussels, Belgium, May 2013